MODELS OF PLANKTON BIOMASS SPECTRA

by

Jose G. Mantilla

B.S. Industrial Engineering
Pontificia Universidad Javeriana, Colombia, 1995

Submitted to the Department of Civil and Environmental Engineering
in Partial Fulfillment of the Requirements for the Degree of

Master of Science
in Civil and Environmental Engineering

at the
Massachusetts Institute of Technology
August 1999

Signature of Author: _____

Department of Civil and Environmental Engineering
August 23,1999

Certified by: _____

Sallie W. Chisholm
Professor of Civil and Environmental Engineering
Thesis Supervisor

Accepted by: _____

Daniele Veneziano
Chairman, Departmental Committee on Graduate Studies

MODELS OF PLANKTON BIOMASS SPECTRA

by

Jose G. Mantilla

Submitted to the Department of Civil and Environmental Engineering on August 23, 1999
in Partial Fulfillment of the Requirements for the Degree of Master of Science in
Civil and Environmental Engineering

Abstract

The goal of this thesis is to study the causes and consequences of the size structure of marine planktonic ecosystems. To this end, a theoretical (continuous) size spectrum model was developed. Phytoplankton and zooplankton biomass is represented in the model as functions of their respective biomass size spectrums. Thus, the model allows the natural recovery of the continuous size spectrum for planktonic ecosystems. The model was developed under the assumption that the structure of planktonic ecosystems is largely dependent on organism size. The generality of the model allows the use of either allometric or random encounter models for the specification of the size-dependent functions in the system.

A "distributed grazing" size-dependent dynamic simulation model is presented as a special (discrete) case of the "general" size spectrum model proposed. The model consists of multiple phytoplankton size classes and one zooplankton size class representative of the entire herbivore community. Zooplankton grazing is described by a dynamic function that distributes grazing pressure among phytoplankton size classes according to their relative biomass. Allometric theory was used to specify the size-dependence of the maximum phytoplankton growth rates. Simulations were carried out to study the dynamics of phytoplankton size structure under different allometric structures, representative of ecosystem diversity. Complementing the analysis, simulations were carried out to study the effects of nutrient enrichment processes on phytoplankton size structure. Size structure varied systematically as a function of the allometric structure and nutrient enrichment process chosen. Two parameters were explored: 1) spectral slope, which indicates the relative contribution of small and large cells to total phytoplankton biomass; and 2) transient spectral shape, which indicates the effects of enrichment on phytoplankton succession as the system goes from its original to a new steady state condition. The model provides a natural and simple way of simulating the transient phytoplankton size structure under nutrient enrichment scenarios. It is argued that this will prove very useful in the analysis of plankton size structure dynamics in natural (e.g. spring blooms) and artificial (e.g. ocean fertilization) enrichment processes.

Thesis Supervisor: Sallie W. Chisholm
Title: Professor of Civil and Environmental Engineering, and Biology

ACKNOWLEDGMENTS

My advisor, Penny Chisholm, provided the resources and direction that made this work possible. Penny has been a role model and I am deeply grateful for her encouragement and support.

I am indebted to Dennis McLaughlin for providing the intellectual motivation and support for the development of the biomass spectrum model.

Many thanks to Dave Marks for his patience and warm advice over these three years.

I thank Jeremy and Paulo for their wonderful friendship. Their companionship and support contributed substantially to this work. I also acknowledge the many other friendships at MIT which have made these last several years more enjoyable (Thor & Raileen, Jed, Bassam, Rolf, and others).

I deeply thank Kim and Susan for their continuous moral support. Along with Penny, Dave, Dennis and Richard, they showed me the wonderful human side of MIT.

I wish to thank my family for helping me bring this work to fruition. My parents, my brother and my sister for their trust, encouragement and support throughout this process. My daughter, Juli, for providing (with her love and innocence) that extra motivation when I mostly needed it. To Tara, I am most grateful for her constant love and encouragement. Without her support, I would not have been able to complete this thesis.

Finally, my deepest gratitude to God for His love and company.

I acknowledge financial support from the following sources: a National Science Foundation Graduate Fellowship; and NSF Grant OCE-9302529 to S.W. Chisholm.

TABLE OF CONTENTS

LIST OF FIGURES

Page

Chapter 2

Chapter 3

Chapter 4

LIST OF TABLES

Page

Chapter 3

Chapter 4

Chapter 1

Introduction

INTRODUCTION

A comprehensive understanding of the structure (species composition and relative abundance) and function (energy flow and nutrient cycles) of the ocean ecosystem is necessary to face the world's ever growing environmental problems. The dynamics and regulation of food webs can only be understood by considering processes at the level of individual populations acting in concert with processes over the domain of the entire community (Pahl-Wostl, 1993). Local processes at the species level permanently change macroscopic properties of the system, which then impose new constraints on the species themselves. Thus, a holistic approach is necessary for the derivation of ecological patterns at the ecosystem level (Gaedke, 1995).

However, the complexity of natural ecosystems does not allow the consideration of ecosystem dynamics in its entirety, forcing one to abstract from the particular situation under study. Therefore, ecosystem dynamics should be studied from as many angles as possible. This task is facilitated by the use of conceptual and mathematical models. Models, as simplified description of the real world, will portray distinct features of the natural systems they are designed to study. Hence, mathematical models are essential in promoting an increased understanding of the dynamics of the ocean ecosystem. Models are designed to either reproduce observed biological patterns in particular ecosystems, or to predict the effects of environmental fluctuations on the temporal and spatial dynamics of the structure and function of the ecosystems they describe.

One of the predominant patterns in phytoplankton ecology is a shifting in the size distribution of phytoplankton communities as one moves from the nutrient-rich coastal waters to the oligotrophic open ocean: small cells dominate the open seas. The size structure of the phytoplankton community dictates the composition and structure of the rest of the food web. The main objective of this work is to contribute to the development of models and a theoretical framework for analyzing the causes and consequences of the size structure of phytoplankton communities, which is a relatively conservative property of the ocean ecosystem.

In order to assist the reader in navigating the contents of this work, an explanation of the thesis layout is provided. Chapter 2 begins with a historical presentation of marine ecosystem modeling and its relevance to understanding ecosystem dynamics. A presentation of the relevance of size as an ecological parameter is followed by a historical review of the progress of size distribution models. I then continue to present the two main theoretical modeling

approaches used to explain the size structure of planktonic ecosystems: biomass distribution models and individual-based models. Chapter 2 ends with a review of size-structured dynamic simulation models (size as an aggregation scheme).

In chapter 3, a theoretical biomass spectrum model is documented. The model describes the flow of biomass in planktonic ecosystems. The phytoplankton and zooplankton communities are classified according to organism size, allowing the derivation of biomass spectra from the model. A special case (simplification) of the general model is presented: distributed grazing model (Armstrong, 1998). The model consists of multiple phytoplankton size classes and one zooplankton compartment representing the totality of the herbivore community. A proposed mathematical approach for the derivation of biomass spectra for this special case follows.

Chapter 4 provides a detailed description of dynamic simulation models and their application for analyzing the size structure of planktonic ecosystems. As a reference, simulations using a basic nutrient-phytoplankton-zooplankton model are presented, along with a theoretical steady state analysis for this system. A distributed grazing model is presented as the model of choice for analyzing phytoplankton size structure. A general description of the model and justification for choice of this model is followed by the presentation of dynamic simulations under different allometric structures and nutrient enrichment scenarios. It is shown that the model provides a natural and simple way of simulating the transient size structure under nutrient enrichment scenarios. This will prove very useful in the analysis of the food web structure dynamics in large scale enrichment processes, such as ocean fertilization.

In chapter 5, the primary conclusions of this work are summarized. Recommendations on future research directions follow.

REFERENCES

Armstrong, R. A. 1998. Stable model structures for representing biogeochemical diversity and size spectra in plankton communities. *Journal of Plankton Research* 21: 445-464.

Gaedke, U. 1995. A comparison of whole-community and ecosystem approaches (biomass size distributions, food web analysis, network analysis, simulation models) to study the structure, function and regulation of pelagic food webs. *Journal of Plankton Research* 17(6): 1273-1305.

Pahl-Wostl, C. 1993. The hierarchical organization of the aquatic ecosystem: an outline on how reductionism and holism may be reconciled. *Ecological Modelling* 66: 81-100.

Chapter 2

Modeling the Size Structure of Planktonic Ecosystems

INTRODUCTION

Marine biota account for almost half of the annual primary production of the planet and play an important role in the control of climate and the atmosphere. They also play an important role in the natural nutrient cycles of the ocean. Hence, a comprehensive understanding of the structure and function of marine ecosystems is essential for predicting the development of community structures and the functional responses of the system to changes in environmental conditions. Mathematical models provide a feasible setting for analyzing the structure and function of marine ecosystems from many different angles. Because they are simplified descriptions of the real world, there is no reason to expect any individual approach to be unequivocally right or wrong. Methodologies based on biomass size distributions and dynamic simulation models are presented in this chapter.

Plankton biomass has been found to be distributed in a continuous manner across entire ranges of size classes. Specifically, observations show that the abundance of organisms per size class is inversely proportional to their body weight. Sheldon et al. (1972) observed that particle concentrations (in ppm, by volume) were uniformly distributed when the data were grouped in logarithmic size intervals, with some indication of a decrease in concentration with increasing logarithmic intervals of organism size. The size structure of the phytoplankton community dictates the composition and structure of the rest of the food web. This chapter reviews the relevance of size distributions in the analysis of planktonic ecosystems. A description of the two main theories for explaining the size distributions observed in pelagic ecosystems, as well as a presentation of the applications of size as an aggregation scheme in simulation models, follows.

BACKGROUND

Marine ecosystem modeling

The initial work in modeling marine ecosystems was carried out by Riley et al. (1949) and Steele (1958). Since then many models have been developed and published and it is only possible here to refer to a few of these. Interest in the analysis of upwelling zones lead to the development of models to simulate the population dynamics of those systems. As an example, the international programs investigating coastal upwelling zones during the 1970s stimulated the development of a number of successful models (Wrobleski, 1977, 1980). Another area of interest for oceanographers during this period was the understanding of the processes

maintaining the deep chlorophyll maximum in oligotrophic waters. The models developed by Jamart et al. (1977, 1979) and Kiefer and Kremer (1981) are the most representative.

Most of the earlier models tended to concentrate on the interaction of phytoplankton and zooplankton only. During the 1980s biological oceanographers became aware of the importance of small organisms, such as picophytoplankton and bacteria, and the organisms that feed on them, such as protozoa (Fasham, 1993). The new awareness of the importance of microbial processes in the analysis of nutrient and plankton dynamics lead to the development of more holistic models that attempt to embrace the totality of knowledge of the components of planktonic ecosystems and the flows of mass and energy between these components. Williams (1981) provided the background for plankton dynamics models incorporating bacteria, protozoans and dissolved organic carbon. The first model to investigate quantitatively the importance of these findings was the one developed by Pace et al (1984). They presented results from a full simulation model incorporating a larger number of groups of organisms and flows than those included in previous models. This model included physical forcing parameterized in the form of variable nutrient inputs. Later Evans and Parslow (1985) emphasized the importance of studying annual cycles, and demonstrated how different cycles of mixed layer depth could give rise to qualitatively different biological cycles. Their phytoplankton-zooplankton-nutrient dynamics model showed how the seasonal recurrence of plankton cycles, in particular the spring bloom, is driven by the interaction of physical mixing with removal by grazers.

All the models referred to so far use deterministic differential equations to describe ecosystem dynamics. Fasham (1977) and Kremer (1983) explored stochastic approaches as an approach for modeling marine ecosystem dynamics, in attempts to account for the high variability characteristic of these systems. Lagrangian (following the water motion) models have been used (Wolf and Woods, 1988) to simulate the light-dependent growth of phytoplankton. They point out that the historical trajectories of phytoplankton within the turbulent mixed layer are a critical factor in the phytoplankton growth. The Lagrangian model involved solving the phytoplankton growth equations for each particle, and the subsequent derivation of the phytoplankton vertical distribution. In the following section, I provide a background on the historical progress of planktonic size distribution models.

Size Distribution Models

Elton (1927) formulated all of the principles on which the modern theory of size distribution in pelagic ecosystems is based. He noted that smaller organisms are much more abundant than larger organisms and characterized this as the "pyramid of numbers". He also stated that elemental food chains comprising the food web are arranged in order of increasing organism size, with the result that the general flow of biomass and energy in the community is from smaller organisms to larger ones. A remarkable feature of Elton's work was that he introduced all the ideas and concepts on organism size in an attempt to simplify the complexity of ecological communities (Platt, 1985). Kerr (1974) developed a theoretical model based on trophic processes, to explain the observed regularities in the size composition of pelagic ecosystems. The model assumes that prey and predator sizes are related and that growth and metabolism satisfy similar functions of organism size when averaged over entire trophic levels. Later, Fenchel (1974) quantified (in operational form) the size-dependence of respiration and growth rate, completing all the necessary pieces for the development of a theory of organism size distribution in the pelagic ecosystem (Platt, 1985).

Allometric relationships between body size and weight-specific process rates enable a rough prediction of community metabolic properties from body mass (size). According to allometric theory, diverse sets of characteristics of organisms scale with body size. The metabolic activity or specific rate process R, e.g. respiration or growth rate, may be estimated from the biomass, W by using the equation $R = aW^b$, where a and b are constants. This relationship seems to hold for a diversity of processes among unrelated organisms. The mass-specific value of b is relative constant (-0.25) for large data sets covering broad size ranges and for a variety of physiological processes. The constant a, on the other hand, is variable and depends on the physiological process under consideration (e.g. respiration or production). Furthermore, its value may differ across major taxonomic groups.

Organism size (in pelagic ecosystems) gains additional predictive power at the community level since body size and trophic position are related to each other (i.e.. autotrophs tend to be smaller than heterotrophs and predators tend to be larger than their prey). The close relationship between body size and physiological and ecological features allows prediction of the abundance, metabolic activity, seasonal variability, reaction time to external perturbations, and other ecosystem attributes, from organism size. In addition, the allometric approach can be

used to parameterize dynamic simulation models for regions where direct measurements of process rates are scarce.

There have been few attempts to develop truly dynamic models for size distributions that would allow a dynamic representation of the pelagic biomass spectrum (Gaedke, 1995). In most cases, size has been used as an aggregation scheme in dynamic simulation models. Figure 2-1 shows a classification of size distribution models. They are divided into theoretical models, attempting to explain the causes of the size distribution and reproduce mathematically, and size-dependent models that are developed using the size distribution theory as an underlying assumption. The theoretical models are divided in biomass distribution models (Platt and co-workers' spectrum theory models) and individual-based models (Kiefer and Berwald's random encounter model). The size-dependent models are divided into steady state and dynamic simulation models. The following section provides a description of two of the main size-based modeling approaches used to study the structure and function of pelagic ecosystems: size distribution models and size-dependent dynamic simulation models.

THEORIES OF SIZE DISTRIBUTION

Biomass Distribution Models

Population dynamics theory based on analysis of species (taxonomy) and stages can not be applied practically to natural planktonic communities (Zhou and Huntley, 1997). Models of population dynamics based on taxa and organism stages require separate determination of individual metabolic rates for each species and stage, making the approach impractical. Biomass spectrum theory is presented as an alternative perspective, based on the classification of plankton on the basis of size alone so that both individual and community changes can be estimated from allometrically-scaled rates.

Interest in understanding the size distribution characteristic to the pelagic ecosystem has resulted in the development of theoretical biomass spectrum models, characterized by the description of a continuous flow of biomass or energy from smaller to larger organisms. These models are based on allometric relationships between organism size and metabolic processes, and have been used mostly as tools to attempt to explain the continuity and regularity of the shape biomass size distributions in pelagic ecosystems (Gaedke, 1995). The models use the correlation between body size and trophic position and describe a mostly continuous flow of

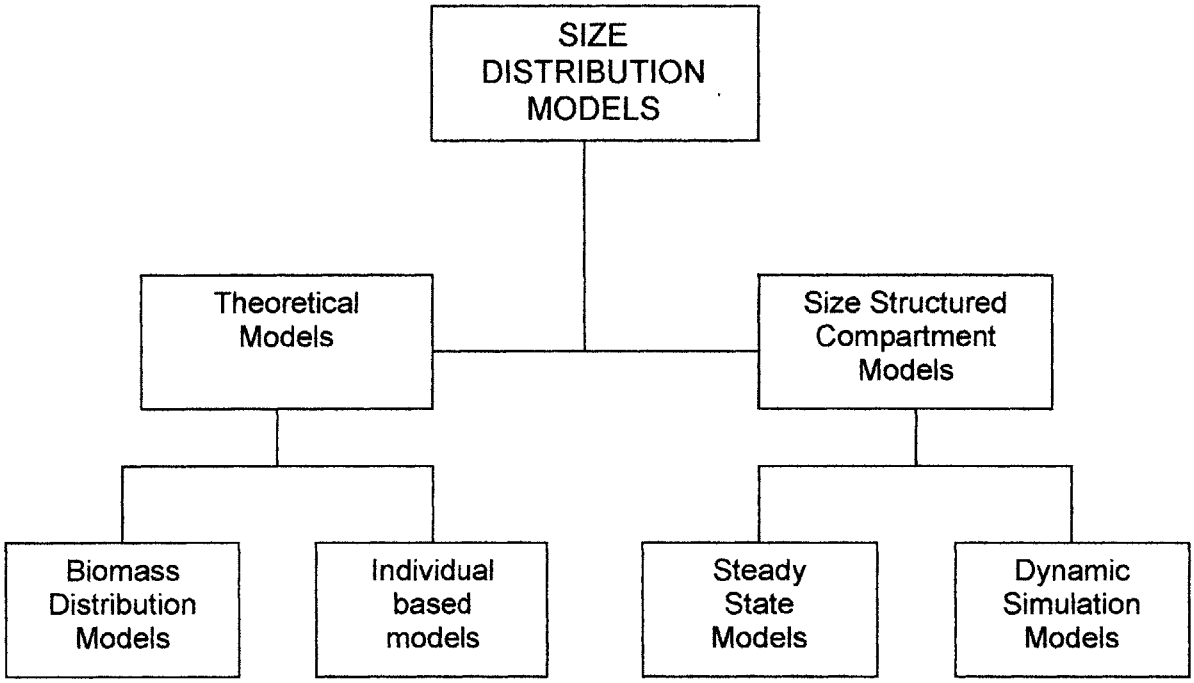

Figure 2-1: Size distribution models in plankton ecology. Theoretical models represent those derived to explain the size distribution of organisms in planktonic ecosystems. Size structured compartment models represent those developed using the size distribution theory as an underlying assumption.

matter from small to larger organisms. Allometric relationships allow the estimation of contributions to metabolic processes like production and respiration. Analysis of the size distributions of species abundance and biomass can provide information on the structural and energetic aspects of the pelagic ecosystem.

Biomass size distributions are constructed by allocating all organisms into logarithmically spaced size classes according to their individual body weight (or size) and summing up the biomass in each weight (size) class. Spectra developed for the ocean ecosystem from observational data show regularity in the continuous distribution of biomass across the entire range of logarithmic classes. This regularity implies that the abundance of organisms per size class is inversely proportional to their body weight, which enables an estimate of the minimum counting volumes required to assess abundance of all size categories with equal accuracy. Hence, the generalizing capacity of body size can be used to reduce the enormous complexity of pelagic food webs in aquatic ecosystems.

The slope of biomass size distributions provides insight into the energy flow and transfer efficiency along the size gradient in complex pelagic food webs. This information is obtained without the necessity to define distinct trophic levels or to distinguish taxonomic groups, as long as the size range under consideration is sufficiently broad to justify the assumption of an energy flow along the size gradient. Trophic transfer efficiencies may be derived from the slope of the biomass spectrum if average predator-prey ratios can be estimated. Among other applications, this technique may provide rough predictions of potential fish yield from plankton measurements.

Platt and Denman (1978) derived a steady-state theory for the distribution of organisms by size in the pelagic zone of the open ocean. The theory was founded on large bodies of research that suggested the size-dependence of physiological processes. The theory developed was independent of the trophic level concept and explored the flow of biomass from smallest to largest organism through a series of size classes arranged on an octave scale, for operational convenience (data collection). They defined the biomass spectrum as $b(w)$, characterized by the arrangement of the nominal weights in an increasing octave scale such that the nominal weight for each size class is double that of the previous class. The biomass spectrum has units $[ML^{-3}]$ and the independent variable is the weight of an individual organism. They then defined the

normalized spectrum, $\beta(w)$, as $b(w)/w$, such that it is integrable over w. The main objective of their work was to examine the flow of biomass from smaller to larger organisms, $F(w)$

(1) $F(w) = \frac{\beta(w)w}{\tau(w)}$, where $\tau(w)$ is the turnover time

(2) $\tau(w) = Aw^x$, where A and x are constants

The general expression for the biomass flow is then

(3) $F(w) = A^{-1}\beta(w)w^{1-x}$

By conservation of flux and by including the processes of respiration and losses to the detritus food chain, Platt and Denman derive a general expression for the unnormalized spectrum

(4) $\frac{b(w)}{w_o} = (w/w_o)^{x-A\alpha-q}$, where α is an allometric constant and q represents the losses through inefficient feeding

By using parameters from the published literature they calculated the theoretical unnormalized biomass spectrum and recovered, from the spectral shape obtained, the fact that biomass decreases in regular manner with increasing size.

As a continuation of the work of Platt and Denman (1978), Silvert and Platt (1978) derived a time-dependent equation for the size structure of the pelagic food chain, based on quantitative relationships for the weight dependence of metabolism and growth. The normalized spectrum is represented as a function of time, $\beta(w,t)$, and represents the density of particles of a given size w at time t. The unnormalized spectrum, $b(w,t)$, is given now by $\beta(w,t)dw$, and represents the mass of particles per unit volume in the interval of sizes between w and $w+dw$ at time t. By defining a continuous growth function they derive a generalization of the steady-state biomass spectrum theory, obtaining a dynamic representation of the normalized biomass spectrum, given by

(5) $\beta(w,t) = \beta(w_o,0)\frac{\beta_o(w)}{\beta_o(w_o)}$

The main advantage of this new dynamic representation is that any peaks in the biomass spectrum will propagate intact through the spectrum. In addition, with this model, the independent variable, *w*, does not need to be measured in an octave scale.

Later, Silvert and Platt (1980) described the energy flow through a pelagic ecosystem by using a nonlinear, time-dependent, and spatially inhomogeneous master equation. As in their previous work, size was used as the main aggregation criteria. For organism description purposes, they assumed that two particles could be regarded as identical if their ecological roles were similar and if they were of the same size and at the same location. The model developed allocated organisms in compartments defined such that all particles of a given typo which fall within a specified size range and lie within a given volume of space are identified with the same compartment and treated as equivalent. The possibility of differentiating organisms by type (ecological role) represents an extension of the previous work of Platt and co-workers described above, where all particles of the same size, regardless of their type, were treated as identical. In this new model, three main categories were considered: plants, animals and detritus. Likewise, all energy (or nutrient) sources and sinks are represented by compartments.

Silvert and Platt define b_i as the energy content (combined biomass) of all particles in the i^{th} compartment. The principle of conservation of energy is expressed by

(6) $\frac{db_i}{dt} = S_i = \Sigma(T_{ij} - T_{ji})$, *where* S_i *is the net rate of energy flow into compartment i*
T *is the transfer rate (energy flow between compartments)*

For their analysis, Silvert and Platt considered two general classes of energy exchange processes: energy exchange between compartments corresponding to very different particle sizes, and energy exchange by transport of particles across the interface between adjacent compartments. In the first group they analyze reproduction and predation processes, whereas in the second group they include the effects of growth, advection and diffusion. Reproduction was represented in the model by a linear function with no density-dependence, so its effect on the dynamics of the model is much smaller than the effect of nonlinear terms (e.g. predation). Predation is defined as all processes whereby particles are consumed by other particles, and its representation is based on a generalization of Holling's disc equation. Predation (in the model)

is very important due to the dynamic effects caused by nonlinearity and feedback. Growth, advection and diffusion are described by a continuous formulation.

Silvert and Platt derived two formulations for their model: a linear and a quadratic representation. For the model in its linear form, the growth term was assumed to be independent of the biomass density function, β, and the source term was assumed to be linear in β. The static form of the linear model equation was derived and solved by Platt and Denman (1978) and the linear dynamic model by Silvert and Platt (1978). The linear model does not include feedback and cannot reflect density-dependent effects and predator-prey cycles. However, it does illustrate some of the main characteristics of pelagic ecosystems close to steady state.

For the model in its quadratic representation, they assumed that all terms but the time derivative are of second order in β. Since reproduction is a linear flow term it is ignored and all mortality is "attributed" to predation in the mathematical representation of the model. The model equation is homogeneous and of second order

$$(7) \qquad \frac{\delta \beta}{\delta t} = -w \frac{\delta}{\delta w} (\beta G) - Z\beta, \qquad \text{where } G = g/w \text{ (specific growth rate)}, \quad Z = \text{predation function (loss term)}$$

In general, the model described by Silvert and Platt to describe the energy flux through the pelagic ecosystem consist of two main components. The first component describes the forcing of the system through primary productivity, i.e. the input of photosynthetically produced material at the small-particle end of the biomass distribution. The second leading component of the master equation is predation, and can be written in terms of the relative sizes of interacting organisms (size selectivity of feeding). The food web structure described by the model is represented then by a transition matrix whose elements express the probability that an organism of a given size will prey on an organism of another size. The formalism described by the model is applicable to discrete and limited parts of the size distribution and not limited to whole ecosystem representations.

Individual-Based Models

Kiefer and Berwald (1992) developed a random encounter model for the microbial planktonic community as an alternative hypothesis to explain the size distribution features in planktonic organisms. Traditionally, the monotonical decrease of biomass with increasing size has been interpreted to be the result of allometric control of growth and respiration rates. Kiefer and Berwald argue that the traditional size distribution theory developed by Platt and co-workers is very general and does not provide sufficient insight into the dynamics of microbial populations, given that they are based on the principle of conservation of energy and assume steady state conditions.

The "random encounter" hypothesis is based on the assumption that the size distribution of cells results from size-selective predation in an environment where populations swim randomly through the water, encountering both prey and predators. Kiefer and Berwald argue that the steady state flow of material through the microbial food web, as well as the size distribution, are determined by the random encounter of predator and prey populations. Finally, they argue that the mathematical model derived explains the fourth power dependence of the frequency of cell size.

They start by defining the differential size distribution of particles, $F(D)$, as the concentration of particles within an infinitesimal band at diameter D. By integration $F(D)$ between the limits of the bandwidth, D_{min} and D_{max}, they calculate $N(D)$, defined as the numeric concentration of cells in a bandwidth from D to $D+dD$. For marine particles, the differential size distribution has generally been described by a hyperbolic function of the form $F(D) = aD^{-b}$, with b having a value of four. This phenomenon is described as the fourth power dependency of the frequency of cell size and has been noted by numerous scientists (Sheldon et al. 1972).

In their presentation, Kiefer and Berwald assume that microbial cells are spherical and start by considering a population of phagotrophic protozoans of diameter D_2 and differential concentration $F(D_2)$. As these cells move randomly through the water they encounter and consume prey of size class 1 with range of diameters (D_{1min} , D_{1max}). The range of cell sizes in this prey class is determined by the ability of size class two cells to ingest them. In addition, the population of cells of size class two encounters predators of size class three with range of diameters (D_{3min} , D_{3max}). Similarly, the range of cell sizes in size class three is determined by their ability to ingest cells in the population of cells of size class two. The rate of ingestion, F_2^I, is

defined as the total rate of encounter of population two with prey multiplied by the mass of an individual prey item. Likewise, the rate of biomass loss through predation, F_2^P, is defined as the total rate of encounter of population two with predators multiplied by the mass of an individual within the size class two population. Under steady state conditions, the ingestion rate of prey must balance the losses to predation and those caused by consumption inefficiencies

(8) $F_2^I = F_2^E + F_2^P$, *where* F_2^E *accounts for the excretion and egestion losses*

By defining the ingestion and predation components in terms of the mean clearance rate, Kiefer and Berwald derive a steady state expression in terms of the population's specific rates of growth, μ_2, and mortality, ω_2. At steady state, $\mu_2 = \omega_2$. Assuming no biochemical selectivity of predation, they define the individual clearance rate as the encounter rate, Z_P. They use the formulation derived by Gerritsen and Strickler (1977) for the rate of encounter of prey by an individual predator

(9) $Z_P = \frac{\pi}{3} R^2 N(D_1) \frac{v_1^2 + 3 v_2^2}{v_2}$, *where* v_1 *is the speed of the prey*
v_2 *is the speed of the predator*
R is the radius of the encounter sphere

Kiefer and Berwald then derived expressions for the mean clearance rate for a predator of constant diameter D_2 feeding on prey of variable diameter D_1, and for the predator's predator with a variable diameter D and feeding on prey of constant diameter D_2. Based on observed distributions of clearance they used a theoretical optimum in prey cell size, characterized by a normal distribution, $\eta(D_2, D_3)$, where larger and smaller cells are less effectively captured by a predator of a given size. Using the expressions for the clearance rate, they derive an expression for the specific rate of mortality, ω_2, in which the capture efficiency is the only term that depends on the cell size of the prey and predator populations.

As an extension of the previous analysis, Kiefer and Berwald continue by including nonphagotrophic populations, e.g. phytoplankton, in their random encounter model. For the nonphagotrophic cells encounter with cells of another species is never beneficial (figure 2-2). The nonphagotrophic population is included in the same size class as the phagotrophic population of size class two in their initial case. The phytoplankton population will consume nutrients, N, and will experience losses by grazing from the phagotrophic population of size class three. For the phytoplankton population, the rate of replacement of individuals is not

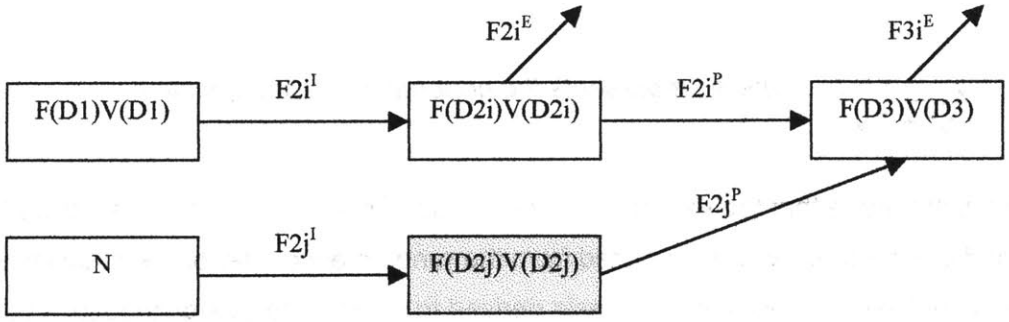

Figure 2-2: Schematic diagram of trophic interactions in the random encounter model when considering the existence of phytoplankton cells in size class 2 (modified from Kiefer and Berwald, 1992). The phytoplankton community is represented by the shaded compartment in the figure. Phytoplankton uptake nutrients and are subject to grazing from the larger size class of phagotrophic organisms. The arrows represents the flows of biomass in the system.

directly dependent on the concentration of cells of another size class, as is the case for the phagotrophic populations. Instead, the rate of replacement for the phytoplankton community will depend on the concentration of a limiting nutrient. The survival of the phytoplankton population requires that it satisfy the steady state conditions for the specific rates of growth and mortality, $\mu_2 = \omega_2$. By assuming that there is no chemical selection by predator between phago and nonphagotrophic populations of the same size class, the ratio of specific growth rates of the two populations is a function of the capture efficiencies and swimming speeds.

(10) $$\frac{\mu_{2j}}{\mu_{2l}} = \frac{v_{2j}^2 + 3\,v_{3j}^2}{v_{2i}^2 + 3\,v_{3i}^2}$$, *where j represents the nonphagotrophic population*

Kiefer and Berwald argue that the expression for the ratio of specific growth rates shows that the growth and death rates can be estimated from the random encounter of the organisms. The main difference between the earlier hypothesis derived to explain the size distribution in the microbial planktonic community and the random encounter hypothesis developed by Kiefer and Berwald involves the treatment of the growth rate of populations. The earlier hypothesis is based on the assumption that the specific growth rates of natural populations are uniquely determined by cell size. The random encounter hypothesis ignores empirical allometry and establishes that the specific growth rate of phagotrophic populations is not only a function of cell size but also a function of the assimilation rate. The specific growth rate of nonphagotrophic populations was found to be "relatively" coupled to the specific growth rates of similarly sized phagotrophic cells. Also, the random encounter model implies that the steady state growth rates will tend to increase with increases in both prey and predator cell concentration.

In addition, Kiefer and Berwald argue that there exists a strong dependence of growth and respiration rates on nutrient and food supply, whereas there is little evidence of dependence of rates on cell size. They state that for phytoplankton and bacteria species, the growth rates of many larger species are faster than those of smaller species. Finally, the random encounter hypothesis ignores the changes in size of individuals and instead focuses on trophic exchange. Based on their analysis and the results of the model developed, Kiefer and Berwald propose that the size distribution of single cells in the ocean is not the result of allometric constraints on metabolism but a consequence of random encounter of prey and predator organisms.

SIZE-STRUCTURED DYNAMIC SIMULATION MODELS

Dynamic simulation models have been used extensively in modeling marine ecosystems due to their unique ability to study the dynamic nature, spatio-temporal organization, direct and indirect cause-effect relationships, and impact of physical forcing on the ecosystem. These models describe explicitly the major dynamics between the important functional groups and with abiotic processes in a particular ecosystem. They are based on non-linear systems of coupled differential or difference equations that have to be solved numerically. Examples include the models developed by Fasham et al (1990) and Moloney and Filed (1991). As with all modeling approaches the principal aim is not a perfect reproduction of the natural system, but to reduce the complexity of ecosystems to a degree that allows analysis.

Dynamic simulation models can be classified in two main categories: those aiming to reproduce natural patterns observed in a particular ecosystem and those designed to derive predictions from the experience on which their development is based. The latter are used to predict the response of the system to environmental changes, e.g. ocean fertilization. The main advantages of dynamic simulation models include the possibility of studying the dynamic nature and spatio-temporal structure, which are of great relevance in the analysis of ecosystems (Gaedke, 1995). Dynamic simulation models represent a coherent way to analyze cause-effect relationships in ecosystems. Their predictive power, however, is limited to a great extent by the large number of parameters usually required, that introduce numerous assumptions and uncertainties. In addition, the existence of positive feedback mechanisms and the chaotic nature of many ecological processes further diminish the predictive ability of these models.

Planktonic ecosystems are commonly described by compartmental models where each compartment represents a trophic level or taxonomic group (Moloney and Field, 1991). Compartmental models range in complexity from the most basic *NPZ* models to connected food webs like the one described by Fasham et al (1990). Such models represent the standing stocks and interactions between the compartments. The compartments most commonly used are phytoplankton, zooplankton and nutrients. When these models are used as the basis for dynamic simulation models a number of problems are encountered. For example, by lumping all phytoplankton size classes with widely disparate metabolic rates in one single compartment, inappropriate rate parameters are commonly used. A logic solution would be to divide the main compartments in subdivisions representing different taxonomic groups. However, the complexity of aquatic ecosystems would require extensive subdivision of the main compartments in order to

produce more realistic results. As complexity is added to the models, parameter estimation becomes increasingly more difficult. In addition, the ability to analyze the significance of the different ecological interactions described by the models is obscured by this added complexity (Armstrong, 1998). This is the most commonly encountered problem for species or trophic level compartment models (Moloney and Field, 1991).

An alternative approach is to develop models based on general ecological principles. Organism size has been identified as a valid scaling factor in the analysis of metabolic processes and ecological interactions in pelagic ecosystems. The structure of planktonic ecosystems is largely dependent on organism size (Sheldon et al., 1972; Platt and Denman, 1978; Silvert and Platt, 1980). In addition, rates of many metabolic processes are size-dependent (Moloney and Field, 1989; Chisholm, 1992). The use of size as an independent ecological criterion for estimating many ecological and metabolic parameters obviates the parameter estimation problems discussed above. The realization of the predictive power of organism size for physiological and ecological properties has lead to the use of organism size as an aggregation scheme in dynamic simulation models for planktonic ecosystems. Two main approaches have been used to reproduce and predict planktonic size distributions: steady state models and dynamic simulation models.

Armstrong (1994) proposed two steady state models: parallel independent food chains and "connected" food web. The phytoplankton and zooplankton communities were divided according to size, and the parameter values for the size classes were derived using allometric relations, with smaller size classes growing more rapidly and being consumed more rapidly than larger size classes. In this model, total nutrient in the system was increased and phytoplankton and zooplankton "invade" the system sequentially, starting with the smallest size classes. The resulting pattern was one of equal biomass in equal logarithmic size categories where total phytoplankton biomass increases by the addition of larger size classes rather than through biomass increases in existing size classes (Armstrong, 1994). This model is effective at describing steady state conditions but is problematic for fitting non steady state data. Armstrong (1994) proposed the connected food web as an alternative to overcome this problem. However, the resulting model presents a new problem: the set of species that will be present at a given nutrient loading becomes extremely sensitive to choices of parameter values and food web structure (Armstrong et al. 1994).

Perhaps the best example of a complex dynamic simulation size-dependent model for planktonic ecosystems is the one developed by Moloney and Field, 1991. The model is represented by compartments organized along a gradient of organism size. The model is comprised of three phytoplankton and zooplankton size classes, bacteria, and nutrients. The equations for the model compartments are parameterized using allometric relationships. The size-based simulation describes the carbon and nitrogen flows in plankton ecosystems. In contrast to size-based energy flow models (Silvert and Platt, 1980), this model simulates the flows of carbon and nitrogen in the ecosystem.

Moloney and Field argue that the model has several clear advantages over size-independent models such as the one developed by Fasham et al. (1990). One of the main problems in the Fasham et al. model comes from the parameterization of zooplankton grazing on multiple resources by means of feeding preferences. The assumption that zooplankton grazing on zooplankton is a size-dependent process obviates that problem: zooplankton graze on their "corresponding" phytoplankton size class. However, the chosen web structure and the imposed grazing limitations are not necessarily representative of actual trophodynamics in a real ecosystem. A more realistic approach would be to allow zooplankton to graze on all equivalent or smaller phytoplankton size classes.

To illustrate the applicability of their model, Moloney and Field simulate the responses of plankton ecosystems to upwelling events. The main goal of the model was to simulate the general features and processes of planktonic ecosystems. Moloney and Field argue that this model represents a first step toward the development of a "generic model" for the dynamics of plankton communities. They argue that the use of size as the independent criterion for classifying planktonic communities allows the systematic estimation of parameters for an unlimited number of size classes. They also state that the model can be applied to the analysis of different environments by changing the parameter values and the input biomass spectrum. However, the "migration" of the model into different ecosystems requires access to a considerable database on plankton size distribution, trophic interactions, and the size dependence of rates and processes.

Finally, they argue that the model structure can be changed to include additional compartments (nutrients, micronutrients, or additional size classes) for added realism. Again, the added complexity translates in greater data requirements, larger sensitivity to parameter values, and

added difficulty in understanding the contribution of the different ecological processes described in the model. As a result of the problems embedded in dynamic simulation models like the one derived by Moloney and Field, Armstrong (1998) proposes the use of a distributed grazing model for analyzing plankton population dynamics (refer to Chapter 4).

More recently, Gin et al. (1998) developed a theoretical model to test hypotheses regarding size structure of plankton communities and their response to perturbations in the environment. They argue that increased understanding of changes in size structure in response to environmental perturbations will be relevant in the analysis of fisheries yields and of the trophic state of ecosystems. The model includes seven size classes of phytoplankton, zooplankton, and nitrate, ammonium, particulate organic nitrogen, and dissolved organic nitrogen. The flows and standing stocks of the different model compartments are driven by external forcing functions, such as light availability and seasonal changes in the vertical structure of the water column. The model was used to simulate the phytoplankton size structure in oligotrophic waters in the Sargasso Sea (BATS). The model is an extension of previous size-based models for the region (Hurtt and Armstrong, 1996). It includes the modeling of the seasonal and depth variation of size spectra, and the results were tested against more recently acquired size spectral data from the BATS station (Gin, 1996). In addition, the model was applied to a mesotrophic coastal ecosystem in Massachusetts Bay. Gin et al. (1998) found that the model was reasonably successfully applied to two very different ecosystems (oligotrophic and eutrophic). This result supports the theory that models based on objective estimators of ecological parameters, such as size, can be effectively used to test hypotheses regarding the structure and function of diverse marine ecosystems.

REFERENCES

Armstrong, R.A. 1994. Grazing limitation and nutrient limitation in marine ecosystems: steady state solutions of an ecosystem model with multiple food chains. *Limnology and Oceanography* 39(3): 597-608.

Armstrong, R.A., S. Bollens, B. Frost, M. Landry, M. Landsteiner, and J. Moisan 1994. Food webs. In Davis, C.S., and J.H. Steele (eds.) *Biological/physical modeling of upper ocean processes.* Woods Hole Oceanographic Institute Tech. Rep. WHOI-94-32.

Armstrong, R. A. 1998. Stable model structures for representing biogeochemical diversity and size spectra in plankton communities. *Journal of Plankton Research* 21: 445-464.

Chisholm, S.W. 1992. Phytoplankton size. In Falkowski, P.G., and A.D. Woodhead (eds.) *Primary productivity and biogeochemical cycles in the sea.* Plenum Press New York.

Elton, C. 1927. Animal ecology. Macmillan, New York, NY.

Evans, G.T., and J.S. Parslow 1985. A model of annual plankton cycles. *Biological Oceanography* 3: 327-347.

Fasham, M.J.R. 1977. The application of some stochastic processes to the study of plankton patchiness. In Steele, J.H. (ed.) *Spatial pattern in plankton communities.* Plenum Press New York and London.

Fasham, M.J.R., H.W. Ducklow, and S.M. McKelvie 1990. A nitrogen-based model of plankton dynamics in the oceanic mixed layer. *Journal of Marine Research* 48: 591-639.

Fasham, M.J.R. 1993. Modeling the marine biota. In Heimann, M. (ed.) *The global carbon cycle.* NATO ASI Series, Vol. I 15, Springer-Verlag Berlin.

Fenchel, T. 1974. Intrinsic rate of natural increase: the relationship with body size. *Oecologia* 14: 317-326.

Gaedke, U. 1995. A comparison of whole-community and ecosystem approaches (biomass size distributions, food web analysis, network analysis, simulation models) to study the structure, function and regulation of pelagic food webs. *Journal of Plankton Research* 17(6): 1273-1305.

Gerritsen, J., and J.R. Strickler 1977. Encounter probabilities and community structure in zooplankton: a mathematical model. *J. Fish. Res. Board Can.* 34: 73-81.

Gin, K.Y.H. 1996. Microbial size spectra from diverse marine ecosystems. ScD. Thesis. Massachusetts Institute of Technology/Woods Hole Oceanographic Institution Joint Program in Applied Ocean Science and Engineering.

Gin, K.Y.H., J. Guo, and H. Cheong 1998. A size-based ecosystem model for pelagic waters. *Ecological Modelling* 112: 53-72.

Hurtt, G.C., and R.A. Armstrong 1996. A pelagic ecosystem model calibrated with BATS data. *Deep-Sea Research* 43: 653-683.

Jamart, B.M., D.F. Winter, K. Banse, G.C. Anderson, and R.K. Lam 1977. A theoretical study of phytoplankton growth and nutrient distribution in the Pacific Ocean of the northwestern US coast. *Deep-Sea Research* 24: 753-773.

Jamart, B.M., D.F. Winter, and K. Banse 1979. Sensitivity analysis of a mathematical model of phytoplankton growth and nutrient distribution in the Pacific Ocean of the northeastern US coast. *Journal of Plankton Research* 1: 267-290.

Kerr, S.R. 1974. Theory of size distribution in ecological communities. *Journal of Fish. Res. Board Can.* 31: 1859-1862.

Kiefer, D.A., and J.N. Kremer 1981. Origins of vertical patterns of phytoplankton and nutrients in the temperate open ocean: a stratigraphic hypothesis. *Deep-Sea Research* 28: 1087-1106.

Kiefer, D.A., and J. Berwald 1992. A random encounter model for the microbial planktonic community. *Limnology and Oceanography* 37(3): 457-467.

Kremer, J.N. 1983. Ecological implications of parameter uncertainty in stochastic simulation. *Ecological Modeling* 18: 187-207.

Moloney, C.L., and J.G. Field 1989. General allometric equations for rates of nutrient uptake, ingestion and respiration in plankton organisms. *Limnology and Oceanography* 34: 1290-1299.

Moloney, C.L., and J.G. Field 1991. The size-based dynamics of plankton food webs. I. Description of a simulation model of carbon and nitrogen flows. *Journal of Plankton Research* 13: 1003-1038.

Pace, M.L., G.A. Knauer, D.M. Karl, and J.H. Martin 1984. A simulation analysis of continental shelf food webs. *Marine Biology* 82: 47-63.

Platt, T. 1985. Structure of the marine ecosystem: its allometric basis. In Ulanowicz, R.E., and Platt, T. (eds.) *Ecosystem theory for biological oceanography.* Canadian Bulletin of Fisheries and Aquatic Sciences 213: 55-64.

Platt, T., and K.L. Denman 1978. The structure of the pelagic marine ecosystems. *Rapp. P.-V. Reun. Const. Int. Explor. Mer.* 173: 60-65.

Riley, G.A., H. Stommel, D.F. Bumpus 1949. Quantitative ecology of the plankton of the western North Atlantic. *Bull. Bing. Ocean. Coll* 12(3): 1-169.

Sheldon, R.W., A. Prakash, and W.H. Sutcliffe 1972. The size distribution of particles in the ocean. *Limnology and Oceanography* 17: 327-340.

Silvert, W., and T. Platt 1978. Energy flux in the pelagic ecosystem: a time-dependent equation. *Limnology and Oceanography* 23(4): 813-816.

Silvert, W., and T. Platt 1978. Dynamic energy-flow model of the particle size distribution in pelagic ecosystems. In Kerfoot, W.C. (ed.) *Evolution and ecology of zooplankton communities.* The University Press of New England, New Hampshire.

Steele, J.H. 1958. Plant production in the northern North Sea. *Scottish Home Department Marine Research report No. 7 HMSO Edinburgh.*

Wolf, K.U., and J.D. Woods 1988. Lagrangian simulation of primary production in the physical environment – the deep chlorophyll maximum and nutricline. In Rothschild, B.J. (ed.) *Towards a theory of biological-physical interaction in the world ocean.* Kluwer Dordrecht.

Wrobleski, J. 1977. A model of phytoplankton plume formation during variable Oregon upwelling. *Journal of Marine Research* 35: 357-394.

Wrobleski, J. 1980. A simulation of the distribution of *Acartia clausii* during Oregon upwelling August 1973. *Journal of Plankton Research* 2: 43-68.

Zhou, M., and M.E. Huntley 1997. Population dynamics theory of plankton based on biomass spectra. *Marine Ecology Progress Series* 159: 61-73.

Chapter 3

Biomass Spectrum Model

INTRODUCTION

The large body of published work dealing with the size dependence of physiological processes and abundance in planktonic ecosystems constitutes the main foundation for the development of a theory of the biomass size distribution. This chapter presents the derivation of a "general" biomass spectrum model that characterizes the flow of biomass in pelagic ecosystems. The model represents the size distribution of organisms and their interactions in a dynamic and continuous way. The analysis is based on organism size as the main variable, but the separate representation of the phytoplankton and zooplankton communities allows the consideration of population dynamics (trophic interactions) in the analysis of the biomass flow between planktonic organisms. The representation of biomass as a function of size allows the derivation of the phytoplankton and zooplankton spectrums from the biomass spectrum model derived.

BIOMASS SPECTRUM MODEL

Mathematical Description

We first define a mathematical representation for the flow of biomass in the ecosystem based on the biomass concentration within discrete compartments of phytoplankton and zooplankton, organized according to organism size. We then derive a continuous form for the biomass flow within the phytoplankton and zooplankton communities that allows for the derivation of biomass spectra.

We start by defining the phytoplankton biomass spectrum, $\rho(s, t)$, as a function of organism size, s, and time, t. Size is defined as a continuous variable and organisms are classified in size classes of width Δs. The total phytoplankton biomass in the size range $(s, s+\Delta s)$, $P(s, \Delta s, t)$, has units *[mass /length^3]*, and is defined as

(1) $P(s, \Delta s, t) = \rho(s,t)\, \Delta s$, *where Δs is the size class width [length], and $\rho(s, t)$ is the phytoplankton biomass spectrum [mass /length^4]*

An equivalent definition applies to the total zooplankton biomass spectrum, $\zeta(s, t)$, derived from

(2) $Z(s, \Delta s, t) = \zeta(s, t)\, \Delta s$, *where Δs is the size class width [length], and $\zeta(s, t)$ is the zooplankton biomass spectrum [mass /length^4]*

The total phytoplankton biomass in the system, $P_T(t)$, can then be defined by

(3) $P_T(t) = \int \rho(s,t)ds$

Similarly, the total zooplankton biomass in the system, $Z_T(t)$, is defined by

(4) $Z_T(t) = \int \zeta(s,t)ds$

The nutrient concentration, $N(t)$, has no size dependency and is only dependent on time.

As explained in the introduction, the model will represent the trophic interactions within the planktonic community. For this, I start by using the general expressions for a simple *NPZ* (nutrients/phytoplankton/zooplankton) model, described by the general differential equations,

(5) $\frac{dN}{dt}$ = *input + regeneration - uptake*

(6) $\frac{dP}{dt}$ = *growth – grazing - loss*

(7) $\frac{dZ}{dt}$ = *growth – predation - loss*

where N, P and Z represent nutrient concentration, phytoplankton biomass and zooplankton biomass, respectively

The trophic interactions described by this system of coupled differential equations represent those most commonly used in the development of basic plankton models. The regeneration term in the nutrient equation accounts for the recycling of phytoplankton and zooplankton. The loss term in the phytoplankton equation accounts for loss of biomass by means other than grazing, e.g. natural death, respiration, sinking, etc. The predation term in the zooplankton equation accounts for predation from higher trophic level organisms, where as the loss term accounts for losses by mechanisms other than predation, e.g. respiration.

Three compartments can represent the general plankton model: nutrient (*N*), phytoplankton (*P*), and zooplankton (*Z*), as seen in figure 3-1. By defining Q_{ij} as the flux from compartment *i* to compartment *j* , with units [mass/length^3 time], and including size as a variable for phytoplankton and zooplankton, we can represent the mass balance for each of the three

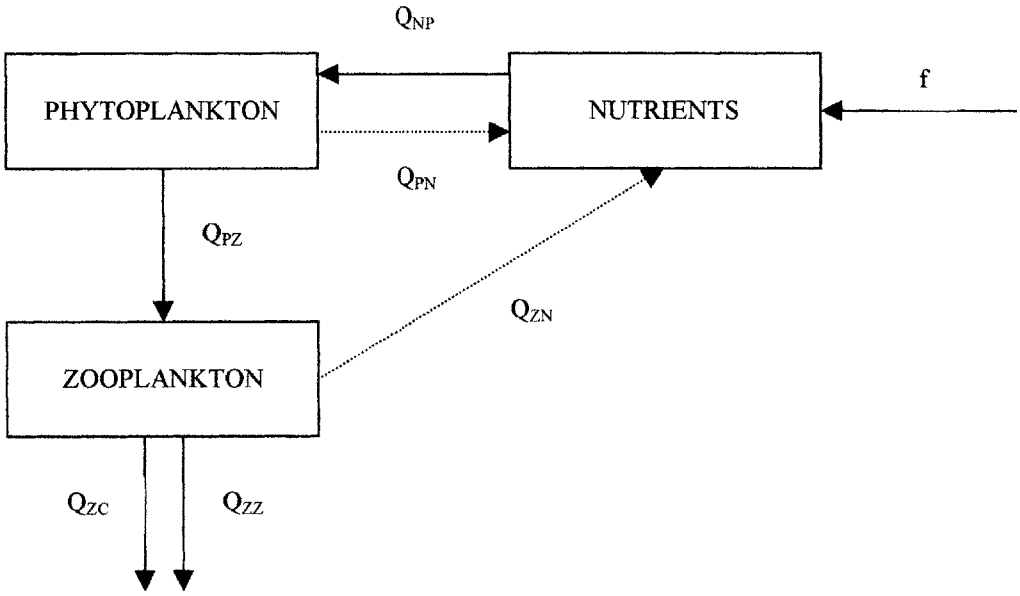

Figure 3-1: "General" biomass spectrum model The compartments ("boxes") in the diagram represent biomass and the arrows represent the flows of biomass from one compartment to another. The phytoplankton and zooplankton compartments represent the continuum of all sizes of phytoplankton and zooplankton. They represent the whole communities and not individual taxa. The nutrient input function, *f*, represents the flow of nutrients into the system from a substrate nutrient source. The nutrient regeneration pathways (for phytoplankton and zooplankton losses) are shown as the dotted lines in the diagram.

compartments in the model. The phytoplankton and zooplankton compartments in figure 3-1 represent the whole phytoplankton and zooplankton communities, respectively, and not particular taxa. Using the biomass flux notation presented in figure 3-1, we can construct a new set of differential equations for the system, where phytoplankton and zooplankton biomass and fluxes are size-dependent. The phytoplankton and zooplankton equations represent their respective biomass in the size range (s, $s+\Delta s$).

(8) $$\frac{dN(t)}{dt} = \phi(t) + Q_{ZN}(t) + Q_{PN}(t) - Q_{NP}(t)$$

(9) $$\frac{\delta(\rho(s, t)\Delta s)}{\delta t} = Q_{NP}(s, \Delta s, t) - Q_{PZ}(s, \Delta s, t) - Q_{PN}(s, \Delta s, t)$$

(10) $$\frac{\delta(\zeta(s', t)\Delta s)}{\delta t} = Q_{PZ}(s', \Delta s', t) + Q_{ZZ}(s', \Delta s', t) - Q_{ZZ}(s', \Delta s', t) - Q_{ZN}(s', \Delta s', t) - Q_{ZC}(s', \Delta s', t)$$

The set of initial conditions $\rho(s, t_o)$, $\zeta(s, t_o)$, *and* $N(t_o)$ needs to be known to analyze the dynamics of the system. We now develop mathematical definitions for the biomass fluxes of the system. Note that the zooplankton equation includes additional terms describing size-based predation (positive and negative) within the zooplankton community. Zooplankton growth is represented by grazing on phytoplankton and by a positive predation term describing the effect of predation on smaller zooplankton. Predation on zooplankton is represented by the traditional closure term (higher predation), and by a negative predation term describing the effect of predation from larger zooplankton. The trophic interactions in the system are based on two main assumptions: all phytoplankton grow by the uptake of nutrient from a common nutrient pool; and all zooplankton graze on all phytoplankton of equivalent or smaller size, and on all smaller zooplankton. This implies that zooplankton grow by the grazing on phytoplankton and the predation on smaller zooplankton, but are at the same time subject to predation from larger zooplankton.

Table 3-1 presents the definition and mathematical representation for all the biomass fluxes in the system. As described above, it is assumed that trophic interactions are dependent on the size of the interacting organisms. The biomass fluxes presented in table 3-1 are determined by functions describing the different metabolic processes involved in the trophic interactions that

Table 3-1: Biomass flux definitions and mathematical representations for the "general" biomass spectrum model. Phytoplankton size is represented by *s* and zooplankton size by *s'*. The sub-indices represent the compartments between which the biomass is being transferred.

Mathematical Representation	Definition
$\phi(t)$	Nutrient input from mixing
$Q_{NP}(t) = \sum_j u(s_j)N(t)\rho(s_j, t)\Delta s$	Nutrient uptake by phytoplankton community
$Q_{PN}(t) = \sum_j \delta_P(s_j)\ \rho(s_j, t)\ \Delta s$	Nutrient input from total phytoplankton community losses
$Q_{ZN}(t) = \sum_i \delta_Z(s_i')\ \zeta(s_i, t)\ \Delta s'$	Nutrient input from total zooplankton community losses
$Q_{NP}(s, \Delta s, t) = u(s)\ N(t)\ \rho(s, t)\ \Delta s$	Growth for phytoplankton of size s
$Q_{PZ}(s, \Delta s, t) = \sum_i g(s, s')\ \rho(s,t)\Delta s\ \zeta(s_i', t)\ \Delta s'$	Total grazing from equivalent or larger zooplankton on phytoplankton of size s
$Q_{PN}(s, \Delta s, t) = \delta_P(s)\ \rho(s, t)\ \Delta s$	Losses (other than grazing) for phytoplankton of size s
$Q_{PZ}(s', \Delta s', t) = \sum_j g(s, s')\ \rho(s_j, t)\Delta s\ \zeta(s', t)\ \Delta s'$	Grazing of zooplankton of size s' on all equivalent or smaller phytoplankton
$Q_{ZZ}(s', \Delta s', t) = \sum_k h(s, s')\ \zeta(s_k, t)\Delta s\ \zeta(s', t)\ \Delta s'$	Predation of zooplankton of size s' on all smaller zooplankton
$Q_{ZZ}'(s', \Delta s', t) = \sum_n h(s', s)\ \zeta(s',t)\Delta s'\ \zeta(s_n, t)\ \Delta s$	Total predation from larger zooplankton on zooplankton of size s'
$Q_{ZN}(s', \Delta s', t) = \delta_z(s')\ \zeta(s', t)\Delta s'$	Losses (other than zooplankton predation) for zooplankton of size s'
$Q_{ZC}(s', \Delta s', t) = c(s')\ \zeta(s', t)\Delta s'$	Losses to higher predation for zooplankton of size s'

characterize the system. The functions' notation and respective descriptions are presented in table 3-2. By substituting the flow terms (table 3-1) in the model equations presented above we obtain general equations for the model based on discrete size classes for the phytoplankton and zooplankton communities,

$$(11)\quad \frac{dN(t)}{dt} = \phi(t) - \sum_j u(s_j)N(t)\rho(s_j, t)\Delta s + \sum_j \delta_P(s_j)\rho(s_j, t)\Delta s + \sum_i \delta_Z(s_i')\zeta(s_i, t)\Delta s'$$

$$(12)\quad \frac{\delta}{\delta t}\rho(s, t)\Delta s = u(s)N(t)\rho(s, t)\Delta s - \sum_i g(s, s')\rho(s,t)\Delta s\zeta(s_i', t)\Delta s' - \delta_P(s)\rho(s, t)\Delta s$$

$$(13)\quad \frac{\delta}{\delta t}\zeta(s', t)\Delta s' = \sum_j g(s, s')\rho(s_j, t)\Delta s\,\zeta(s', t)\,\Delta s' + \sum_k h(s, s')\zeta(s_k, t)\Delta s\,\zeta(s', t)\,\Delta s' -$$

$$\sum_n h(s', s)\zeta(s',t)\Delta s'\,\zeta(s_n, t)\,\Delta s - \delta_z(s')\zeta(s', t)\Delta s' - c(s')\zeta(s', t)\Delta s'$$

To express the model in terms of continuous equations (continuous description of size and biomass flow) we calculate the limits of the equations as Δs and $\Delta s'$ tend to zero. We then obtain a set of three general equations for the model. The integro-differential equations describing the ecosystem dynamics are

Nutrient Equation

$$\frac{dN(t)}{dt} = \phi(t) - \int_{Spmin}^{Spmax} u(s)N(t)\rho(s,t)ds + \int_{Spmin}^{Spmax} \delta_P(s)\rho(s\,t)ds + \int_{Szmin}^{Szmax} \delta_Z(s')\zeta(s,t)ds' \qquad (14)$$

Phytoplankton Equation

$$\frac{\delta\rho(s,t)}{dt} = u(s)N(t)\rho(s, t) - \int_{Szmin(s)}^{Szmax(s)} g(s,s')\rho(s, t)\zeta(s',t)ds' - \delta_P(s)p(s,t) \qquad (15)$$

Zooplankton Equation

$$\frac{\delta\zeta(s,t)}{dt} = \int_{Spmin(s')}^{Spmax(s')} g(s,s')\rho(s,t)\zeta(s',t)ds + \int_{Sz(s')}^{Sz(s')} h(s,s')\zeta(s,t)\zeta(s', t)ds' - \qquad (16)$$

$$\int_{Sz'(s')}^{Sz'(s')} h(s',s')\zeta(s',t)\zeta(s,t)ds - c(s')\zeta(s', t) - \delta_z(s')\zeta(s', t)$$

Table 3-2: Size-dependent metabolic and trophic interaction functions for the system biomass fluxes. Phytoplankton size is represented by *s* and zooplankton size by *s'*.

Notation	Definition
u(s)	nutrient uptake function for phytoplankton of size s
$\delta_P(s)$	loss function for phytoplankton of size s
$\delta_Z(s')$	loss function for zooplankton of size s'
g(s, s')	grazing function for zooplankton of size s' on phytoplankton of size s
h(s, s')	predation function for zooplankton of size s' on zooplankton of size s
h(s', s)	predation function for zooplankton of size s on zooplankton of size s'
c(s')	higher predation (closure term) function on zooplankton of size s'

The limits of the integrals in the system are defined as follows. S_{pmin}, S_{pmax}, S_{zmin}, and S_{zmax} represent the minimum and maximum sizes of phytoplankton and zooplankton present in the ecosystem. $S_{zmin(s)}$ and $S_{zmax(s)}$ represent the minimum and maximum sizes of zooplankton grazing on phytoplankton of size *s*. $S_{pmin(s')}$ and $S_{pmax(s')}$ represent the minimum and maximum sizes of phytoplankton grazed upon by zooplankton of size *s'*. $S_{Z(s')}$ and $S_{Z(s')}$ represent the minimum and maximum sizes of zooplankton subject to predation by zooplankton of size *s'*. $S_{ZZ(s')}$ and $S_{ZZ(s')}$ represent the minimum and maximum sizes of zooplankton preying on zooplankton of size *s'*. The system of integro-differential equations describes an ecosystem in which all trophic interactions are size-dependent. The grazing and predation processes are based on the general assumption that all zooplankton graze on all phytoplankton of equivalent or smaller size, and on all zooplankton of smaller size.

The generality of the biomass spectrum model presented allows the use of either allometric or random encounter models to represent the size dependency in the system (refer to Chapter 3 for a description of both models). Given the size dependent parameters we should in principle be able to solve the system for the steady state spectra, $\rho^*(s,t)$, $\zeta^*(s',t)$. First we need to define functional forms for the biomass fluxes (uptake, grazing, predation and loss) and the metabolic and trophic interaction functions. Then, we continue by establishing the size-dependence by the use of an allometric or random encounter structure. The model equations can then be solved to derive the continuous spectrum for phytoplankton and zooplankton.

To solve for the steady state spectra we set the ordinary and partial derivatives equal to 0 and solve the steady state equations for the steady state conditions for nutrient biomass, N^*, and the spectrum for phytoplankton, $\rho^*(s,t)$, and zooplankton, $\zeta^*(s',t)$. Approximate solutions for the phytoplankton biomass spectra can be chosen. An example can be the use of a hyperbolic function to describe plankton biomass spectra, since numerous scientists sampling geographically diverse waters (Kiefer and Berwald, 1992) have noted hyperbolic distributions for plankton biomass. The coefficients of the distribution function can then be estimated by using a least-squares method.

Distributed Grazing Model

A model of "distributed grazing" was chosen as a special case of interest for analyzing the generation of steady state biomass spectra from the general model described previously. The model consists of multiple phytoplankton size classes and one zooplankton population representative of the total grazing biomass in the system. Hence, size-dependence only applies to phytoplankton biomass and the grazing function for zooplankton. The specifics regarding the grazing distribution will be discussed later in the analysis. Refer to Chapter 4 to review a discussion of the biological relevance of this model, as well as a presentation of different allometric and nutrient enrichment simulation scenarios.

For simplification purposes, I will assume that the phytoplankton community has no losses other than those to the zooplankton community by grazing. I will also assume that the system is closed, i.e. no nutrient input; in other words, the whole system is driven by recycled nutrients. I also introduce the concept of grazing inefficiencies, represented by the use of the function g' in the model. The inefficiencies in the grazing process imply that a fraction of the biomass grazed is not transformed to zooplankton growth but lost in the feeding process. The general integro-differential equations for this system are

$$\frac{dN(t)}{dt} = -\int_{Spmin}^{Spmax} u(s)N(t)\rho(s,t)ds + \delta_Z Z(t) \qquad (17)$$

$$\frac{\delta\rho(s,t)}{dt} = u(s)N(t)\rho(s,t) - g(s)\rho(s,t)Z(t) \qquad (18)$$

$$\frac{dZ(t)}{dt} = \int_{Spmin(s')}^{Spmax(s')} g'(s)\rho(s,t)Z(t)ds - \delta_Z Z(t) \qquad (19)$$

To analyze the system at steady state we set the ordinary and partial derivatives equal to 0, obtaining

$$0 = -\int_{Spmin}^{Spmax} u(s)N(t)\rho(s,t)ds + \delta_Z Z(t) \qquad (20)$$

$$0 = u(s)N(t) - g(s)Z(t) \qquad (21)$$

$$0 = \int_{Spmin(s')}^{Spmax(s')} g'(s)\rho(s,t)ds - \delta_Z \qquad (22)$$

Following the hypothesis presented above that phytoplankton biomass spectra can be derived from the model by assuming approximate solutions of the size structure, I define a hyperbolic spectrum for the size dependent functions in the system.

(23) $u(s) = u_o s^{u1}$

(24) $g(s) = g_o s^{g1}$

(25) $g'(s) = g'_o s^{g'1}$

(26) $\rho(s,t) = \rho_o s^{\rho 1}$

It is assumed that all parameters of the hyperbolic distributions are known, except for those for the phytoplankton biomass spectra function. Substituting the hyperbolic distributions in equations (20), (21) and (22), we obtain a new set of equations characterized by the hyperbolic distributions chosen

$$0 = -\int_{Spmin}^{Spmax} u_o s^{u1} N \rho_o s^{\rho 1} ds + \delta_Z Z \qquad (27)$$

$$0 = u_o s^{u1} N - g_o s^{g1} Z \qquad (28)$$

$$0 = \int_{Spmin(s')}^{Spmax(s')} g'_o s^{g'1} \rho_o s^{\rho 1} ds - \delta_Z \qquad (29)$$

I assume that the hyperbolic coefficients for the phytoplankton growth and zooplankton grazing functions are equivalent ($u_1 = g_1$). This assumption is consistent with observational data and has been used in previous theoretical analysis of plankton biomass distributions (Kiefer and Berwald, 1992). Multiplying equation (28) by s^{-u1} and solving the integrals in equations (27) and (29) we obtain a set of three steady state equations in four unknowns

$$0 = - u_o \rho_o N \frac{s^{\rho 1+u1+1}}{\rho_1+u_1'+1} \Big|_{S_{pmin}}^{S_{pmax}} + \delta_Z Z \qquad (30)$$

$$0 = u_o N - g_o Z \qquad (31)$$

$$0 = g'_o \rho_o \frac{s^{\rho 1+g1'+1}}{\rho_1+g_1'+1} \Big|_{S_{pmin}}^{S_{pmax}} - \delta_Z \qquad (32)$$

Solving equations (30) and (31) for Z and equating them, and then solving the result and equation (32) for δ_Z and equating them, I obtain

$$(g'_o/g_o)[(\rho_1+u_1+1)/(\rho_1+g_1'+1)] = \frac{s^{\rho 1+u1+1}}{s^{\rho 1+g'1+1}} \Big|_{S_{pmin}}^{S_{pmax}} \qquad (33)$$

By defining $a=u_1+1$, $b=\rho_1$, $c= g_1'+$, $G=g'_o/g_o$, $x=S_{pmax}$, *and* $y= S_{pmin}$, and substituting in equation (33), we obtain

$$\frac{X^{a+b} - Y^{a+b}}{X^{c+b} - Y^{c+b}} = G \frac{a+b}{c+b} \qquad (34)$$

Solving for b and calculating the roots of the resulting polynomial we can calculate ρ_1 if u_1, g'_1, g'_o, g_o, S_{pmax}, and S_{pmin}. Once we calculate ρ_1 we substitute it in equation (29) and solve for ρ_o. However, without any further information we can not solve for N and Z.

A similar approach for deriving the steady state phytoplankton biomass spectra consists in using the same steady state conditions, described by equations (27), (28), and (29). If the size-

dependent coefficients for the hyperbolic distributions for growth, grazing, zooplankton growth efficiency are known, and the loss function for zooplankton is given, we can derive the spectra by assuming a given steady state nutrient level. We then solve the system by calculating Z from equation (28) and substituting in the nutrient equation (27) to obtain a system of two equations in two unknowns, ρ_1 and ρ_0. The calculation of the two unknowns completes the derivation of the phytoplankton biomass spectra, under the assumption that it is represented by a hyperbolic distribution. In this case, the assumption of growth equivalent to grazing is not necessary to derive the phytoplankton biomass spectra.

The analysis presented above shows that the "general" biomass spectrum model developed provides a natural way of deriving the phytoplankton biomass spectra from the size-dependent trophic interactions of the ecosystem described. The analysis was carried out for the "distributed grazing" special case but can be extended to the "general" model.

REFERENCES

Kiefer, D.A., and J. Berwald 1992. A random encounter model for the microbial planktonic community. *Limnology and Oceanography* 37(3): 457-467.

Chapter 4

Size-Structured Dynamic Simulation Models

INTRODUCTION

Models of nutrient cycles in the ocean are a very important tool for elucidating short- and long-term patterns in chemical fluxes. This chapter presents a description and simulations for a basic *NPZ* model and a "distributed grazing" size-dependent model. The most basic categorization for ocean systems, and the most widely used (Franks et al .1986; Wroblesky et al. 1988; Evans and Parslow 1985; Steele and Henderson 1992) has three components: nutrients (*N*), phytoplankton (*P*), and grazing zooplankton (*Z*). This model is a simplification of the biomass spectrum model (Chapter 3) with no size-dependence given that the phytoplankton and zooplankton compartments represent their respective communities in their entirety.

The structure of the general biomass spectrum model developed (Chapter 3) allows the inclusion of either allometric or random encounter structures for the size-dependent rate coefficients. The research objectives of the present study lead to the selection of allometric theory for analyzing plankton population dynamics. This chapter presents the description and results of a set of dynamic simulations carried out with a "distributed grazing" (discrete) size-dependent model under different allometric structure and nutrient enrichment scenarios. This alternative model structure consists of multiple phytoplankton size classes and one zooplankton compartment representing the entire herbivore community. Grazing pressure is distributed across phytoplankton size classes according to their relative biomass.

BASIC 'NPZ' MODEL

Background

The incredible complexity of the dynamics of plankton ecosystems limits the number of taxonomic categories that can be feasibly used. The multiple interactions between taxonomic categories in a planktonic food-web results in the need for many parameters, increasing the data requirements and obscuring the mechanisms involved. In general, most models are limited to about seven compartments (Fasham et al. 1990). It is argued that valuable results can still be achieved using very simple systems. The nonlinearity of the dynamics of basic *NPZ* models has made them a model of choice for many scientists interested in studying the dynamics of marine plankton. Simple models such as these have a relatively long history (e.g. Riley, 1946). There has been a recent revival of interest in their study in an attempt to simulate and predict the fluxes of elements such as carbon and nitrogen at regional or global scales (Steele, 1984). The relatively good agreement between models and observations (Steele and Henderson, 1992) is a

measure of the validity of these simple compartment models and of their simplifying assumptions.

General Description

The model consists of three components: nutrients (*N*), phytoplankton (*P*), and grazing zooplankton (*Z*) (figure 4-1). The model is driven by physical processes, such as mixing or upwelling, that introduce nutrients into the system and are closed at the upper level by some loss of zooplankton. In the model, nutrients are regarded as a third variable and are introduced to the system by some physical supply function. The system represented is driven by a single limiting nutrient, *N*.

Mathematical Representation

The biomass flows for the *NPZ* model can be expressed by a system of coupled ordinary differential equations,

(1) $\frac{dN}{dt} = input - uptake + regeneration\ (phytoplankton\ and\ zooplankton)$

(2) $\frac{dP}{dt} = uptake - grazing - losses$

(3) $\frac{dZ}{dt} = growth - losses$

I define functions for the nutrient input, $\phi(t)$, nutrient uptake by phytoplankton, m, phytoplankton grazing by zooplankton, g, and for the phytoplankton and zooplankton losses, δ. The model can then be represented by the following set of three coupled ordinary differential equations,

(4) $\frac{dN}{dt} = \phi(t) - mPN + \delta_P P + \delta_Z Z + (1-\alpha)gPZ$

(5) $\frac{dP}{dt} = mPN - gPZ - \delta_P P$

(6) $\frac{dZ}{dt} = \alpha gPZ - \delta_Z Z$

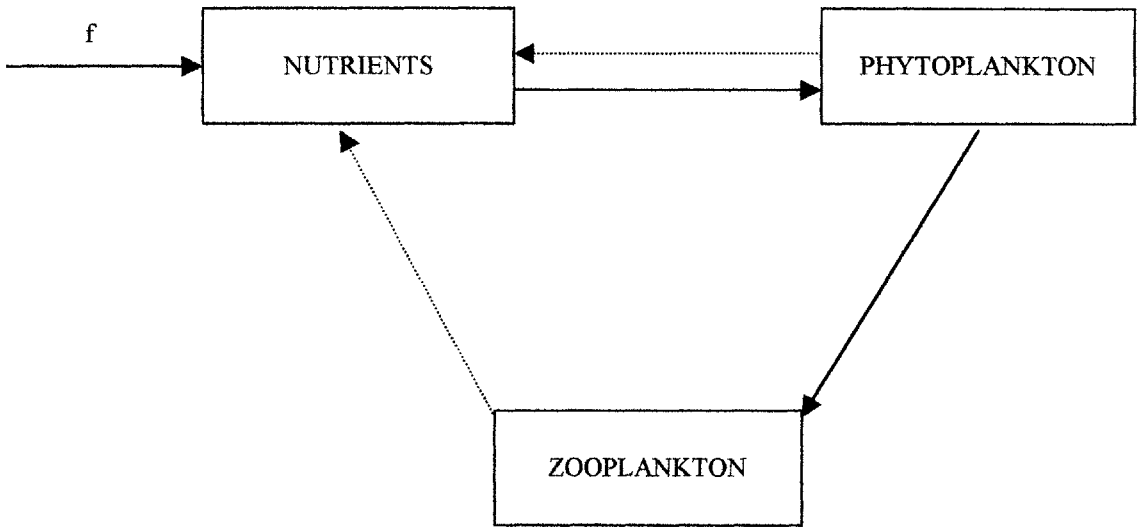

Figure 4-1: Basic NPZ model (modified from Truscott and Brindley, 1994). The compartments ("boxes") in the diagram represent biomass and the arrows represent the flows of biomass from one compartment to another. Nutrients are introduced in the system from a substrate nutrient source, as described by an input function, *f*. Phytoplankton uptake nutrients and are grazed upon by zooplankton. These main biomass flows are represented by the solid arrows. The dotted arrows represent the regeneration of nutrients as a result of phytoplankton and zooplankton losses. It is assumed that all losses are regenerated instantaneously.

where N, P, and Z represent the concentration of nutrients, and the biomass of phytoplankton and zooplankton, and α represents the efficiency of zooplankton grazing. The model assumes the instantaneous regeneration of nutrients through phytoplankton and zooplankton losses and zooplankton grazing inefficiencies. The specifics of the functions for nutrient input (ϕ), phytoplankton uptake/growth (m), zooplankton grazing (g), and loss (δ) are described as follows.

The nutrient input function, ϕ, was specified as in Steele and Henderson (1992), assuming a single 'box' with mixing from a deeper high nutrient source. A Michaelis-Menten function was used to parameterize the effect of nutrient limitation on phytoplankton growth, as well as the grazing of zooplankton on phytoplankton. Linear loss terms for phytoplankton and zooplankton were chosen. The model is then represented by the following set of coupled differential equations,

$$(7) \quad \frac{dN}{dt} = s(N_o - N) - \frac{\mu PN}{k_P+N} + \delta_P P + \delta_Z Z + (1-\alpha)\frac{\alpha \gamma Z P}{k_z+P} .$$

$$(8) \quad \frac{dP}{dt} = \frac{\mu PN}{k_P+N} - \frac{\gamma Z P}{k_Z+P} - \delta_P P$$

$$(9) \quad \frac{dZ}{dt} = \frac{\alpha \gamma Z P}{k_z+P} - \delta_Z Z$$

where μ is the maximum phytoplankton growth rate; k_P is the nutrient concentration at which the (phytoplankton) nutrient uptake velocity is half its maximum value; γ is the maximum grazing rate; k_Z is the half-saturation constant for zooplankton grazing on phytoplankton; and α is the assimilation efficiency for zooplankton grazing. The function describing the input of limiting nutrient to the system (from an outside nutrient source) is described by the rate of mixing for the nutrient supply, s; and by the concentration (at the source) of the limiting nutrient, N_o. Table 4-1 summarizes the variable and parameter definitions and their units. It is assumed that nutrients are regenerated instantly, as seen from the nutrient equation above.

Table 4-1: Variable and parameter definitions and units for the basic plankton model, *NPZ*. Units for the nutrient, phytoplankton and zooplankton biomass are in mmol m^{-3} of an equivalent limiting nutrient (i.e. nitrogen).

Notation	*Description*	*Units*
P, Z	Phytoplankton and zooplankton concentration	mmol m^{-3}
N, N_o	System and supply limiting nutrient concentration	mmol m^{-3}
s	Limiting nutrient supply mixing rate	d^{-1}
μ	Maximum phytoplankton growth rate	d^{-1}
k_p	Half-saturation nutrient concentration for phytoplankton	mmol m^{-3}
δ_p	Intrinsic phytoplankton loss rate	d^{-1}
γ	Maximum zooplankton grazing rate	d^{-1}
α	Zooplankton growth efficiency	dimensionless
k_z	Half-saturation phytoplankton concentration for zooplankton	mmol m^{-3}
δ_z	Intrinsic zooplankton loss rate	d^{-1}

Theoretical Steady State Analysis

The equilibrium solutions of the system are the solutions to the equations,

$$(10) \quad s(N_o - N) - \frac{\mu P N}{k_P + N} + \delta_P P + \delta_Z Z + (1-\alpha)\frac{\alpha \gamma Z P}{k_z + P} = 0,$$

$$(11) \quad \frac{\mu P N}{k_P + N} - \frac{\gamma Z P}{k_Z + P} - \delta_P P = 0,$$

$$(12) \quad \frac{\alpha \gamma Z P}{k_z + P} - \delta_Z Z = 0.$$

We first note that N_o must be less than or equal to N. Otherwise, since α is greater than zero and less than or equal to 1, either P or Z would have to be less than zero, which is biologically inadmissible. This result is consistent with the assumption made by Steele and Henderson (1992). Solving the set of equations we obtain a steady state (equilibrium) solution for the system. The equilibrium solution of biological relevance, (N', P', Z'), is that in which the biomass for nutrients, phytoplankton, and zooplankton is positive (greater than zero).

$$(13) \quad N' = N_o$$

$$(14) \quad P' = \frac{\delta_Z k_Z}{\alpha\gamma - \delta_Z} .$$

$$(15) \quad Z' = \frac{k_Z \alpha (N_o \mu - N_o \delta_P - \delta_P k_P)}{(k_P + N_o)(\alpha\gamma - \delta_Z)} .$$

A detailed analysis of the stability of the equilibrium solutions for a general *NPZ* model is presented in Truscott and Brindley (1994). The analysis is applicable to the model described above. They start by constructing a Jacobian (stability) matrix in order to calculate their eigenvalues and determine the stability of the system by studying their signs. Truscott and Brindley found that the general expression for the characteristic equation of the stability matrix is positive-definite. Therefore, the Routh-Hurwitz[1] conditions are satisfied and the equilibrium solution *(N', P', Z')* is stable.

Simulations

Representative model parameters were chosen from Frost (1987), Fasham et al (1990), Fasham (1993), Ducklow and Fasham (1992), Pahl-Wostl (1997), Steele and Henderson (1992), and Edwards and Brindley (1996). The input of nutrients to the system is assumed to be derived from a deeper high nutrient source, N_o. Following Edwards and Brindley (1996), I choose N_o with a value of 0.6 mmol N m^{-3} and the mixing nutrient rate with a value of 0.05 m d^{-1}. The phytoplankton parameters were chosen from Fasham et al (1990) and Armstrong (1994). The value chosen for the maximum phytoplankton growth, μ was 1.25 d^{-1}. The half-saturation nutrient concentration for phytoplankton, k_p, was chosen to be 0.5 mmol N m^{-3} and the intrinsic phytoplankton loss rate, δ_p, was chosen to be 0.09 d^{-1}. The maximum zooplankton grazing rate, γ, was chosen from Fasham et al (1990) with a value of 1.0 d^{-1}. Following Edwards and Brindley (1996) I use a zooplankton assimilation efficiency, α, of 0.25. Finally, I use the value of 0.05 d^{-1} for the intrinsic zooplankton loss, δ_z, used by Fasham et al (1990). Table 4-2 summarizes the model parameters used for the simulations that follow.

Following Edwards and Brindley (1996), the grazing half-saturation constant, k_z, was chosen as the primary bifurcation parameter. Hence, two different simulation scenarios were developed, with values of 1.0 mmol m^{-3} and 2.0 mmol m^{-3}, as in Fasham et al (1990) and Pahl-Wostl (1997), respectively. For both scenarios, the model equations were solved numerically over time using a Runge-Kutta (4,5) with the set of parameters presented in Table 4-2. Different sets of initial conditions were used and it was found that the steady state biomass concentrations are independent of the initial conditions chosen. This is result is in accordance with the theoretical stability analysis developed by Truscott and Brindley (1994).

[1] Routh-Hurwitz conditions refer to stability conditions based on the analysis of the eigenvalues of the community matrix (Jacobian) of a particular ecosystem.

Table 4-2: Parameter values for the basic plankton model, *NPZ*.

Notation	*Value*	*Units*
N_o	0.6	mmol m^{-3}
s	0.05	d^{-1}
μ	1.25	d^{-1}
k_p	0.5	mmol m^{-3}
δ_p	0.09	d^{-1}
γ	1.0	d^{-1}
α	0.25	dimensionless
k_z	1.0 or 2.0	mmol m^{-3}
δ_z	0.05	d^{-1}

The system was modeled and projected to steady state, and time series and phase portraits for the nutrient, phytoplankton and zooplankton biomass were developed. Using the parameters defined above, I simulate the system from the initial conditions *(N, P, Z) = (0.4, 0.2, 0.1)* to obtain both the time series and the trajectory in *N-P-Z* space of the system (figure 4-2). The system was simulated over a period of 200 days. For the first scenario, $k_z = 1.0$ *mmol* m^{-3}, the nutrient, phytoplankton and zooplankton concentrations settle down to steady state values of *(N', P', Z') = (0.6, 0.25, 0.72)*. The initial large rise in the phytoplankton community is due to the excitable nature of the system.

Phytoplankton bloom as they take up nutrients from the system. The nutrient levels decrease in this process. Zooplankton start grazing on phytoplankton with a delay of about 10 days with respect to the beginning of the phytoplankton bloom. As grazing pressure builds, the phytoplankton biomass starts leveling off and then decreasing. However, as zooplankton grazing saturates, zooplankton biomass starts leveling off and then decreasing. Simultaneously, nutrient levels are increasing due to the external input and regeneration, and to the decreased uptake by phytoplankton. Nutrient levels peak at a certain biomass, time at which the phytoplankton start a new bloom. This process repeats itself, making the system settle to a periodic orbit, or limit cycle, after a relatively short transient time. The oscillations have a period of 35 days which is consistent with observational data and output of large pelagic ecosystem models (Edwards and Brindley, 1996). The cycles are shown in the phase portrait diagram, which shows the decreasing amplitude and eventual settling of the system to the steady state values presented above. The behavior of the system is independent of initial conditions, as expected from the theoretical analysis.

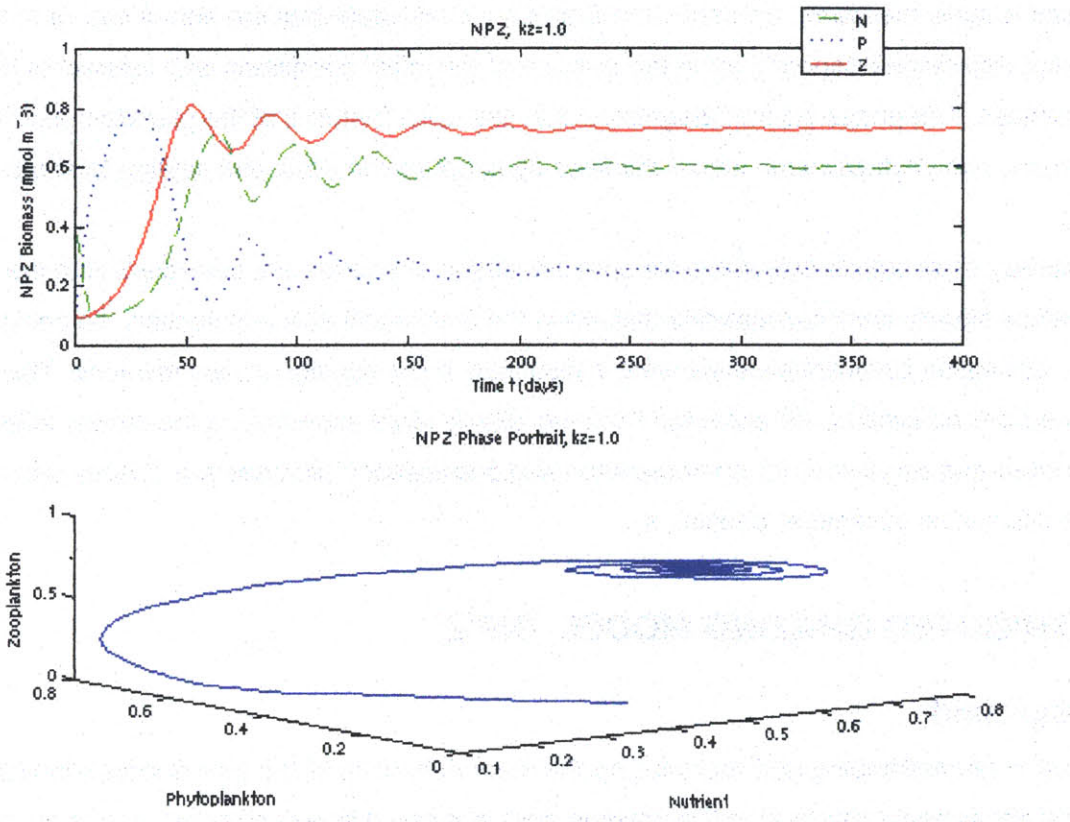

Figure 4-2: Time series and phase space trajectory for NPZ model with k_Z =1.0 mmol m^{-3}. The system settles down to a stable limit cycle and eventually to steady state values of (0.6,0.25,0.72).

Starting from the same set of initial conditions, a second set of simulations was carried out changing the value of the half-saturation constant for zooplankton, k_Z, to the value *2.0 mmol* m^{-3} used by Pahl-Wostl (1997). The system settles down to steady state values of *(N', P', Z') = (0.6,0.5,1.45)* after a transient time of about 80 days (figure 4-3). Again, the behavior and steady state conditions of the system are independent of the initial conditions. Starting from a range of other initial conditions, trajectories converge to the same steady-state and the transient time remains roughly the same. Edwards and Brindley (1996) state that the actual nature of the transient trajectories depends upon the position of the initial conditions with respect to the nullsurfaces. The phase portrait diagram shows the main features of the plankton population dynamics; one phytoplankton bloom followed by zooplankton peak and settling to steady state.

The steady state values calculated for both simulation scenarios are consistent with the theoretical steady state expressions derived in the theoretical analysis section. To compare them, simulation parameter values were substituted in the equilibrium expressions. The results obtained are equivalent. As expected from the steady state expressions the steady state values (estimated and simulated) for phytoplankton and zooplankton biomass are directly proportional to the bifurcation parameter chosen, k_Z.

DISTRIBUTED GRAZING MODEL, 'NP^{i}Z'

Background

Interest in understanding and reproducing the main dynamics of the size distribution features of pelagic ecosystems has lead to the development of many different size-dependent modeling approaches. Armstrong (1994) developed a model of independent parallel food chains where each pair of phytoplankton and zooplankton represented a different size class. Parameter values for the different size classes were taken to vary allometrically with size, with smaller size classes growing more rapidly and being consumed more rapidly by their respective zooplankton grazers. The model produced the pattern of "equal biomass in equal logarithmic size classes" (Chisholm, 1992). However, the simple model of parallel food chains was found to have several undesirable properties when used to model time-series data (Armstrong, 1998). The model was found to be effective at describing steady state conditions but inadequate at fitting non-steady state data.

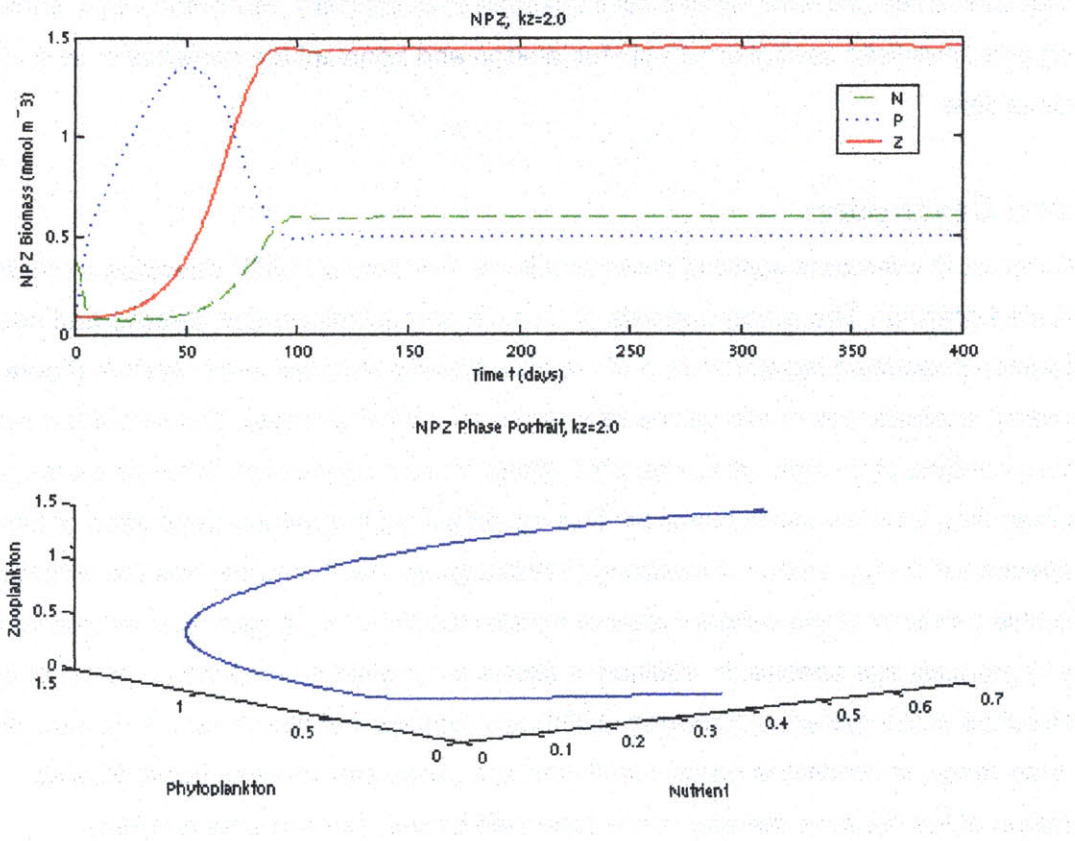

Figure 4-3: Time series and phase space trajectory for NPZ model with k_Z =2.0 mmol m^{-3}. After one phytoplankton bloom, the system settles down to steady state values of (0.6,0.5,1.45).

Generalizations of this model have been developed by allowing zooplankton predation on smaller zooplankton size classes and on all equivalent and smaller phytoplankton size classes (Armstrong, 1994; Moloney and Field, 1991; Moloney et al., 1991). The added food web complexity makes the model structure much more realistic, as it is representative of a much wider set of ecosystem dynamics. However, the added complexity results in very high sensitivity to the choices of parameter values and food web structure. In addition, these more complex food web structures are often dynamically unstable in biologically unrealistic ways, showing striking and unrealistic oscillations in phytoplankton and zooplankton densities in very short periods of time.

General Description

In an attempt to overcome some of these problems, Armstrong (1998) develops a model of "distributed grazing". The model consists of multiple phytoplankton size classes and one zooplankton population representative of the total grazing biomass in the system (figure 4-4). In the present analysis, this model will be referred to as the NP^iZ model. The NP^iZ food web structure consists of multiple (discrete) phytoplankton size classes and a single state variable, Z, representing total herbivore biomass. This model allows the natural generation of biomass size spectra for phytoplankton. Armstrong (1998) argues that the model has the simplicity and predictable behavior of the simple model of parallel food chains, in particular as related to its ability to produce size spectra. In addition, it allows a dynamic representation of the changes of size structure in the system. Armstrong (1998) also argues that the system is dynamically stable for a wide range of conditions (initial conditions and parameter values). For a detailed description of the dynamic stability of this food web model, see Armstrong (1998).

In this model, grazing intensity among size classes is distributed in response to changes in phytoplankton densities. The grazing model is qualitatively similar to the switching grazer model used by Fasham et al. 1990 to distribute zooplankton grazing among bacteria, phytoplankton and detritus. However, in this case, size-specific grazing is modeled as a community level phenomenon rather than as the switching among prey types of a single zooplankton species (Armstrong 1998). In addition, the state variable Z represents the biomass of the entire grazing community and not the abundance of a single species.

The potential grazing is distributed among phytoplankton size classes in proportion to their current abundance, allowing size classes that are currently in lower abundance to bloom while

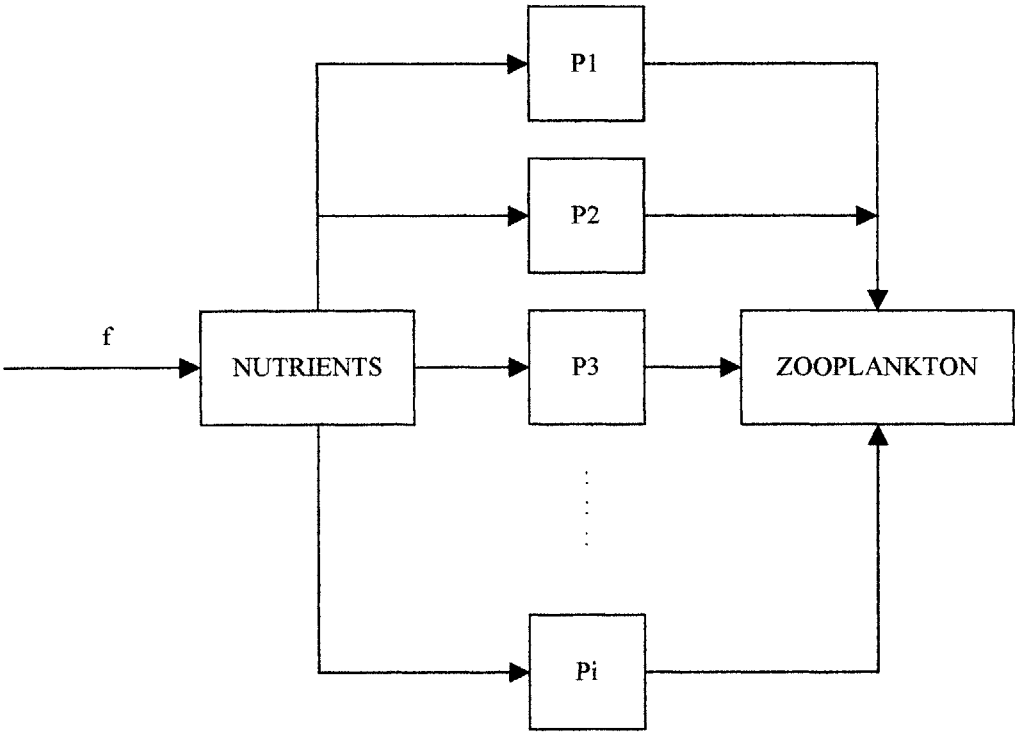

Figure 4-4: Distributed grazing model (modified from Armstrong, 1998). The compartments ("boxes") in the diagram represent biomass and the arrows represent the flows of biomass from one compartment to another. The phytoplankton community is divided in multiple discrete size classes, P_i. The zooplankton community grazes on all phytoplankton size classes, and these in turn grow by the uptake of nutrients from the system. The nutrient input function, f, represents the flow of nutrients into the system from a substrate nutrient source. The nutrient regeneration pathways (for phytoplankton and zooplankton losses) are omitted for simplicity.

size classes that are currently dominant are not blooming (Armstrong 1998). The distribution of grazing based on relative phytoplankton biomass recovers some of the complexity and realism "lost" by the inclusion of the entire grazing community in one state variable, *Z*. The distribution of grazing relative to the phytoplankton biomass at different size classes is quantitatively represented (mathematically) using the grazing model of Fasham et al. (1990). Armstrong (1998) introduces a lag in then redistribution of grazing (as phytoplankton densities change) which is not considered in the present analysis.

The size-dependence of the phytoplankton community is determined by imposing an allometric structure on the phytoplankton metabolic rates. For present purposes, maximum phytoplankton growth rate is selected as the parameter of choice for determining the allometric structure of the model. The different structures selected are described in the simulations section.

Mathematical Representation

The model is described by a set of *n* coupled differential equations,

$$(16) \quad \frac{dN}{dt} = \phi(t) - \sum m_i P_i N + \sum \delta_{Pi} P_i + \delta_Z Z + (1-\alpha)\sum g_i P_i Z$$

$$(17) \quad \frac{dP_i}{dt} = m_i P_i N - g_i P_i Z - \delta_{Pi} P_i$$

$$(18) \quad \frac{dZ}{dt} = \sum \alpha g_i P_i Z - \delta_Z Z$$

where N, P_i, and Z represent the biomass of nutrients, phytoplankton in each size class i and zooplankton. The specifics of the functions for nutrient input (ϕ), phytoplankton uptake/growth (m), zooplankton grazing (g), and loss (δ) will be described in the simulations section.

One of the main problems that arises for the use of this model is the definition of a grazing function for the zooplankton community. It is argued that grazing should be distributed among phytoplankton size classes in proportion to their abundance, so that the zooplankton community exert more grazing on the most readily available food source. In particular, grazing should be distributed so that it changes dynamically as a function of the relative proportion of biomass in the different phytoplankton size classes. Following Fasham et al 1990, I define weighted preferences ρ_i for each of the phytoplankton size classes in the model, of the form

(19) $\rho_i' = \frac{\rho_i P_i}{\sum \rho_j P_j}$, *where ρ_i is the nominal preference for P_i*

Nominal preferences are defined as the grazing preferences for the different phytoplankton size classes when they are equally abundant. The use of this grazing model will guarantee that the zooplankton community will actively select the most abundant phytoplankton size class. Grazing was parameterized using a Michaelis-Menten model; and defining *PT* as the total phytoplankton biomass available for grazing in the system ($PT = \sum \rho_j P_j$), we obtain

(20) $g_i = \frac{\alpha \gamma Z \rho_i' P_i}{k_z + PT}$, *where γ is the maximum specific grazing rate, and kz is the half-saturation constant for grazing*

Substitution of the expression for the weighted preferences in the grazing function yields

(21) $\Gamma_i = \frac{\alpha \gamma Z \rho_i P_i^2}{k_z(\sum \rho_j P_j) + \sum \rho_j P_j^2}$, *where γ_i represents the grazing of Z on P_i*

I assume no grazing preference when the biomass of phytoplankton from different size classes is equal. Hence, the grazing distribution is solely determined by the relative concentrations of phytoplankton size classes and is represented by

(22) $\Gamma_i = \frac{\alpha \gamma_i Z P_i^2}{k_z(\sum P_j) + \sum P_j^2}$.

Using a Michaelis-Menten function to parameterize the effect of nutrient limitation on phytoplankton growth, and linear loss terms for phytoplankton and zooplankton, the model is represented by the following set of coupled differential equations,

(23) $\frac{dN}{dt} = s(N_o - N) - \sum \frac{\mu_i P_i N}{k_{Pi} + N} + \sum \delta_{Pi} P_i + \delta_Z Z + (1-\alpha) \sum \frac{\alpha \gamma_i Z P_i^2}{k_z(\sum P_j) + \sum P_j^2}$.

(24) $\frac{dP_i}{dt} = \frac{\mu_i P_i N}{k_{Pi} + N} - \frac{\gamma_i Z P_i^2}{k_z(\sum P_j) + \sum P_j^2} - \delta_{Pi} P_i$

(25) $\frac{dZ}{dt} = \sum \frac{\alpha \gamma_i Z P_i^2}{k_z(\sum P_j) + \sum P_j^2} - \delta_Z Z$

where μ_i is the maximum phytoplankton growth rate for size class i, k_{Pi} is the half-saturation constant for phytoplankton of size class i, s is the mixing rate of nutrients, N_o is the substrate nutrient concentration, and α is the assimilation efficiency for zooplankton grazing. Table 4-3 summarizes the variable and parameter definitions and their units. It is assumed that nutrients are regenerated instantly, as seen from the nutrient equation above.

The phytoplankton parameters are specified by means of allometric relations among phytoplankton based on different size classes. Following Armstrong (1994) I use an allometric model of the form $R_i = R_o(L_i / L_o)^{\beta_R}$, that relates a rate constant, R_i, for phytoplankton of size class i, to a corresponding constant, R_o, for a reference phytoplankton size class. L_i and L_o are the nominal sizes for phytoplankton of size class i and reference. β_R represents the allometric constant for rate constant R.

Table 4-3: Variable and parameter definitions and units for the "distributed grazing" model. Units for the nutrient, phytoplankton and zooplankton biomass are in mmol m^{-3} of an equivalent nutrient (i.e. nitrogen).

Notation	*Description*	*Units*
P, Z	Phytoplankton and zooplankton concentration	mmol m^{-3}
N, N_o	System and substrate nutrient concentration	mmol m^{-3}
s	Substrate mixing rate with system	d^{-1}
μ	Maximum phytoplankton growth rate	d^{-1}
k_p	Half-saturation nutrient concentration for phytoplankton	mmol m^{-3}
δ_p	Intrinsic phytoplankton loss rate	d^{-1}
γ	Maximum zooplankton grazing rate	d^{-1}
α	Zooplankton growth efficiency	dimensionless
k_z	Half-saturation phytoplankton concentration for zooplankton	mmol m^{-3}
δ_z	Intrinsic zooplankton loss rate	d^{-1}
β_r	Allometric constant for rate process r	dimensionless

Simulations

I begin by dividing the phytoplankton size spectrum into discrete size classes. For calculation of the phytoplankton rates, I take the smallest phytoplankton size class as the reference class. Moloney and Field (1991) define phytoplankton size classes that are of equal width on a logarithmic scale. Hence, following Armstrong (1994) I define size classes so that the nominal size of phytoplankton in adjacent size classes differs by a factor of four. The upper limit of the

smallest phytoplankton size class is chosen to be 2μm and its corresponding nominal size to be 1μm . Accordingly, the upper limits of the additional four phytoplankton size classes are 8μm, 32μm, 128μm, and 512μm. And their corresponding nominal size classes are 4μm, 16μm, 64μm, and 256μm. The widths of the five phytoplankton size classes are 2μm, 6μm, 24μm, 96μm, and 384 μm, respectively. By this process we have discretized the phytoplankton community into five separate size classes, covering a spectrum of size between 0 and 512μm. Phytoplankton range in size from ~0.6 to ~500 microns in diameter, so our five phytoplankton size classes cover the complete range of phytoplankton size, as intended.

Representative model parameters were chosen from Moloney and Field (1991), Armstrong (1994), Fasham et al. (1990), Ducklow and Fasham (1992), Frost and Franzen (1992), and Edwards and Brindley (1996). The input of nutrients to the system is assumed to be derived from a deeper high nutrient source, N_o. Following Edwards and Brindley (1996), I choose N_o to be 0.6 mmol N m^{-3} and the mixing nutrient rate to be 0.05 m d^{-1}. Zooplankton parameter values of $\gamma = 1.0\ d^{-1}$, $k_Z = 1.0\ mmol\ N\ m^{-3}$, and $\delta_Z = 0.05\ d^{-1}$ were taken from Fasham et al (1990) and Ducklow and Fasham (1992).

For the phytoplankton community, I assume that the only size-dependent parameter is the maximum phytoplankton growth rate (Armstrong, 1994). Moloney and Field (1991) include size dependence for the half-saturation constants and loss rates for phytoplankton. However, their constancy will suffice for the purpose of the present analysis. Values of $k_P = 0.1\ mmol\ N\ m^{-3}$ and $\delta_P = 0.016\ d^{-1}$ were chosen from Armstrong (1994) and were taken to be constant across all five phytoplankton size classes. Maximum phytoplankton growth rate for the reference (smallest) size class was taken as $\mu_i = 1.4\ d^{-1}$. The allometric coefficient for the maximum phytoplankton growth rate was allowed to vary across cases.

I start by carrying out simulations for a reference case in which there is no size-dependency for the maximum growth rate, $\beta_\mu = 0$. I then used a value $\beta_\mu = -0.75$, as in Moloney and Field (1991), Armstrong (1994) and Chisholm (1992). This value for the allometric coefficient is the most used in size-dependent models for phytoplankton maximum growth rate, and will be referred to as the "traditional" case. The third case is representative of a phytoplankton community in which larger size classes are comprised mostly of diatoms. Maximum phytoplankton growth rate declines less fast within taxa than across taxa, so the allometric

exponent for a community composed of the same type of phytoplankton should be less negative. Following Armstrong (1994) I use $\beta_\mu = -0.4$. This case will be referred to as the "diatom" case.

I also study a fourth case based on the fact that in some planktonic communities the maximum growth rate increases with size instead of decreasing, as it is normally assumed (Chisholm, 1992). For this case I use $\beta_\mu = 0.125$ so that the maximum growth rate for the larger size class is 2.8 d^{-1}. The allometric structure was chosen to represent a system composed mainly of cyanobacteria and diatoms. '*Synechococcus*', a class of cyanobacteria, are tiny organisms (~1 micron) whose maximum growth rates are around 1.5 d^{-1}. They represent the smaller size classes in the system. Diatoms represent the larger size classes in the system and have growth rates of around 2.5 d^{-1}. The allometric structure chosen produces maximum growth rates ranging in value from 1.4 to 2.8 d^{-1}, appropriate for the system described. This case will be referred to as the "positive slope" case. Finally, I analyze the potential of the model for use in the study of nutrient enrichment processes. For this purpose, I study the effects on the system dynamics of pulse and press perturbations for the "diatom" ($\beta_\mu = -0.4$) and the "positive slope" ($\beta_\mu = 0.125$) cases.

For each of the eight different scenarios, the model equations were solved numerically over time using a Runge-Kutta (4,5) with the set of parameters described above. I used the same initial conditions as in the simulations for the basic NPZ model. Different sets of initial conditions were used and it was found that except for some ranges of biomass that lead to unrealistic oscillations, steady-state biomass concentrations are independent of the initial conditions chosen. This is result is in accordance with the stability analysis carried out by Armstrong (1998) in which he concludes that the system is dynamically stable under a wide range of conditions. In particular it was found that the resulting phytoplankton size distribution is not affected by their initial biomass distribution.

The system was modeled and projected to steady state, and time-series for the nutrient, phytoplankton and zooplankton biomass were developed. At steady state, size spectra were constructed to study the resulting size structure of the ecosystem under the different scenarios. For the perturbation cases, I modeled the transient size structure of the system from the moment of the perturbation to the time of settling to steady state. This analysis may prove to be

very helpful in the study of micronutrient[2] enrichment processes, such as iron fertilization. In these processes, models such as the one presented here may be used to predict the community response, in terms of species composition and size distribution, to the addition of micronutrients to the system.

"Size-Independent" Simulation

Consider first the case with no size-dependence for the maximum phytoplankton growth rate. In this case, the five phytoplankton size classes are dynamically equivalent since they are subject to the same growth (nutrient uptake), grazing, and loss rates. Hence, all phytoplankton size classes settle to the same steady state values. In particular, the steady state biomass for each phytoplankton size class is consistent with the theoretical steady state representation derived for the basic *NPZ* model ($P^s_i = \delta_Z k_Z / \alpha\gamma$). Since I used the same parameters for the zooplankton community here as I did for the *NPZ* model, the phytoplankton steady state concentrations have the same value of *0.25 mmol* m^{-3}. Time-series for the biomass concentrations of the phytoplankton size classes, as well as cumulative biomass distributions are presented in figure 4-5. Cumulative distributions are presented to illustrate the individual contribution to total system biomass of each phytoplankton size class and of the zooplankton community, as in Armstrong (1994). From the time-series data we observe that the system has a transient time (time for settling to steady-state) of about 400 days. We also observe that the total phytoplankton biomass supported by the system at steady-state is of *1.25 mmol* m^{-3}. The nutrient biomass is *~0.01 mmol* m^{-3} and the total ecosystem biomass (including the zooplankton community) at steady state is *~1.84 mmol* m^{-3}.

Biomass spectra for the phytoplankton community at steady-state are developed as synoptic images of the size structure of the taxon-independent system under consideration. The unnormalized biomass spectrum is obtained by plotting the phytoplankton biomass for each size class against their respective size ranges.

The normalized spectrum is obtained by following the framework presented by Platt and Denman (1978) [$\beta(w) = b(w)/\Delta w$, where $b(w)$ is the biomass in a certain weight/size class, w, and Δw is the width of the weight/size class]. As shown in figure 4-6, the unnormalized spectra is flat, since there is no size-dependence. The normalized spectra is presented in figure 4-7.

[2] 'Micronutrients' are nutrients typically required by organisms in relatively small quantities in order to grow and reproduce .

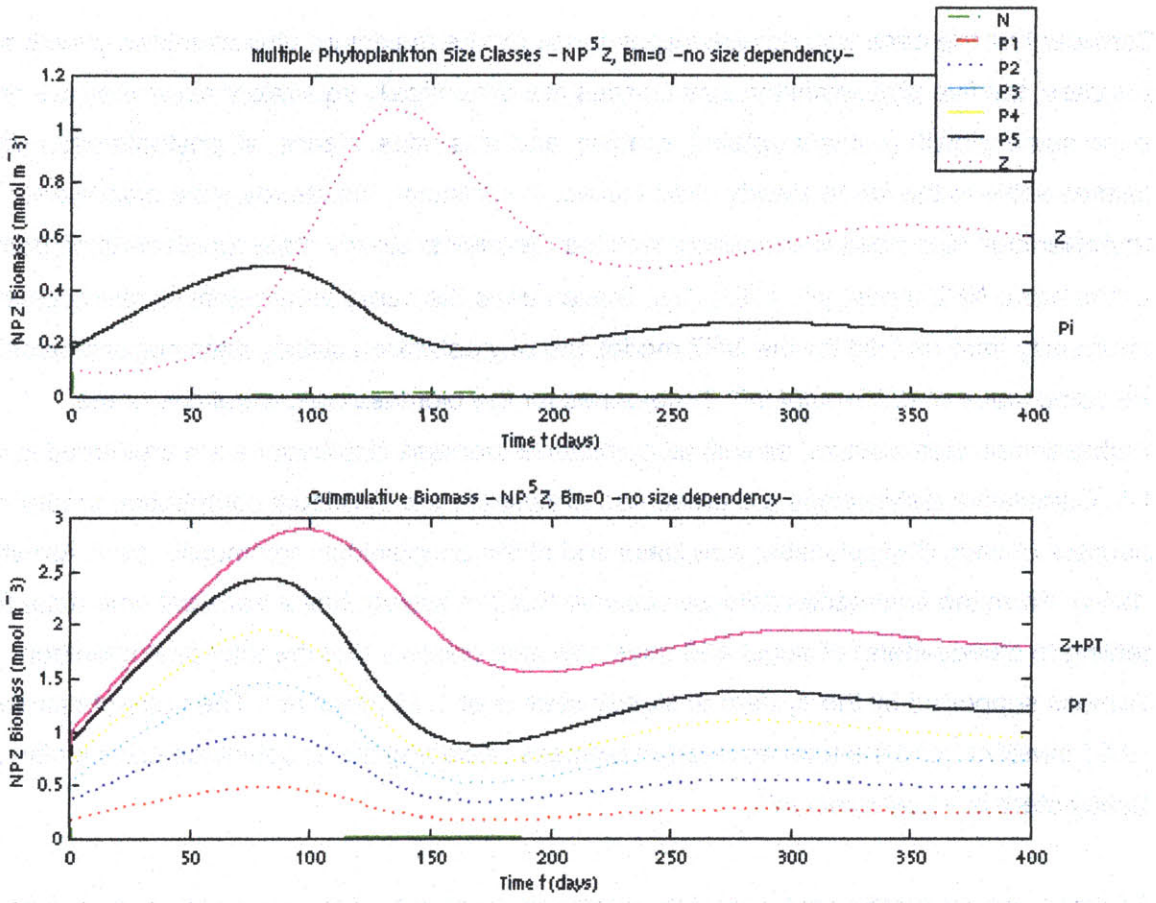

Figure 4-5: Time-series data for individual and cumulative biomass distributions for the "size-independent" simulation. P_i in the individual time-series graph represents all five phytoplankton size classes, since they are dynamically equivalent.

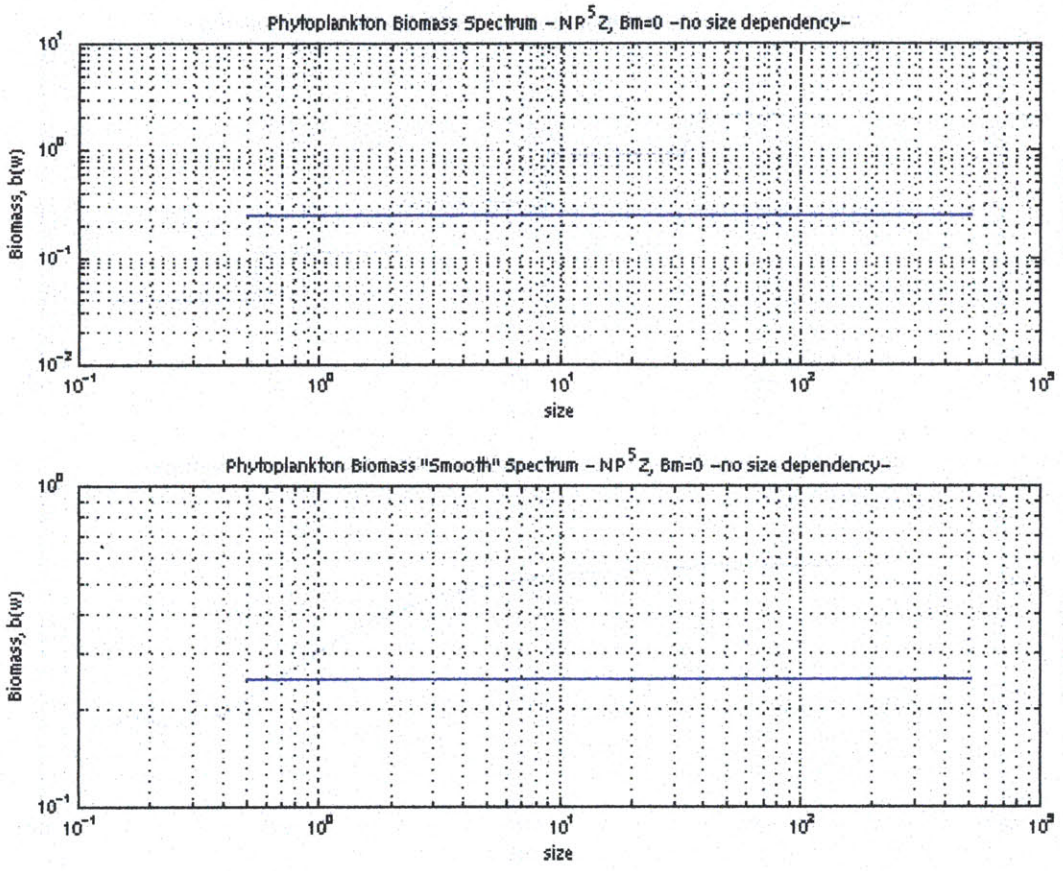

Figure 4-6: Unnormalized steady state spectra for "size-independent" simulation. The no size-dependency of maximum phytoplankton growth rate determines the flat shape of the spectra. Steady state biomass concentrations are equal in all phytoplankton size classes.

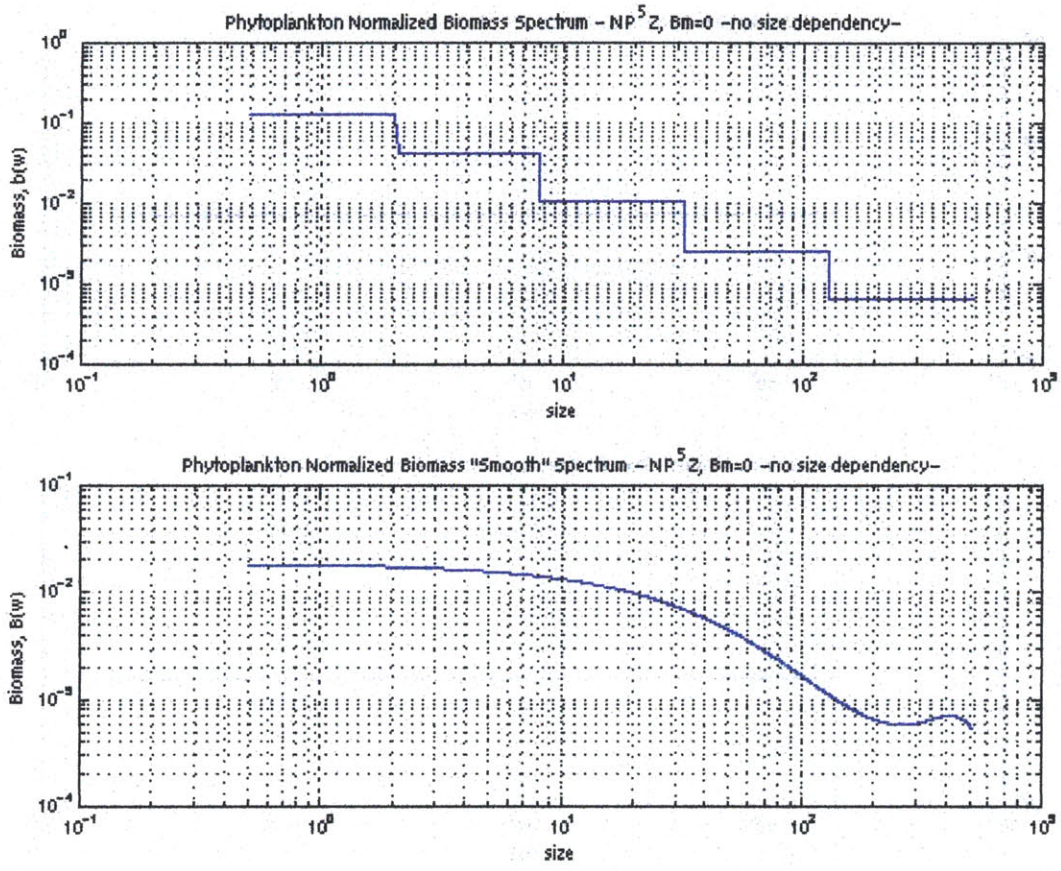

Figure 4-7: Normalized steady state spectra for "size-independent" simulation. The normalization (by size class width) is responsible for the uniformly declining shape of the spectra. Biomass in each size class is equal but size class width increases with size, so the normalized biomass decreases with size.

For both cases, an approximation ("smooth" spectrum) was developed using a third power logarithmic model that, although not very exact, produces the main features of the size distribution depicted in the biomass spectrums (unnormalized and normalized). The biomass spectrum slopes for the phytoplankton community can be derived as follows

$b(w_i)/b(w_o) = (w_i/w_o)^x$, *where x is the unnormalized b.s slope*

$\beta(w_i)/\beta(w_o) = (w_i/w_o)^{xn}$, *where x_n is the normalized b.s slope*

The biomass spectrum slope has been given considerable attention in theoretical studies of planktonic size spectra. In idealized form, the slope of the normalized spectrum allows one to infer the relative contribution of small and large sized cells to total biomass (Kent 1999). Using the steady state data generated by the model simulation, I obtain $x = 0$, and $x_n = -0.95$. The slope of the unnormalized spectrum is zero given the no size-dependency condition of this first case. The normalized spectrum slope, however, is similar to the slope of actual biomass spectra (i.e., close to –1) (Cavender-Bares, 1999).

"Traditional" Simulation, $\beta_\mu = -0.75$

The "traditional" simulation is representative of the most commonly used allometric structure in the size-dependent models literature. This value for the allometric coefficient was determined following Chisholm (1992), and Moloney and Field (1991). Figure 4-8 shows the relationship between maximum phytoplankton growth rate and size of the organism for this allometric structure.

Time-series for the biomass concentrations of the phytoplankton size classes, as well as cumulative biomass distributions are presented in figure 4-9. From the time-series data, we observe that the system has a transient time of about 160 days, much shorter than that estimated for the model with no size-dependence. As a result of the allometric structure chosen, smaller phytoplankton size classes have a clear competitive advantage over larger phytoplankton organisms. This advantage comes from the decreasing magnitude of uptake/growth rates as we move from smaller to larger cells. Independent of the set of initial conditions chosen, the system settles to steady state, with the smaller three phytoplankton size classes surviving and the larger two going extinct after a certain period of time. For the parameters chosen, these two larger size classes remain in the system for an extended period of time but ultimately decay to extinction.

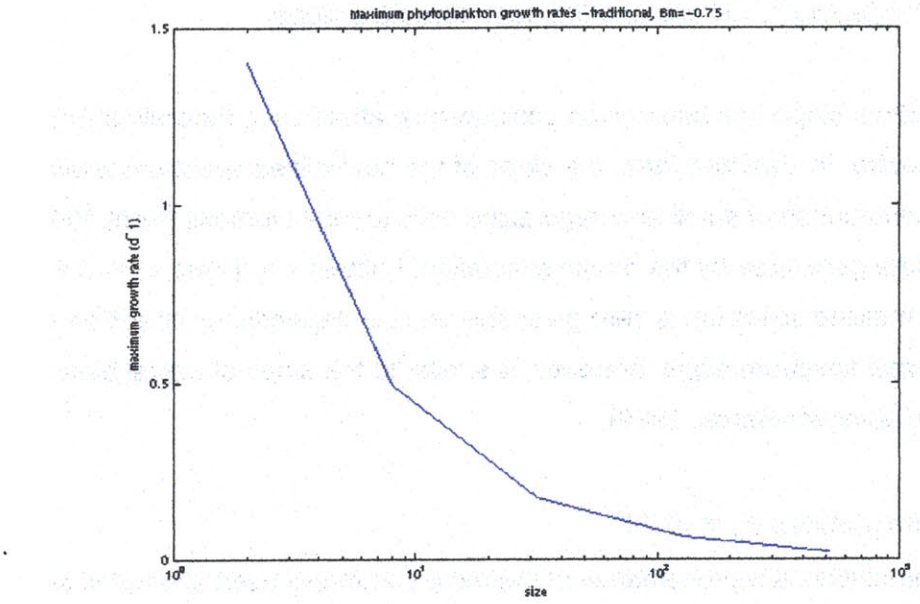

Figure 4-8: Maximum phytoplankton growth rates as a function of size for the "traditional" simulation. The graph displays a continuous representation of the maximum growth rate. The maximum growth rate data used for the model simulations is discrete.

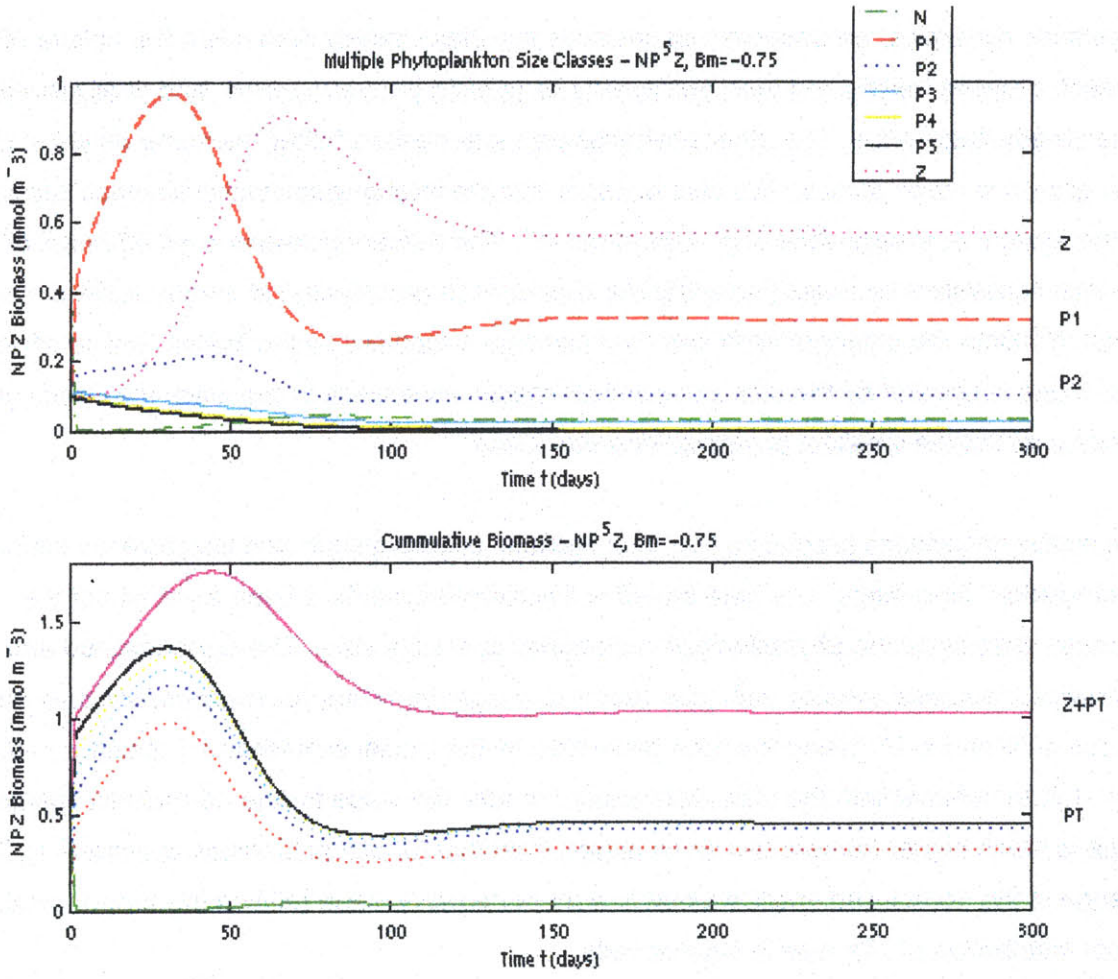

Figure 4-9: Time-series data for individual and cumulative biomass distributions for the "traditional" simulation. Graphs show the clear dominance of the two smallest phytoplankton size classes at all times during the simulation.

The cumulative biomass time-series clearly shows that the smallest phytoplankton size class is the main contributor to phytoplankton biomass. The distribution presented in the cumulative biomass time-series at steady-state is very similar to that obtained by Armstrong (1994) in his independent food chain (steady-state) model. One advantage of the present approach is the ability to display the temporal dynamics of the system. This is particularly relevant to study the short-term dynamics of the system before it settles to steady-state. By analyzing the short-term population dynamics, we observe that smallest size class clearly dominates the uptake of nutrient, growing rapidly and then decreasing as grazing pressure builds, and finally leveling off to its steady-state value. The other phytoplankton size classes follow the same dynamic but their growth is much smaller. We also observe that the total phytoplankton biomass supported by the system at steady-state is of *0.44 mmol* m^{-3}. The nutrient biomass is *~0.03 mmol* m^{-3} and the total ecosystem biomass (including the zooplankton community) at steady state is *~1.01 mmol* m^{-3}. Both the phytoplankton and total biomass supported by the system are much lower than those supported by the size-independent model, as a result of the lower maximum growth rates for all but the smallest phytoplankton size class.

The model simulations produce a matrix of nutrient, phytoplankton and zooplankton biomass at *n* "simulation" time-steps. The data stored in the biomass matrix is used to construct the biomass spectra for the phytoplankton community at steady state. The unnormalized and normalized biomass spectra, with their respective logarithmic approximations, are presented in figures 4-10 and 4-11. Using the data generated by the model simulations, I obtain $x = -0.9$, and $x_n = -1.8$. In contrast with the size-independent model, the value for the normalized spectrum slope is much higher (almost two times larger) than that for actual biomass spectra (–1). The change in the normalized spectra slope to a more negative value reflects the proportionally larger distribution of biomass in smaller cells.

"Diatom" Simulation, $\beta_\mu = -0.4$

The "diatom" simulation is representative of a system in which larger phytoplankton size classes are comprised mostly of diatoms. Following Armstrong (1994), I choose the value *–0.4* for the allometric coefficient. The relationship between maximum phytoplankton growth rate and size of the organism is shown in figure 4-12.

Time-series data for the biomass concentrations of the phytoplankton size classes, as well as cumulative biomass distributions are presented in figure 4-13. Using the same set of initial

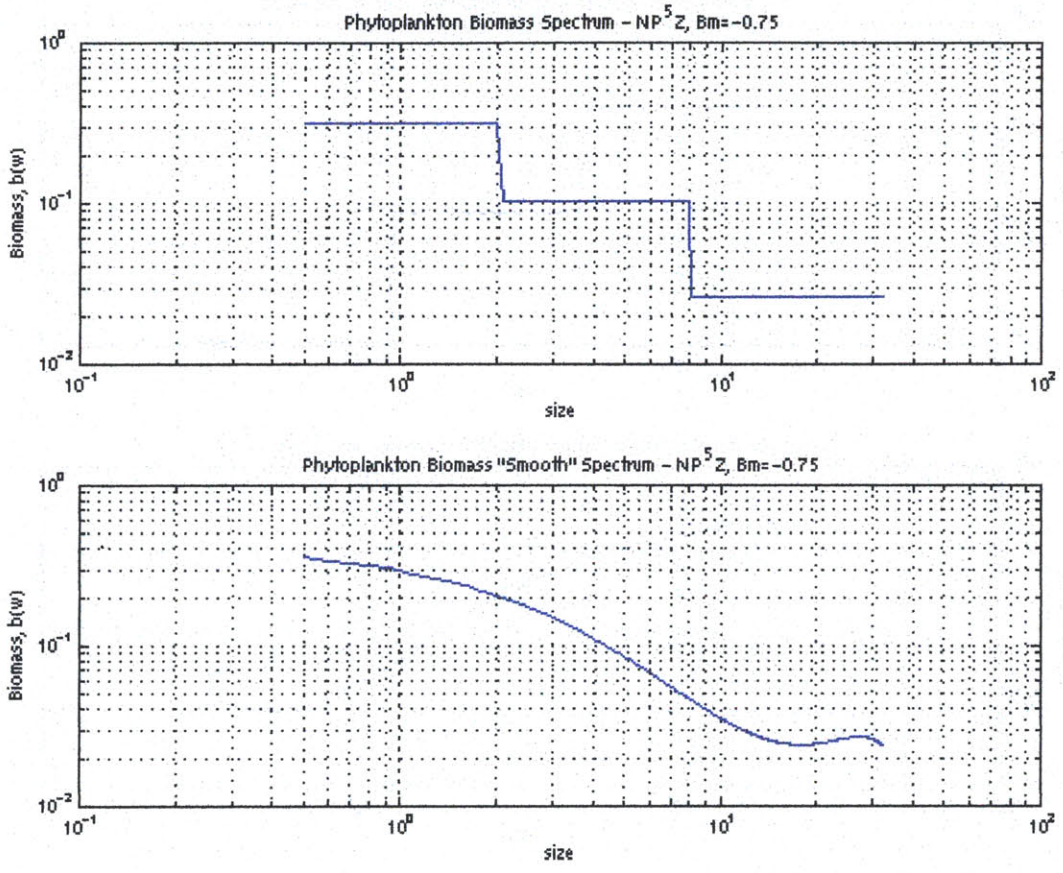

Figure 4-10: Unnormalized steady state spectra for the "traditional" simulation. The spectra shows that only the three smaller phytoplankton size classes are present at steady state. Phytoplankton biomass is inversely proportional to size as a result of the allometric structure chosen.

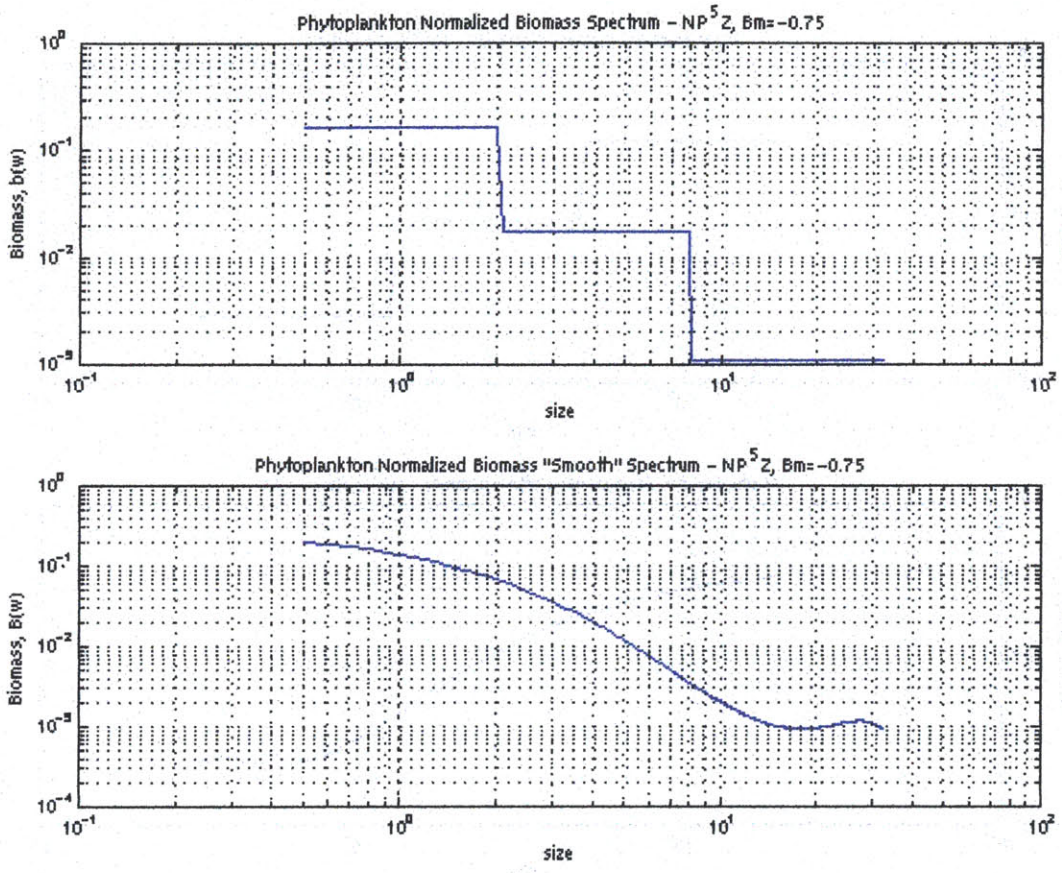

Figure 4-11: Normalized steady state spectra for the "traditional" simulation. The normalization is responsible for the decrease (more negative) in biomass spectra slope.

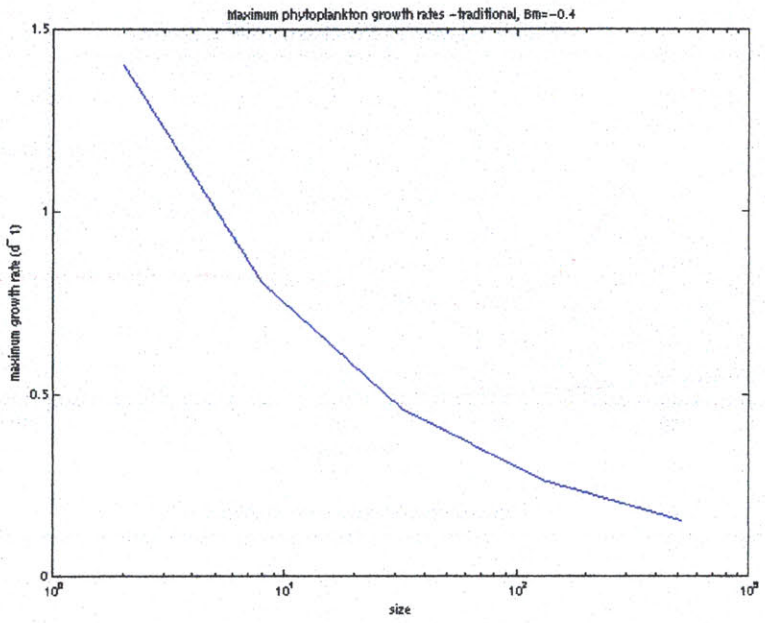

Figure 4-12: Maximum phytoplankton growth rates as a function of size for the "diatom" simulation. The graph displays a continuous representation of the maximum growth rate. The maximum growth rate data used for the model simulations is discrete.

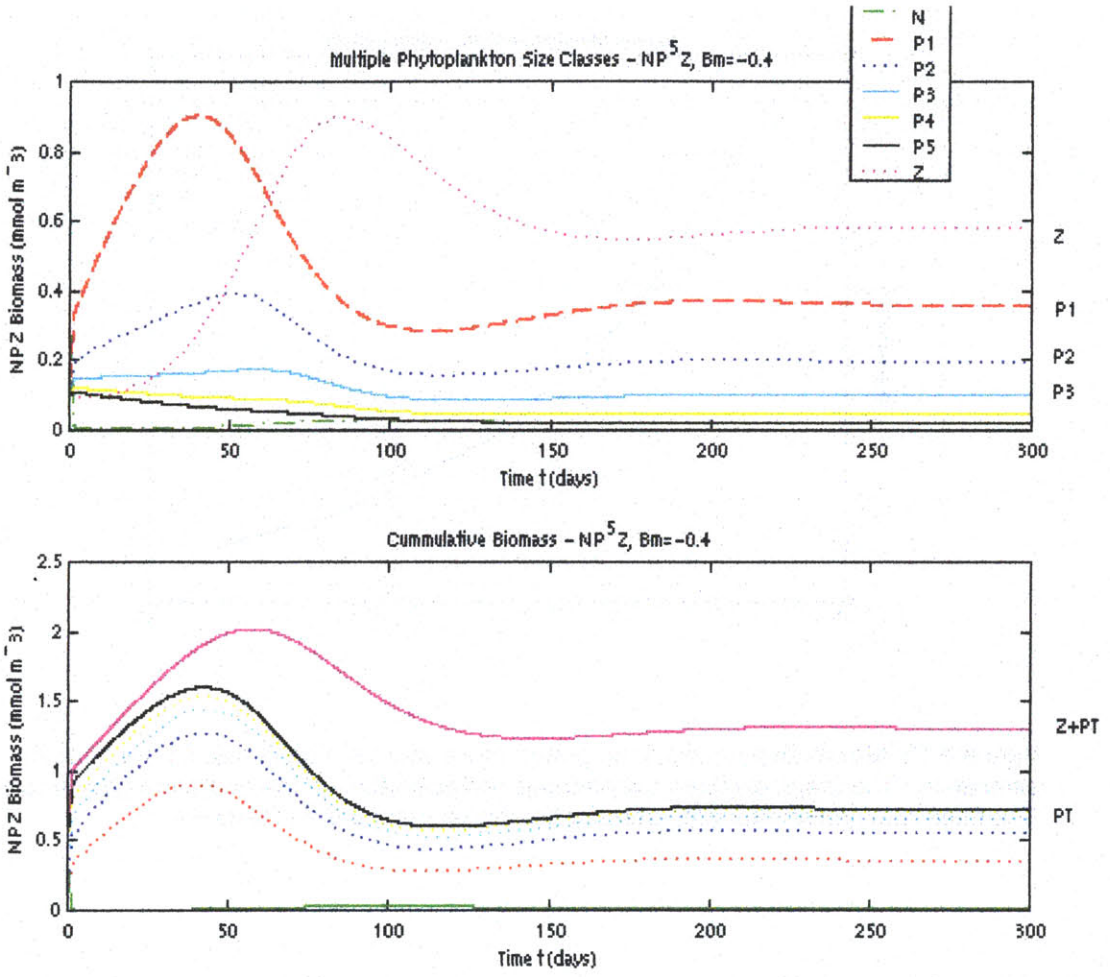

Figure 4-13: Time-series data for individual and cumulative biomass distributions for the "diatom" simulation. Graphs show the clear dominance of the two smallest phytoplankton size classes at all times during the simulation. All phytoplankton species settle to non-zero steady state conditions.

conditions as in the previous two cases we observe that the transient time is of about 240 days. This value is intermediate between those obtained for the "size-independent" and "traditional" models. This is expected, given that the allometric coefficient is less negative than that used in the traditional case. As in the "traditional" case, the allometric structure determines that smaller phytoplankton size classes have a competitive advantage over larger phytoplankton organisms. However, this new structure allows for all five phytoplankton size classes to thrive and survive in the system and settle to steady state. Again, the steady state conditions are independent of the set of initial conditions chosen.

The cumulative biomass time-series clearly shows that the smallest phytoplankton size class is the main contributor to phytoplankton biomass, but in this case, the second size class contributes to total phytoplankton biomass significantly as well. When compared to Armstrong's (1994) steady state conditions for the "diatom" case we find that the two models produce equivalent results. In both cases, the "diatom" simulations are characterized by allowing the survival of a larger number of size classes than the "traditional" case.

By analyzing the short-term population dynamics, we observe that the two smallest size classes clearly dominate the uptake of nutrient, growing rapidly and then decaying as grazing pressure increases. Eventually, all five phytoplankton size classes eventually level off to steady state, as grazing and growth rates closely balance each other. The total phytoplankton biomass supported by the system at steady state is of *0.72 mmol* m^{-3}. The nutrient biomass is *~0.02 mmol* m^{-3} and the total ecosystem biomass (including the zooplankton community) at steady state is *~1.3 mmol* m^{-3}.

The total phytoplankton biomass supported by the system at steady state is larger than that supported by the "traditional" simulation, but lower than that for the size-independent model, as a result of the respective allometric structures. Comparing the total biomass supported by the system we find that for all three simulations described ("size-independent", "traditional", and "diatom"), the steady state concentration for the zooplankton community is constant. Comparing all three cases we also observe that the lower the steady state nutrient concentration, the larger the total phytoplankton biomass at steady state.

The unnormalized and normalized biomass spectra, with their respective logarithmic approximations, is presented in figures 4-14 and 4-15. Using the data generated by the model

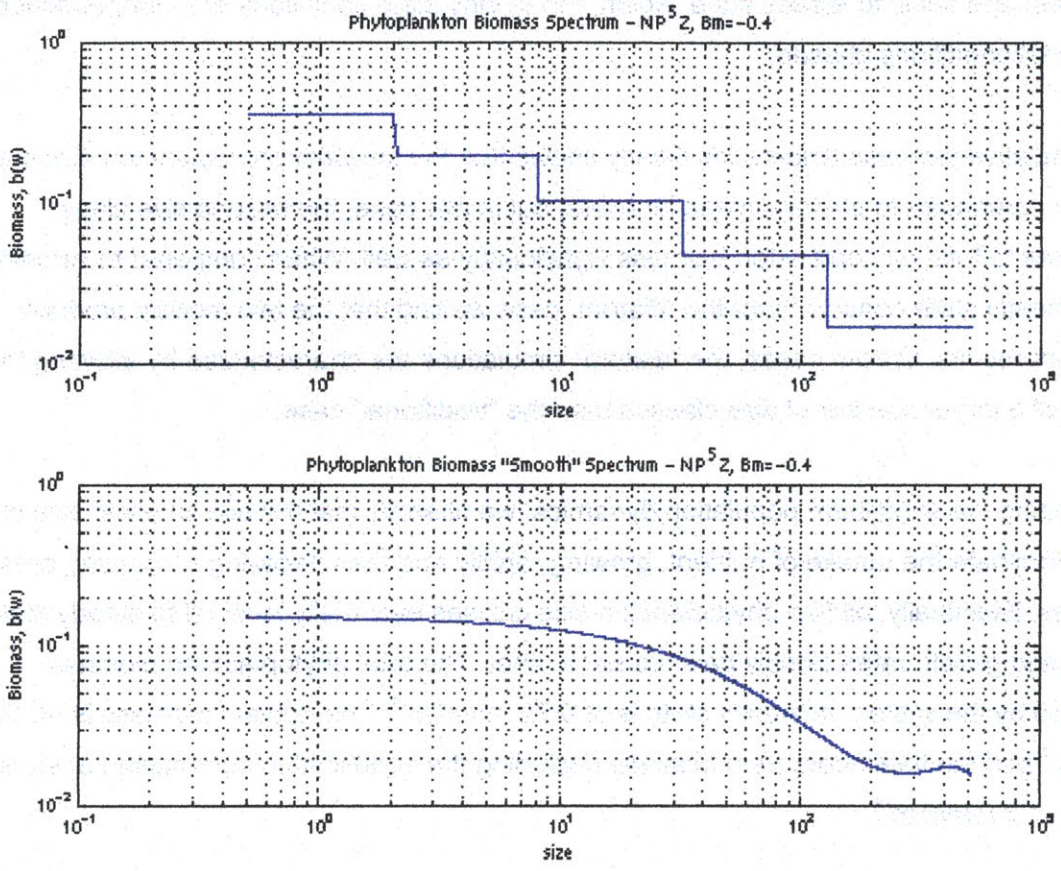

Figure 4-14: Unnormalized steady state spectra for the "diatom" simulation. The spectra shows that all phytoplankton size classes are present at steady state. Phytoplankton biomass is inversely proportional to size as a result of the allometric structure chosen.

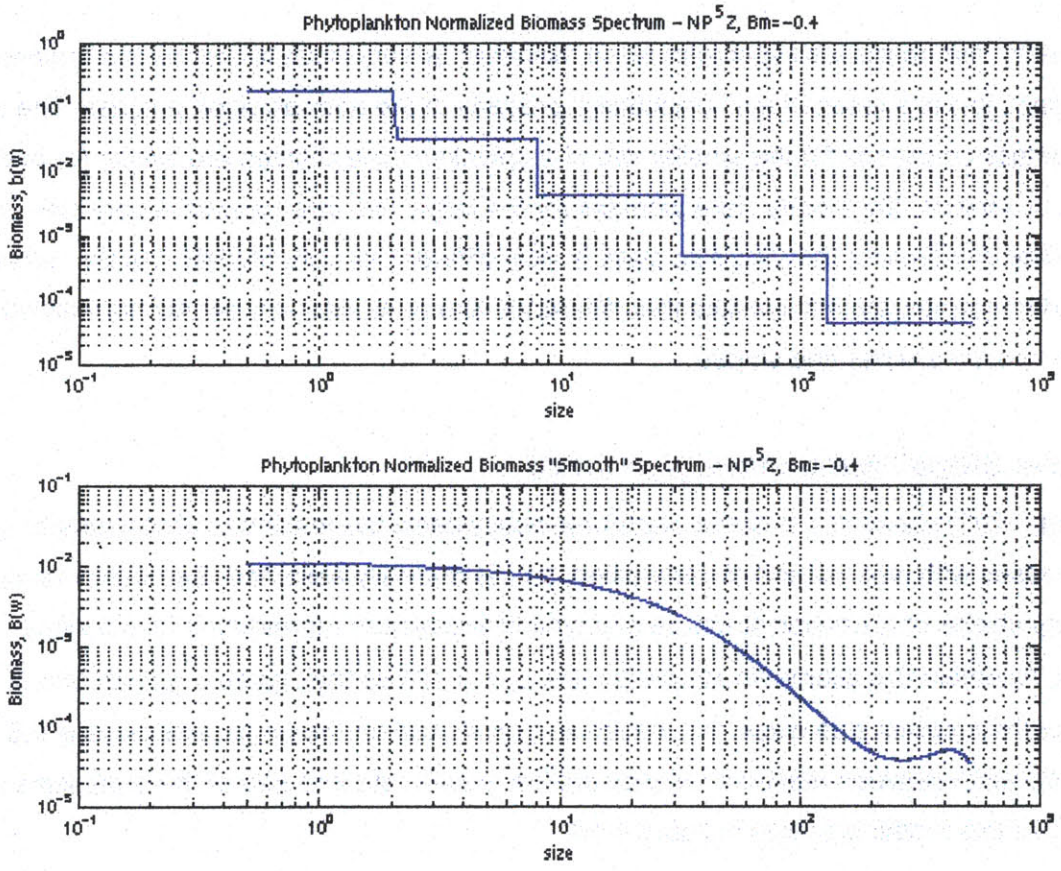

Figure 4-15: Normalized steady state spectra for the "diatom" simulation. The normalization is responsible for the decrease (more negative) in biomass spectra slope, as compared to the unnormalized spectra.

simulations, I calculate values of $x = -0.55$, and $x_n = -1.9$ for the unnormalized and normalized spectra slopes, respectively. The value for the unnormalized spectra slope is less negative than that for the "traditional" simulations; a direct result of the difference in the allometric structures for both simulations. Both allometric structures are based on the principle that smaller phytoplankton cells grow faster than larger phytoplankton cells, but the competitive advantage is smaller in the "diatom" case, and less biomass is distributed in the small size classes.

The value for the normalized spectrum slope, however, is very close to that for the "traditional" case. Again, this is a result of the "smoothing" property of the normalization process. The steady state biomass conditions for the smaller two phytoplankton size classes are similar for both models. In addition, the steady state biomass for the larger two size classes is very low. The steady state biomass for the third size class is very different for both models, but the "size-class-width" normalization minimizes that difference and produces very similar normalized biomass spectra shapes and slopes.

"Positive Slope" Simulation, $\beta_\mu = 0.125$

Chisholm (1992) states that in some planktonic ecosystems the maximum phytoplankton growth rate increases with size instead of decreasing, as it is normally assumed. See earlier comment explaining choice of allometric structure and type of ecosystem represented (simulations section). To obtain this allometric structure I use $\beta_\mu = 0.125$ so that, given a growth rate of 1.4 d^{-1} for the smallest size class, the maximum growth rate for the larger size class is 2.8 d^{-1}. The relationship between maximum phytoplankton growth rate and size of the organisms (size classes) for this model is shown in figure 4-16.

Time-series for the biomass concentrations of the phytoplankton size classes, as well as cumulative biomass distributions are presented in figure 4-17. The use of a positive allometric coefficient results in a proportionally larger distribution of biomass in larger phytoplankton size classes, since they will have larger maximum growth rates. Simulations in this case result in steady state conditions with all five phytoplankton size classes present. This is a result of the higher maximum growth rate values used across all size classes. As in the three models described previously, the steady state conditions are independent of the set of initial conditions chosen. The cumulative biomass time-series clearly shows that the largest phytoplankton size class is the main contributor to phytoplankton biomass. However, the other four size classes are all significant contributors to total phytoplankton biomass. The "weighted" model of distributed

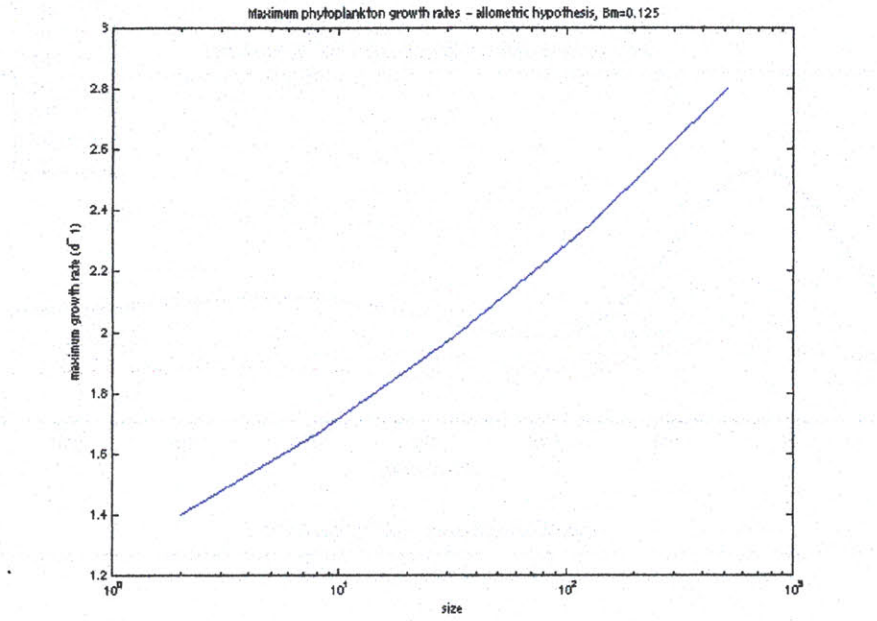

Figure 4-16: Maximum phytoplankton growth rates as a function of size for the "positive slope" simulation. The graph displays a continuous representation of the maximum growth rate. The maximum growth rate data used for the model simulations is discrete.

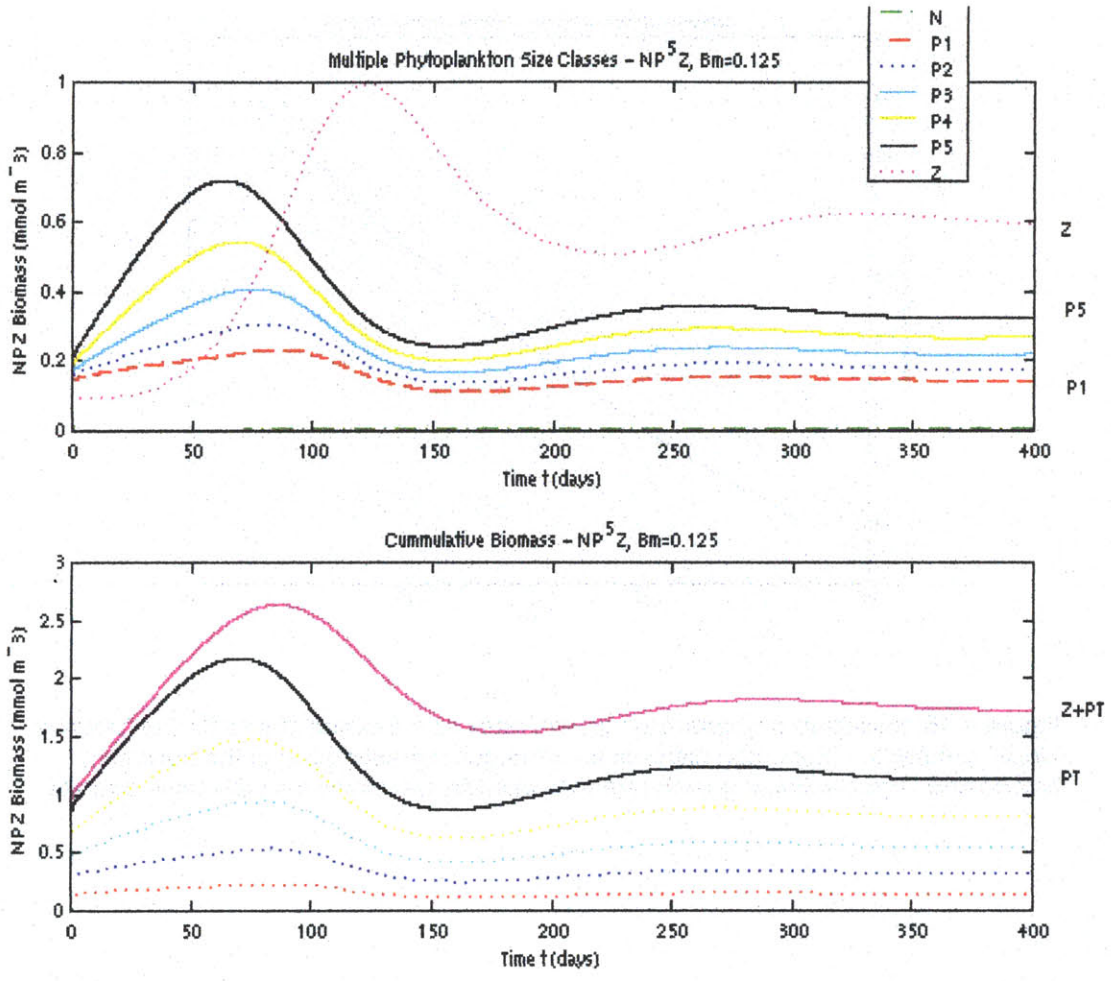

Figure 4-17: Time-series data for individual and cumulative biomass distributions for the "positive slope" simulation. Graphs show dominance of the larger phytoplankton size classes at all times during the simulation. Biomass differences across size classes are smaller than for previous models. All phytoplankton species settle to non-zero steady state conditions.

grazing allows for the coexistence of all phytoplankton size classes at relatively large biomass levels, by allowing the grazing community to exert greater grazing pressure on the relatively more abundant size classes.

The short-term population dynamics of the system indicate that the largest size classes dominate the uptake of nutrient, growing rapidly and then decaying as grazing pressure increases. Smaller size classes bloom at a slower rate than larger size classes, and the magnitude of their biomass at peak stages is sequentially smaller as we move from the largest to the smallest size class. The steady state biomass concentrations are all within the same order of magnitude. The grazing response to phytoplankton growth is slower in this case, resulting in a longer transient time value than that obtained in the previous simulations. In this case, the transient time (time to steady state) is about 400 days. This value is close to that obtained for the size-independent model and higher than those obtained for both the "traditional" and "diatom" simulations.

The total phytoplankton biomass supported by the system at steady state is *1.16 mmol* m^{-3}. The nutrient biomass is *~0.006 mmol* m^{-3} and the total ecosystem biomass (including the zooplankton community) at steady state is *~1.75 mmol* m^{-3}. We observe that the phytoplankton biomass supported by the system is larger than that supported by both the "traditional" and the "diatom" simulations. This result is consistent with the increase in phytoplankton biomass from the "traditional" to the "diatom" simulations, as the allometric coefficient becomes less negative. However, the total phytoplankton biomass is smaller than that for the size-independent case. This may indicate that total phytoplankton biomass is largest with no size-dependency, and decreases as the allometric coefficient used for the model becomes either more positive or more negative. Consistent with the results for the previous simulations we find that the steady state concentration for the zooplankton community is constant. Another relevant feature of this model is that, contrary to the results obtained when comparing the previous three models, the steady state nutrient concentration is not directly related to total phytoplankton biomass.

The unnormalized and normalized biomass spectra, with their respective logarithmic approximations, are presented in figures 4-18 and 4-19. Using the data generated by the model simulations, I obtain respective spectra slopes of $x = 0.15$, and $x_n = -0.8$. As a direct result of the allometric structure chosen, the slope of the unnormalized spectra is positive. However, the size-fractionation method implies that the larger the size class, the larger the range in size. As a

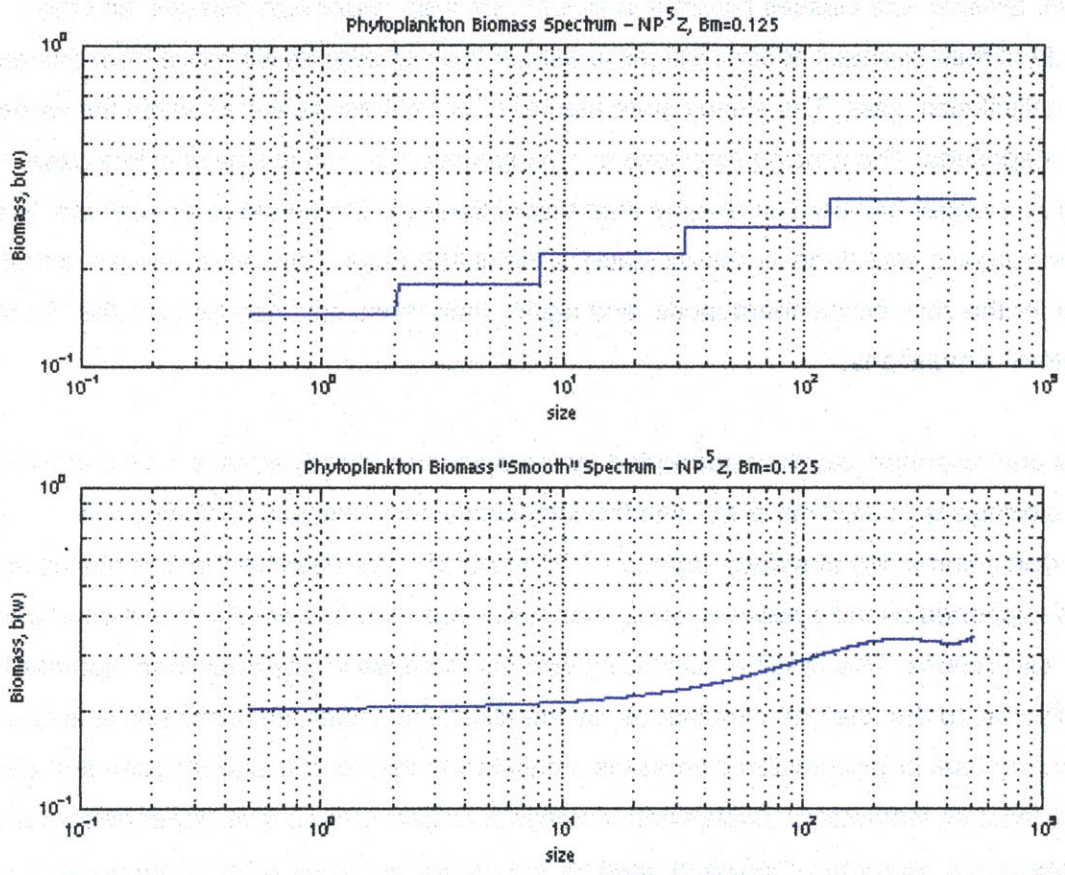

Figure 4-18: Unnormalized steady state spectra for the "positive slope" simulation. The spectra shows that all phytoplankton size classes are present at steady state. Phytoplankton biomass is directly proportional to size producing a positive spectra slope.

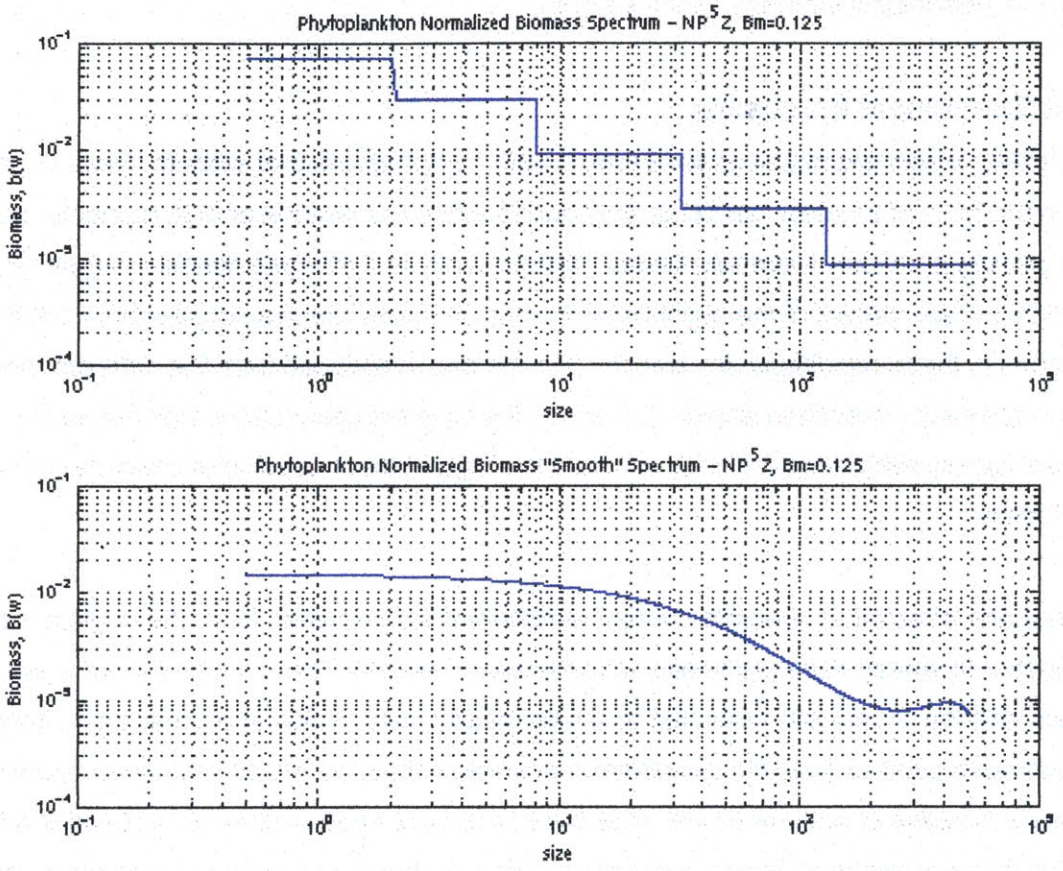

Figure 4-19: Normalized steady state spectra for the "positive slope" simulation. The normalization accounts for the shift in biomass spectra, from an increasing (positive slope) trend to a decreasing trend (negative slope) with increasing size.

result, the normalization (with respect to size class width) of the biomass spectra produces a slope value close to the value for the actual biomass spectra (-1). This result is very important, because it implies that even under a positive allometric structure, the normalized biomass spectra is in substantial agreement with observational oceanographic data, reflecting the uniform decrease in normalized biomass with increasing size. Except for the "size-independent" simulation, the slope of the normalized spectra for the "positive slope" simulation is the one closest to –1 (theoretical biomass spectra slope).

Nutrient Enrichment Processes

Based on field observations Cavender-Bares (1999) hypothesizes that smooth, linear microbial spectra in the form of a power law occur only during extended periods of high nutrients, perhaps with low grazing pressure. Cavender-Bares (1999) suggests that these conditions may be expected in surface waters of the oligotrophic ocean. Biomass spectra constructed from field observations in these conditions are smooth, like the ones produced from the different model simulation scenarios described above. Cavender-Bares (1999) also states that nutrient enrichment experiments should ideally simulate the high nutrient conditions characteristic of spring blooms.

The model was adapted to simulate nutrient enrichment experiments. First, the original model was projected to steady state (as shown in the analysis above). Then, nutrient input was increased, and the model was projected to a new steady state. Pulse and press perturbation techniques were used to illustrate the different possible scenarios. Pulse enrichment consists of a temporary increase in nutrient levels; after the enrichment ends, nutrient input level is returned to its initial background level. Press enrichment differs in that the nutrient enrichment is constant and maintained until the system reaches new steady state conditions. We intend to use the results of these simulations to analyze the changes in community structure and size spectra brought about by the different nutrient enrichment scenarios.

The nutrient enrichment simulations are developed only as illustrative examples of the potential of the model for simulating nutrient enrichment experiments, such as iron fertilization. To this effect, the "diatom" and "positive slope" simulations were used to analyze the pulse and press perturbation scenarios. The change in the nutrient environment can be characterized by an increase in substrate nutrient concentration, or by the addition of a new nutrient, such as a micronutrient, to the system. To account for preferential response to the nutrient enrichment

process, it was assumed that the larger two size classes experience an enhanced benefit from the new nutrient environment. Changing the model's allometric structure at the time of enrichment simulated this effect. A new allometric coefficient of *0.25* was used for the two larger size classes. This change produces larger maximum growth rates for the two larger size classes, and is representative of their competitive advantage under the new nutrient conditions.

More complex and realistic approaches can be incorporated into the model by adding a new compartment representing a new nutrient source. However, for the purpose at hand, it was decided that the nutrient increase would be included as increased substrate concentration and that the competitive advantage of the larger size classes would be represented by the altered allometric structure. For all simulations, the model was initially run for 600 days, time by which the steady state conditions are well established. At this time, the substrate concentration was increased from 0.6 mmol m^{-3} to 5 mmol m^{-3} and the new allometric structure was established.

"Pulse" enrichment

For both the "diatom" and "positive slope" simulations, a period of 100 days was used as the period of perturbation (nutrient enrichment). As explained above, the nutrient level is increased at *t=600 days* and then reduced back to the original background concentrations at *t=700 days*. At the time of enrichment, the allometric structure for size classes 4 and 5 was changed, using the new coefficient of *0.25* for the two larger size classes. At the end of the perturbation period, the allometric coefficient was set back to its original value of *-0.4* or *0.125* for the "diatom" and "positive slope" simulations, respectively.

The simulations for both models show that after the perturbation stops the system returns to its original steady state conditions. The resulting phytoplankton biomass spectra is unchanged as well. However, the community structure is affected by the nutrient enrichment and its effects are present in the system for a period of about 200 days after the perturbation ceases. In the "diatom" case, there is evidence of species succession, represented in changes in the community structure, as the growth of the larger size classes is enhanced by their competitive advantage for uptake and growth under the new nutrient conditions. During the enrichment period, the larger size classes go from having the lowest contribution to phytoplankton biomass, to being the dominant phytoplankton size classes in the system. As seen in the time-series graph (figure 4-20), the change in the size structure of the community starts occurring immediately after the enrichment starts. The system returns to its original size structure only

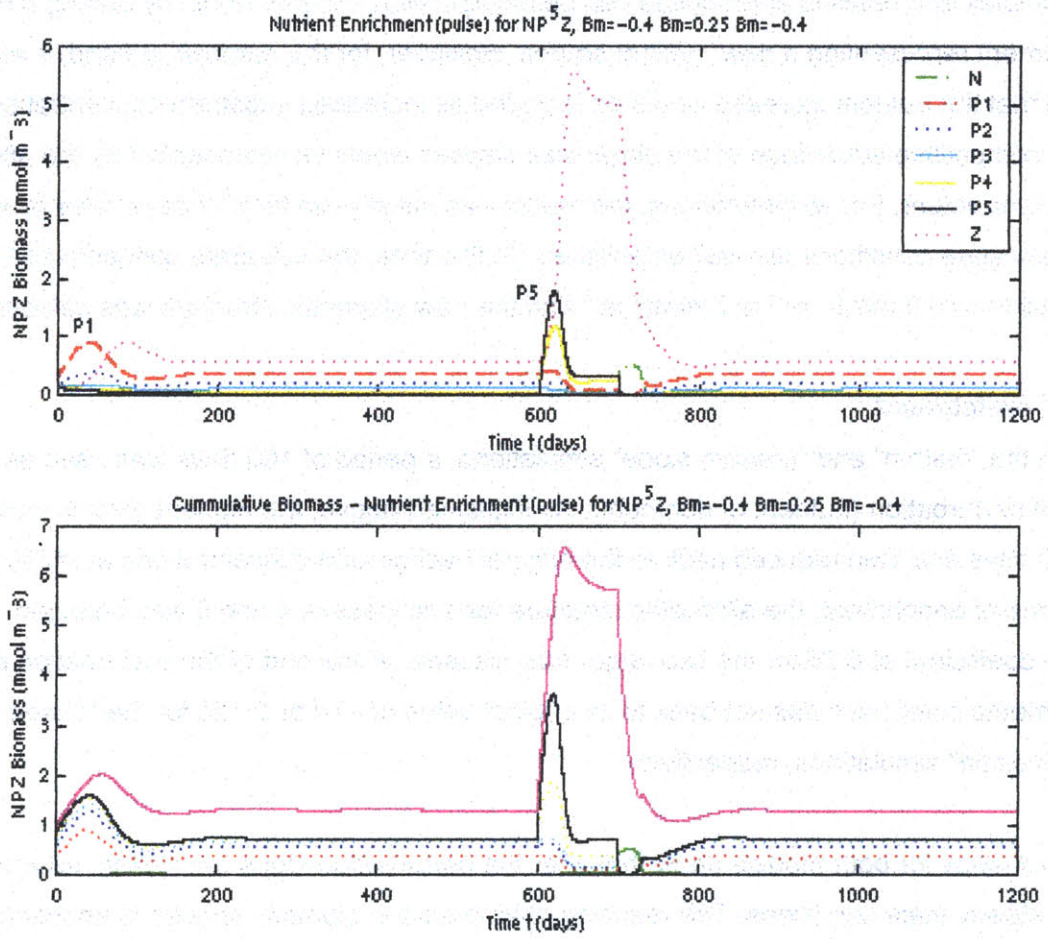

Figure 4-20: Time-series data for individual and cumulative biomass distributions for the "diatom" pulse-enrichment simulations. Graphs show the shift in community structure during the enrichment period. Larger size classes bloom shortly into the perturbation and become the dominant classes in the system. After the perturbation stops, the system returns to its original steady state conditions, with larger biomass distributed in the smaller size classes.

after the perturbation stops. It is important to emphasize that under both "pulse" enrichment scenarios, the zooplankton biomass also returns to its original steady state value.

In the "positive slope" case, the resulting steady state conditions are the same as those for the original "unperturbed" system. The larger size classes experience the largest bloom after the nutrient enrichment due to their increased ability to grow under the new conditions established (figure 4-21). The relative distribution of phytoplankton biomass is unchanged however, as the size classes benefited are the same ones that dominated the system before the enrichment.

The settling to the original steady sate implies that there is no change in the resulting biomass spectra for either one of the two "pulse" perturbation simulations. The return to the original steady state conditions is evidence of the stability of the system and of its independence on initial conditions.

"Press" (continuous) enrichment

Press perturbations are characterized by a continued and constant enrichment process. Hence, the system is perturbed by the addition of nutrient at a certain time and the new nutrient environment is maintained until the system reaches a new set of steady state conditions. For both the "diatom" and "positive slope" simulations, the perturbation was carried out at *t=600 days*, increasing the substrate nutrient level to 5 mmol m^{-3}. As in the "pulse" perturbation case, the allometric structure for size classes 4 and 5 was changed at the time of enrichment. The same value of *0.25* for the allometric coefficient was used. The resulting vector of maximum phytoplankton growth rates is μ_{max} = *[1.4 1.67 1.98 3.96 5.6]*, starting with the smallest size class. The system was then projected to steady state and the new conditions were used to produce new biomass spectral representations.

The simulations show that for both models the system settles to a new set of steady state conditions after about 100 days. The stability of the system and the independence of steady state on initial conditions are illustrated by the fact that the resulting phytoplankton biomass spectra is the same for the "diatom" and "positive slope" simulations in the "press" perturbation simulations. This is particularly relevant given that the size structure of the system at original steady state conditions is very different for both cases. In the "diatom" case, we have a larger proportion of total phytoplankton biomass distributed in the smaller size classes. In the

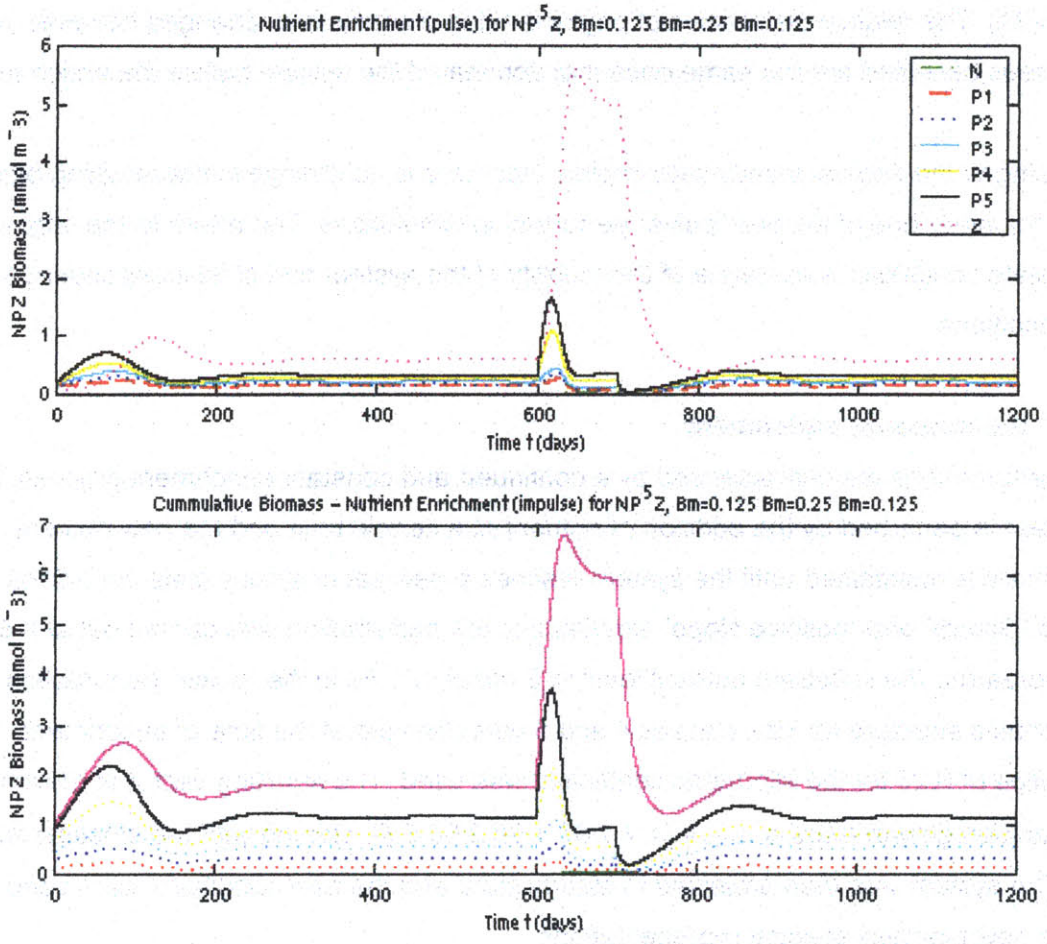

Figure 4-21: Time-series data for individual and cumulative biomass distributions for the "positive slope" pulse-enrichment simulations. Graphs show the larger biomass increase (bloom) for larger size classes during the enrichment period. This results in an even larger distribution of biomass in larger size classes during the enrichment. At the end of the enrichment, lower nutrient substrate biomass and grazing dramatically reduce phytoplankton biomass in all size classes. Phytoplankton then grow and the system returns to its original steady state conditions, with larger biomass distributed in the larger size classes.

"positive slope" model, on the contrary, we have a community characterized by dominance of the larger phytoplankton size classes. However, once both systems are perturbed by equivalent "press" nutrient enrichment processes, they both settle to steady state after equivalent transient times. The new biomass steady state conditions, however different, produce equivalent biomass slopes (unnormalized and normalized).

In the "diatom" simulation, there is a rapid species succession following the enrichment and the establishment of the new allometric (resource uptake competition) structure. The community structure changes are displayed clearly from the time-series data (figure 4-22). Immediately after the enrichment process starts we observe that the two larger phytoplankton size classes (previously the less abundant) experience a large bloom determined by their resource uptake competitive advantage over the smaller phytoplankton size classes. After the bloom, grazing pressure builds up and they decay to new steady state condition values an order of magnitude larger than those for the "pre-enrichment" conditions. The smaller size classes decay after the nutrient enrichment process begins due to their relative decreased ability for nutrient uptake and growth. The three smaller size classes decay and settle to biomass steady state values an order of magnitude smaller than those for the "pre-enrichment" conditions. Hence, the new steady state conditions are representative of a new community structure in which the dominant size classes are those who were less abundant prior to the enrichment process, and vice versa.

The total phytoplankton biomass supported by the system at the new steady state conditions is equivalent to that for the system at steady state before the enrichment process. However, contrary to the equivalency of "pre" and "post" enrichment steady state values for the zooplankton community, the "press" perturbation environment results in an almost 10-fold increase in the zooplankton steady state biomass. The increase in the zooplankton biomass is caused by the bloom of the larger phytoplankton size classes at the beginning of the nutrient enrichment, which causes the zooplankton to respond by exerting increasing grazing on the most abundant size classes. Eventually, grazing pressure results in the decay of phytoplankton, until grazing and phytoplankton growth rates are closely balanced and the system settles to steady state.

The changes in the size structure of the system are evident when we compare the biomass spectra for the "pre" and "post" enrichment steady state conditions. The steady state unnormalized biomass spectra slope, x, changes from a value of -0.55 to 0.26. The shape of

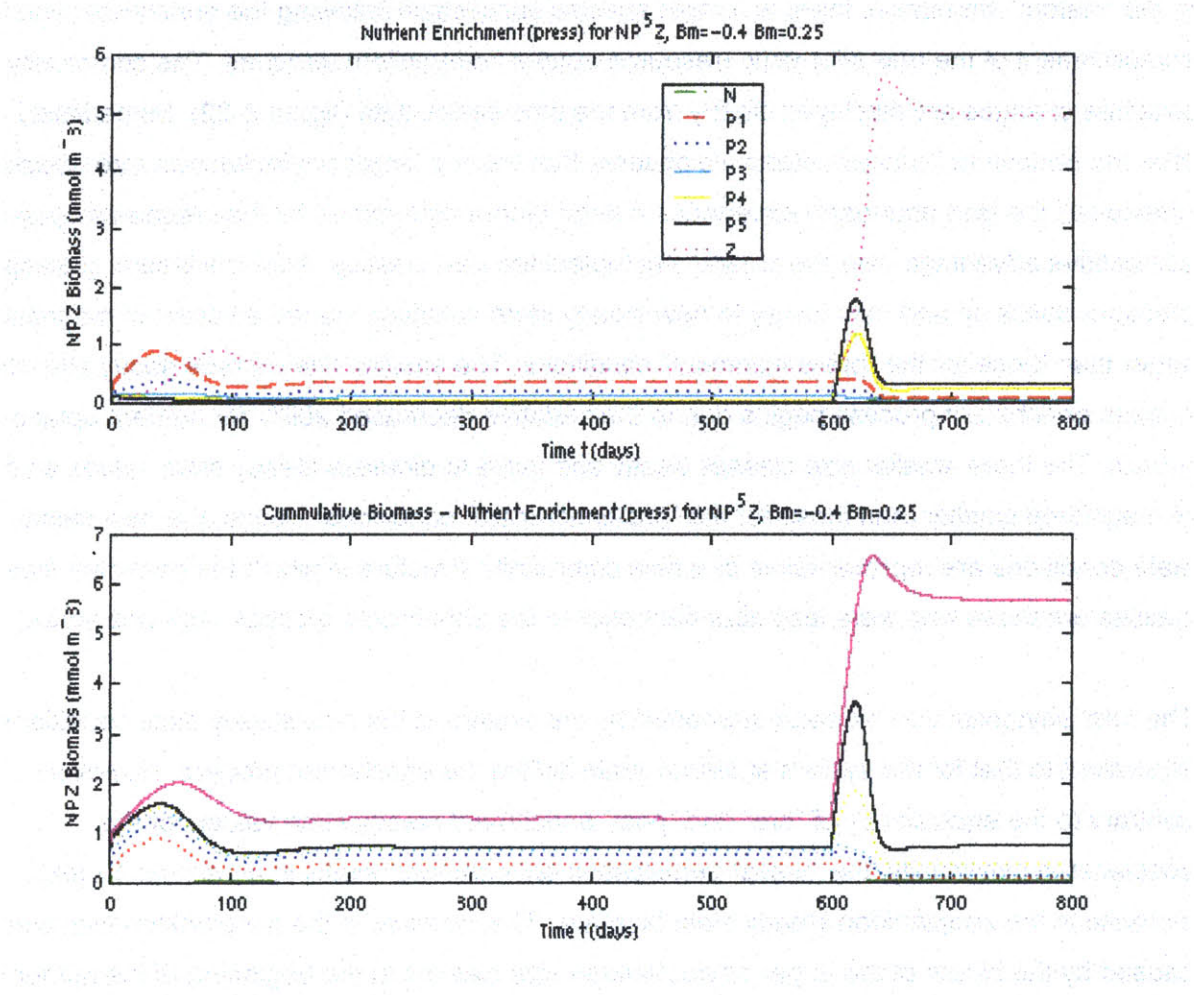

Figure 4-22: Time-series data for individual and cumulative biomass distributions for the "diatom" press-enrichment simulation. Graphs show the shift in community structure during the enrichment period. Larger size classes bloom shortly into the perturbation and become the dominant classes in the system. The system settles to a new set of steady state conditions with larger biomass distributed in the larger size classes. New steady state community size structure is opposite to that before the enrichment process.

the spectra for the smaller three size classes is unchanged since we did not alter their maximum growth rates, and their biomass decreases as size increases. The two larger size classes have the largest contribution to total phytoplankton biomass, with P_5 having the largest contribution of all size classes. The unnormalized biomass spectra data (figure 4-23) shows that the shape of the spectra is non-uniform (decreasing at first, and then increasing), in contrast with the uniform shape for the "pre" enrichment spectra. This feature (non-uniformity) is in accordance with the spectra developed from nutrient enrichment experiments such as the IronEx II (Cavender-Bares, 1999).

The slope for the normalized biomass spectra, x_n, at steady state changes from -1.9 to -0.69, a value much closer to -1. The shape of the spectra for the smaller three size classes is unchanged by the enrichment process, but the slope is less steep than that for the "pre" enrichment conditions. From the normalized biomass spectra graph (figure 4-24) we observe that the shape of the spectra is still non-uniform, but less so than that for the unnormalized spectra. The normalized spectra is decreasing for the first three size classes, increases with the fourth size class and then decreases again with the largest size class. This feature is in contrast with the smooth shape of the normalized spectra for the "pre" enrichment model, and in accordance with biomass spectra developed from observational data for nutrient enrichment experiments.

Analysis of the "positive slope" press-enrichment simulation dynamics shows an increase in all size classes after the enrichment process begins. The allometric structure determines that the magnitude of the bloom will be larger for larger size classes, and vice versa. Analogous to the initial growth at the beginning of the simulation (initial nutrient conditions), the largest size class blooms and peaks first, followed in order by the other classes in descending order of size. During their respective blooms, all phytoplankton size classes are subject to increasing grazing pressure and after their peaks in biomass they decay and settle to the new set of steady state conditions. The three smaller size classes decay and settle to biomass steady state values about two times smaller than those for the "pre-enrichment" conditions. The steady state values for the larger size classes are very close to those for the "pre" enrichment conditions. Hence, the new steady state conditions are representative of a new community structure in which the proportional distribution of biomass in larger size classes is even greater than before the enrichment process. The community structure dynamics for the system before and after enrichment are displayed in figure 4-25.

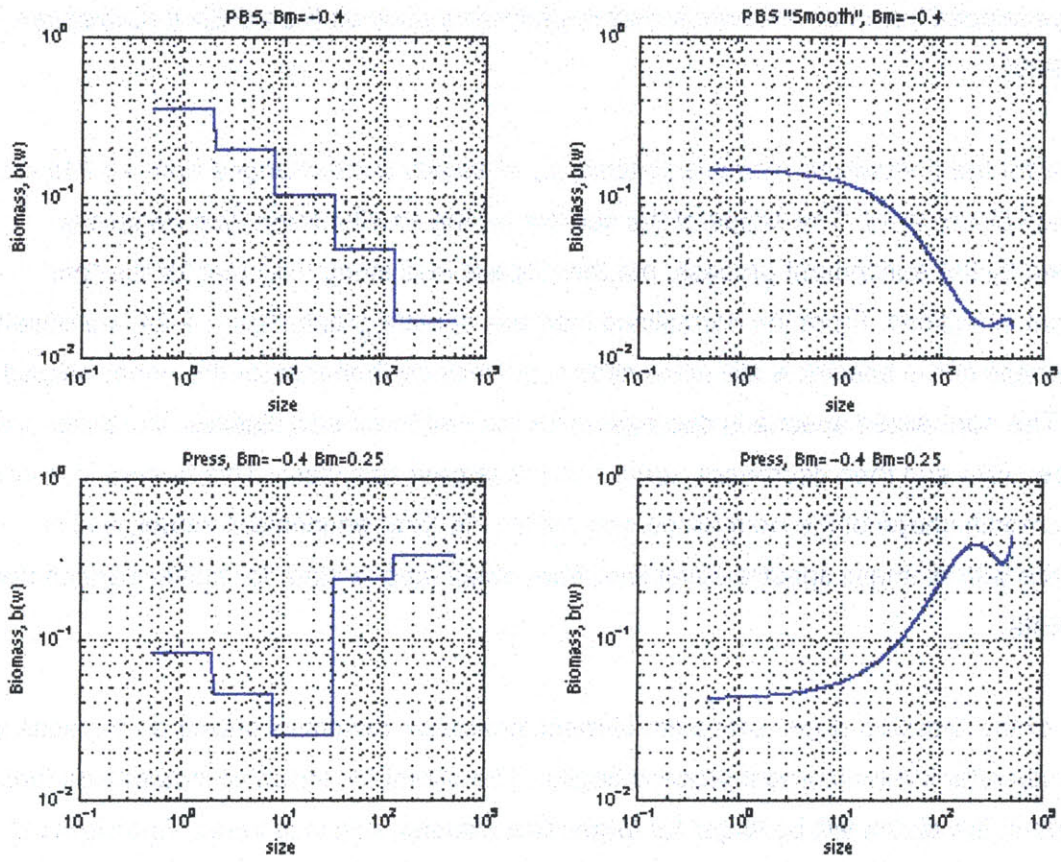

Figure 4-23: Unnormalized steady state spectra for the "diatom" press-enrichment simulation (bottom) compared to "pre" enrichment steady state spectra (top). The non-uniform shape of the spectra (bottom) is representative of the species succession following the enrichment process.

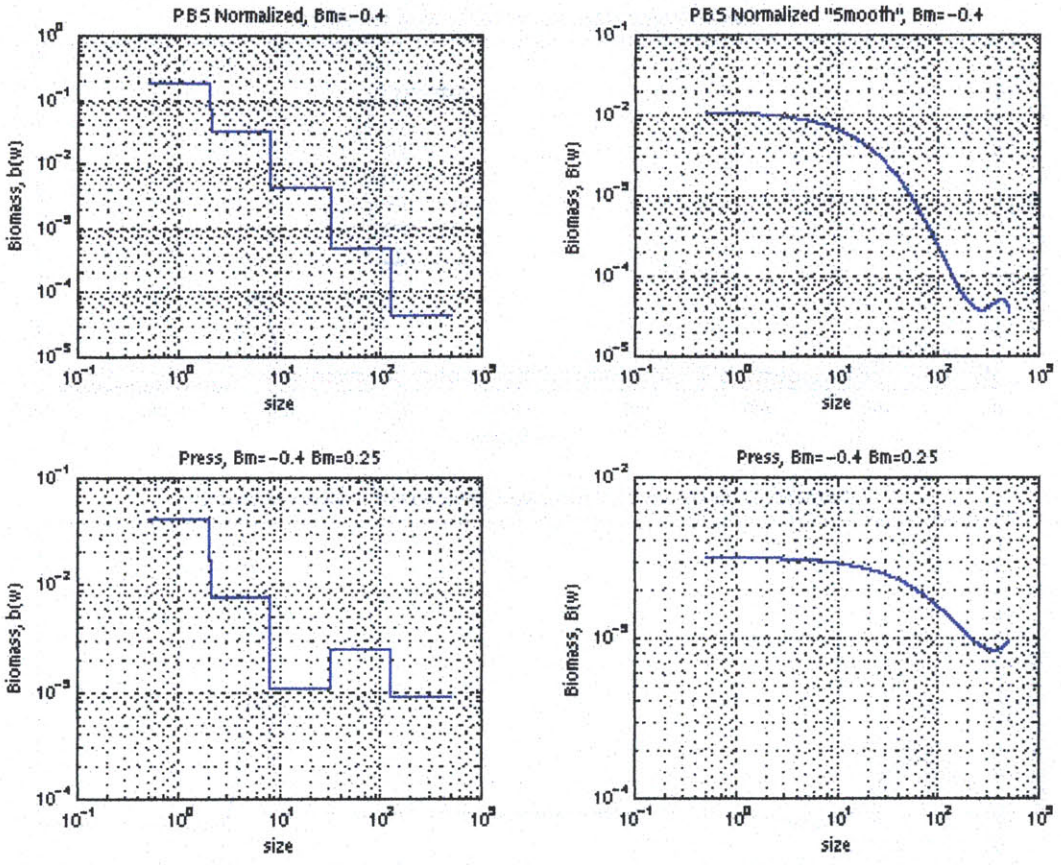

Figure 4-24: Normalized steady state spectra for the "diatom" press-enrichment simulation (bottom) compared to "pre" enrichment steady state spectra (top). The non-uniform shape of the spectra (bottom) is representative of the species succession following the enrichment process.

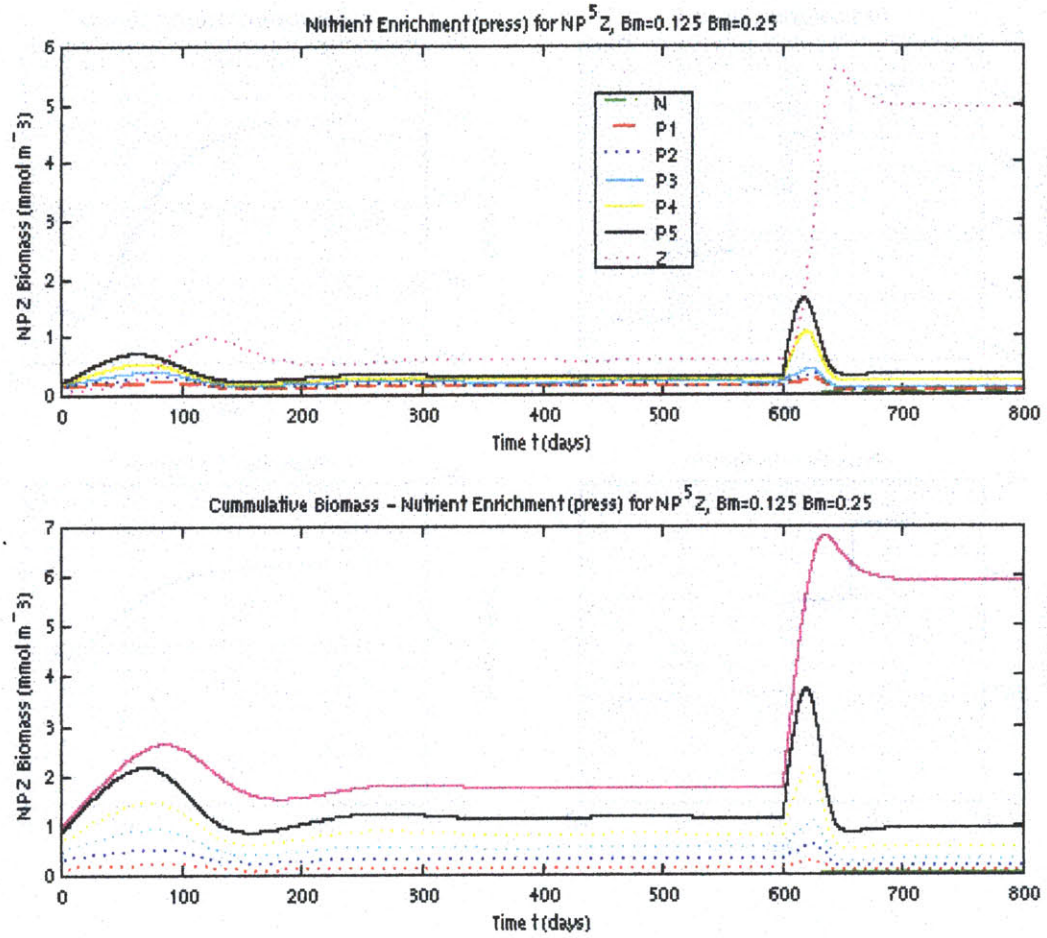

Figure 4-25: Time-series data for individual and cumulative biomass distributions for the "positive slope" press-enrichment simulation. Graphs show the changes in the community structure during the enrichment period. Larger size classes bloom shortly into the perturbation and become even more dominant in the system. The system settles to a new set of steady state conditions with larger biomass proportionally more distributed in the larger size classes. New steady state community size structure is equivalent (but accentuated) to that before the enrichment process.

The total phytoplankton biomass supported by the system at the new steady state conditions is smaller than that supported by the system before enrichment, due to the 2-fold reduction in biomass for the smaller size classes. Analogous to the "diatom" enrichment simulation, the "positive slope" enrichment simulation shows that the system experiences an almost 10-fold increase in the biomass of the zooplankton community. The increase in the zooplankton biomass is caused by the bloom of all phytoplankton size classes at the beginning of the nutrient enrichment, which causes the zooplankton to respond by exerting increasing grazing on the most abundant size classes. Eventually, grazing pressure results in the decay of phytoplankton, until grazing and phytoplankton growth rates are closely balanced and the system settles to steady state.

The biomass spectra for the "pre" and "post" enrichment steady state conditions allows the analysis of the changes in the size structure of the system. The steady state unnormalized biomass spectra slope, x, changes from a value of 0.15 to 0.26. The general shape of the unnormalized spectra (increasing) is unchanged since the new allometric structure is analogous to the original allometric structure in the sense that maximum growth rate increases as we move from smaller to larger size classes. The new allometric structure, however, produces larger maximum growth rates for the two larger size classes, producing an even more marked larger contribution to total phytoplankton biomass by them (more positive slope). The shape of the new unnormalized biomass spectra (figure 4-26) is less smooth than that for the original model. Comparison of the two graphs shows that the "post" enrichment steady state spectra displays a large increase in biomass as we move from the third to the fourth size class. Again, the change in the smoothness of the spectra is consistent with spectra developed from field observations during and after nutrient enrichment experiments.

The slope for the normalized biomass spectra, x_n, for the "post" enrichment system at steady state changes from -0.8 to -0.69. The shape of the spectra is very similar to that for the "pre" enrichment conditions, but the slope is less steep. From the normalized biomass spectra graph (figure 4-27) we observe that the shape of the spectra is somewhat less uniform than that for the "pre" enrichment conditions, but not dramatically so. This is a result of the similarity of the steady state community structure for the system before and after the enrichment process. When comparing the "post" enrichment spectra for the "diatom" and "positive slope" simulations we observe that the steady state biomass spectra slopes (unnormalized and normalized) are equivalent. The equivalency of the spectra slopes is a result of the equivalency of the steady

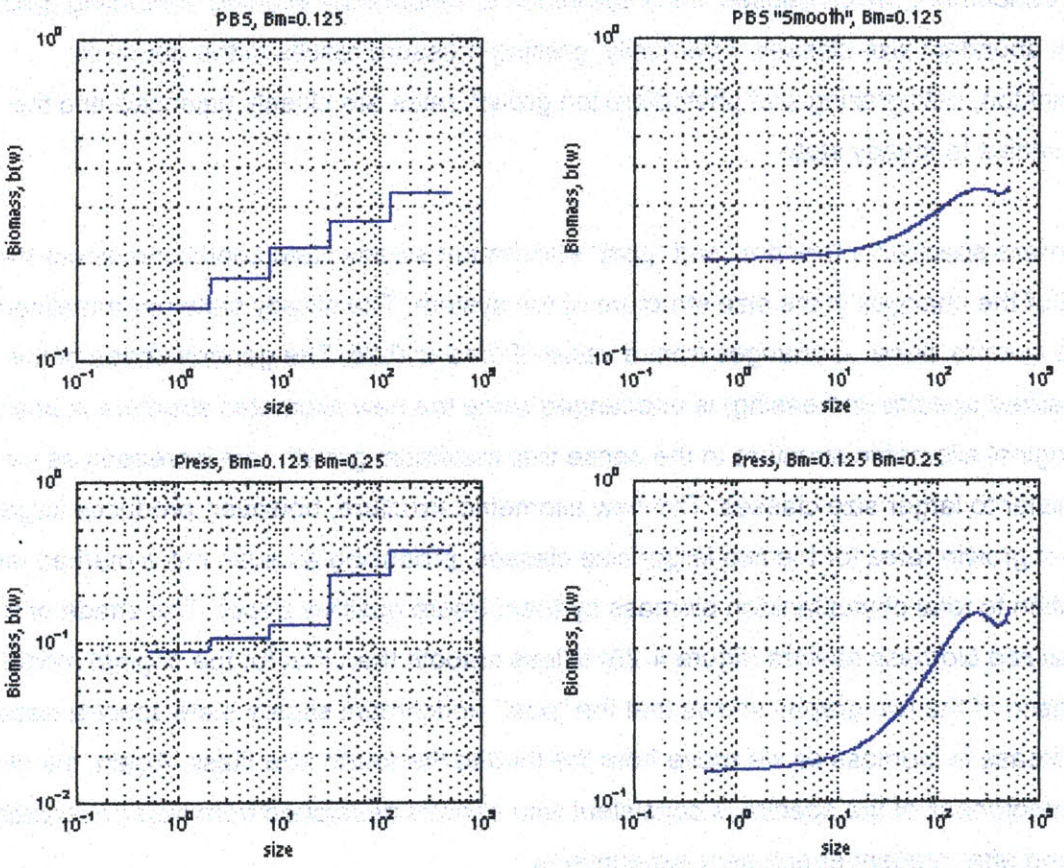

Figure 4-26: Unnormalized steady state spectra for the "positive slope" press-enrichment simulation (bottom) compared to "pre" enrichment steady state spectra (top). The less uniform shape of the spectra (bottom) is representative of the changes in relative size distribution following the enrichment process.

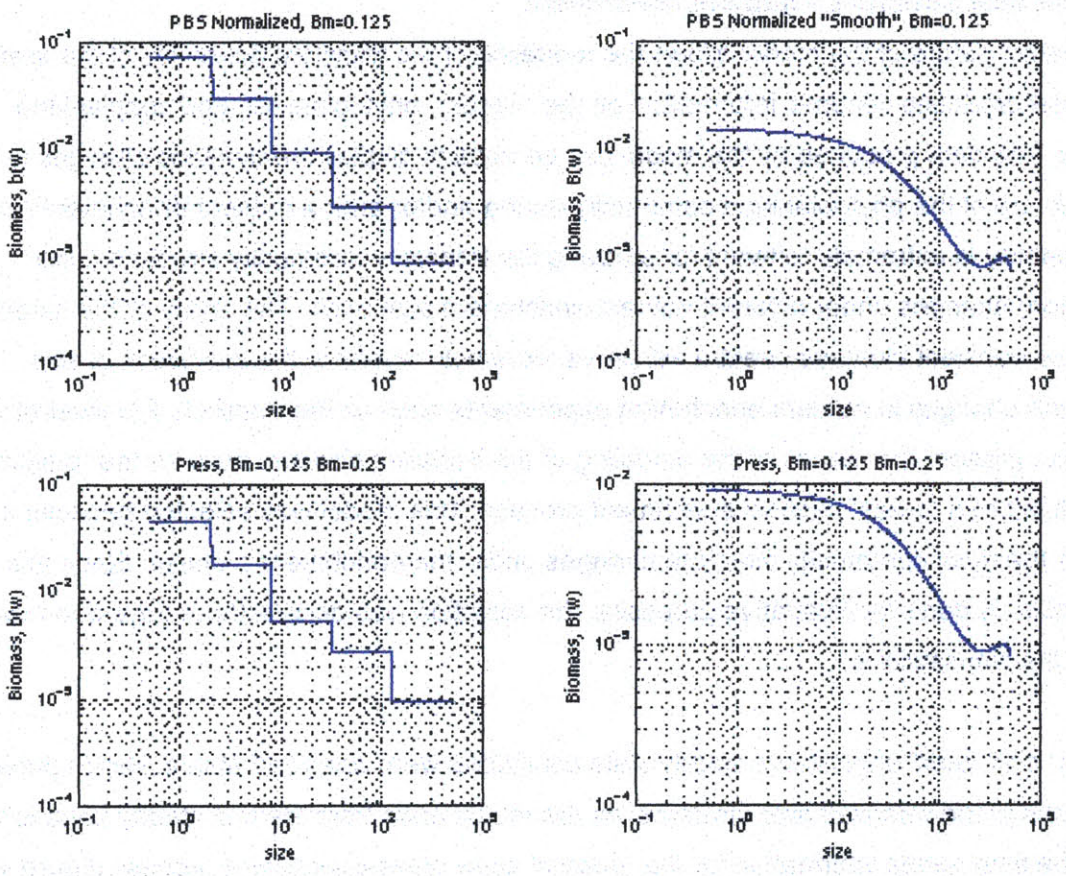

Figure 4-27: Normalized steady state spectra for the "positive slope" press-enrichment simulation (bottom) compared to "pre" enrichment steady state spectra (top). The normalization produces a close-to-uniform shape of the spectra (bottom).

state biomass for the smallest and largest size class in both cases. However, the shapes of the spectra for both cases are very different, being much less uniform in the "diatom" simulation. This difference results from the marked differences in steady state biomass for the second and third phytoplankton size classes. As explained above, the "diatom" spectra after enrichment is much less uniform given the shift in biomass distribution (species succession).

Transient Size Structure – nutrient enrichment

The dynamic nature of the model allows the modeling of the transient dynamics of the system. The model produces dynamic information on the nutrient, phytoplankton and zooplankton biomass. The data produced by the model can be used to display the dynamic changes in the size structure of the phytoplankton community during and/or after a nutrient enrichment process. This capability is extremely relevant for studying the transient community structure (size distribution) changes under different nutrient enrichment scenarios. The ability of the model to reproduce transient biomass spectra will prove extremely helpful in the prediction of size distribution changes in nutrient enrichment experiments such as the IronEx II. For illustrative purposes I present the results of the modeling of the transient size structure for the "diatom" case subject to a "press" nutrient enrichment process. This model was selected because it presents the most community structure changes under the enrichment process. Since this presentation is done for illustrative purposes, the selection was done without regard to how realistic the simulation is.

The "pre" and "post" enrichment steady state conditions were analyzed above. Here I present an analysis of the transient size structure, as the model goes from the first steady state to the latter. The time series information for the "diatom" case press-enrichment process (figure 4-22) shows that the community size structure changes as the larger size classes go from being the less abundant to being the most abundant in the system. After the biomass of the two larger phytoplankton size classes peaks, grazing pressure makes them decay to the new steady state conditions. Hence, the main shift in the relative biomass distribution takes place between the time when the enrichment begins and the peak in biomass for the two larger size classes (*t=~20 days* after enrichment begins). After the peak in biomass, the proportionality in the relative distribution still changes, but the main features of the size spectra are unchanged.

Unnormalized spectra for the transient conditions is displayed in figure 4-28. By analyzing the transient size structure we observe that the changes in the relative abundance of populations

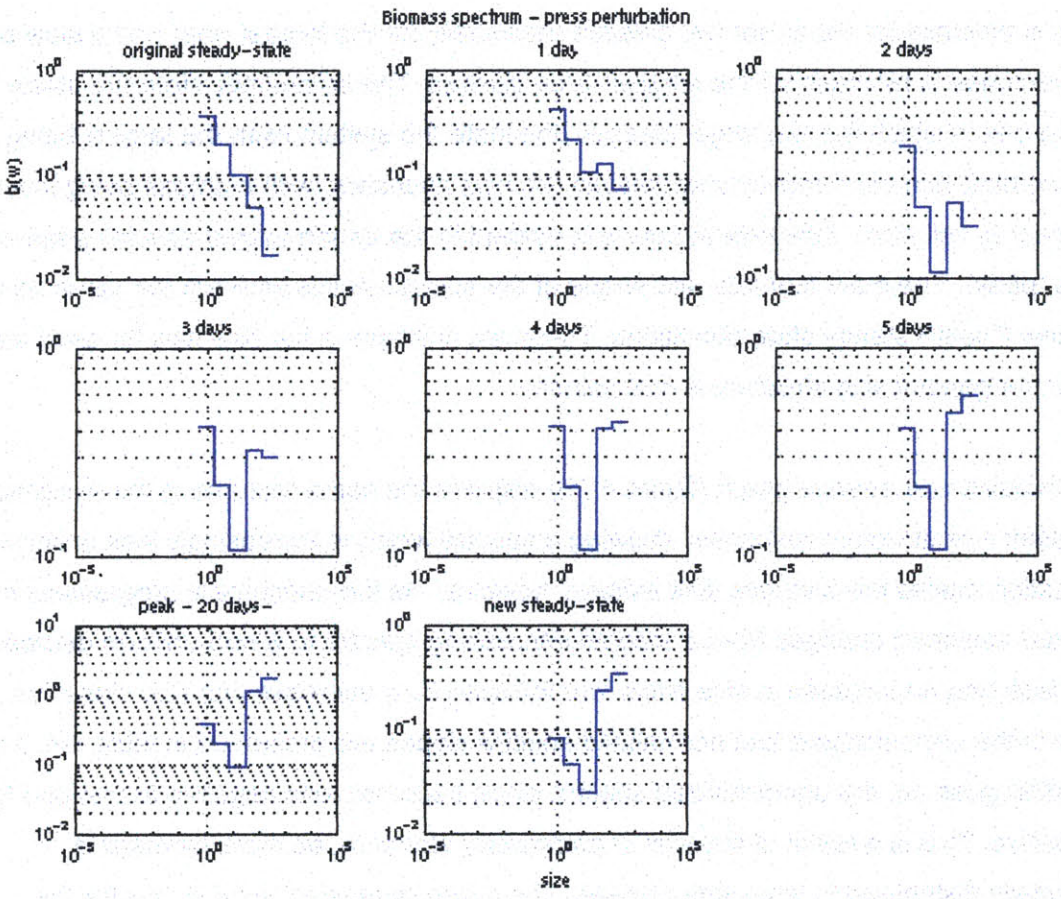

Figure 4-28: Transient unnormalized biomass spectra for "diatom" press nutrient enrichment simulation. The graph shows the size distribution dynamics from the beginning of the enrichment process (original steady state) to the establishment of the new steady state conditions. Each of the other figures is representative of the number of days after the beginning of the enrichment. Enrichment results in non-uniform spectra.

occur on time scales of several days following the enrichment. This result is in accordance with spectra developed from field "nutrient enrichment experiments" (Cavender-Bares *et al.* 1999). We observe that one day into the enrichment process there is already evidence of species succession, as the biomass of the larger size classes increases much faster than that for the smaller classes. At this point, we already see a change from a uniform shape to a non-uniform one. The species succession in the following days is characterized by a rapid and steady increase in biomass for the larger two classes (especially for the largest one) and a slow but steady decrease in biomass for the smaller three classes. The community structure starts shifting to one in which the two larger classes dominate the system (with the largest being the most abundant) and the three smaller classes are less abundant (with biomass being inversely proportional to cell size). This new structure is evident in the unnormalized spectra graph for the biomass "peak". The main features and shape of the spectra at this time are the same as those for the new ("post") steady state conditions. There are changes in the biomass for each size class but the general size structure is maintained.

The normalized size spectra graph (figure 4-29) displays the same features in the dynamics of the transient size structure response, showing a spectra which is increasingly less uniform. The normalization makes the changes less evident, however. As the enrichment progresses, the normalized spectrum changes from a smooth decreasing spectra to a non-uniform decreasing spectra featuring an increase in size class four followed by a decrease into size class five. The changes in the unnormalized and normalized spectra slopes are presented in table 4-4. As the perturbation goes on, the unnormalized spectra slope becomes less negative at first and then more positive. This is a result of the shift in community structure, as more biomass is proportionally distributed in large size classes. The same increasing trend is true for the normalized spectra but the slope is always negative.

Table 4-4: Transient biomass spectra slopes for "diatom" press-enrichment process

Time (after enrichment)	Unnormalized spectra slope	Normalized spectra slope
Initial steady state	-0.56	-1.91
t = 1	-0.32	-1.25
t = 2	-0.17	-1.10
t = 3	-0.06	-1.01
t = 4	0.01	-0.93
t = 5	0.06	-0.89
t = 20 ("peak")	0.27	-0.68
New steady state	0.26	-0.69

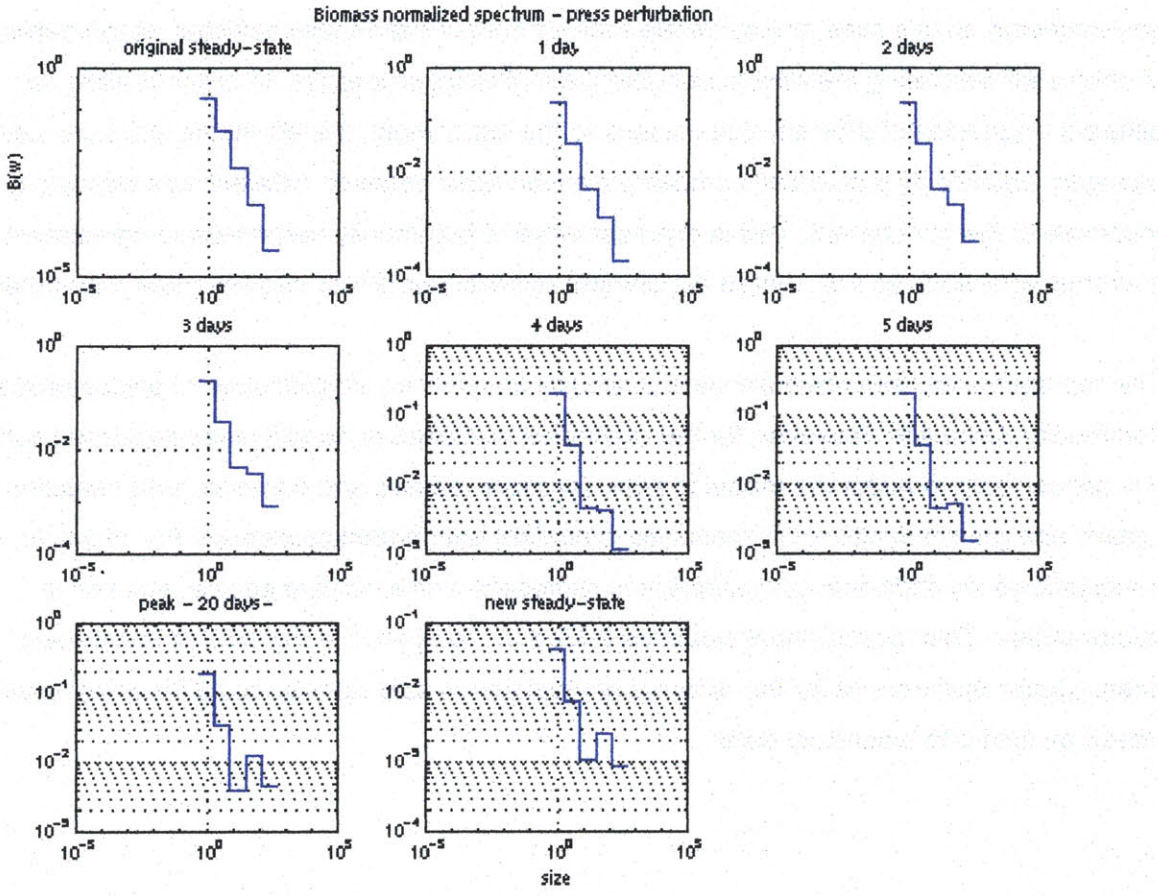

Figure 4-29: Transient normalized biomass spectra for "diatom" press nutrient enrichment simulation. The graph shows the size distribution dynamics from the beginning of the enrichment process (original steady state) to the establishment of the new steady state conditions. Each of the other figures is representative of the number of days after the beginning of the enrichment. Enrichment results in non-uniform spectra.

The dynamic nature of the model allows the modeling of the transient size structure (biomass spectra) response of the system to an external perturbation, and its projection to steady state. In this case, I decided to model the response of the system to nutrient enrichment processes to predict the community response in terms of its size distribution. This feature of the model is extremely relevant for studying system ecosystem responses to enrichment processes such as the IronEx II or to model spring blooms or changes in the system under changing nutrient environments. In this case, the substrate nutrient concentration was selected as the parameter of choice for simulating the effects of nutrient enrichment processes. In order to allow for different responses of different size classes to the enrichment, the allometric structure was changed, representing potential competitive advantages between different size classes in response to the enrichment. This is representative of community responses to enrichment with micronutrients such as iron, where enrichment benefits some size classes more than others.

The representation described above is obviously an extreme simplification of phytoplankton community dynamics. However, for the illustrative purposes at hand it was considered sufficient. It is conceivable to adapt the model to allow for more realistic and complex representations of uptake and growth dynamics in response to nutrient enrichment processes. For example, one could include an additional compartment to represent a new nutrient source, such as a micronutrient. This micronutrient would be added to the system at the time of enrichment. In this case, uptake preferences for the different phytoplankton size classes could be determined based on field and laboratory data.

REFERENCES

Armstrong, R.A. 1994. Grazing limitation and nutrient limitation in marine ecosystems: steady state solutions of an ecosystem model with multiple food chains. *Limnology and Oceanography* 39(3): 597-608.

Armstrong, R. A. 1998. Stable model structures for representing biogeochemical diversity and size spectra in plankton communities. *Journal of Plankton Research* 21: 445-464.

Cavender-Bares, K. Size distributions, population dynamics, and single-cell properties of marine plankton in diverse nutrient environments. Ph.D. Thesis, M.I.T. Civil and Environmental Engineering, 1999.

Chisholm, S.W. 1992. Phytoplankton size. In Falkowski, P.G., and A.D. Woodhead (eds.) *Primary productivity and biogeochemical cycles in the sea.* Plenum Press New York.

Ducklow, H., and M.J.R. Fasham 1992. Bacteria in the greenhouse: modeling the role of oceanic plankton in the global carbon cycle. In Mitchell, R. (ed.) *New Concepts in Environmental Microbiology*, Wiley-Liss Inc. New York.

Edwards, A.M., and J. Brindley 1996. Oscillatory behaviour in a three-component plankton population model. *Dynamics and Stability of Systems* 11(4): 347-370.

Evans, G.T., and J.S. Parslow 1985. A model of annual plankton cycles. *Biological Oceanography* 3: 327-347.

Fasham, M.J.R., H.W. Ducklow, and S.M. McKelvie 1990. A nitrogen-based model of plankton dynamics in the oceanic mixed layer. *Journal of Marine Research* 48: 591-639.

Fasham, M.J.R. 1993. Modeling the marine biota. In Heimann, M. (ed.) *The global carbon cycle.* NATO ASI Series, Voll. I 15, Springer-Verlag Berlin.

Franks, P.J.S., J.S. Wroblewski, and G.R. Flierl 1986. Behavior of a simple plankton model with food-level acclimation by herbivores. *Marine Biology* 91: 121-129.

Frost, B.W. 1987. Grazing control of phytoplankton stock in open sub-Arctic Pacific Ocean. *Marine Ecology Progress Series* 39: 49-68.

Frost, B.W., and N.C. Franzen 1992. Grazing and iron limitation in the control of phytoplankton stock and nutrient concentration: a chemostat analog of the Pacific equatorial upwelling zone. *Marine Ecology Progress Series* 83: 291-303.

Moloney, C.L., and J.G. Field 1991. The size-based dynamics of plankton food webs. I. Description of a simulation model of carbon and nitrogen flows. *Journal of Plankton Research* 13: 1003-1038.

Pahl-Wostl, C. 1997. Dynamic structure of a food web model: comparison with a food chain model. *Ecological Modelling* 100: 103-123.

Platt, T., and K.L. Denman 1978. The structure of the pelagic marine ecosystems. *Rapp. P.-V. Reun. Const. Int. Explor. Mer.* 173: 60-65.

Riley, G.A. 1946. Factors controlling phytoplankton populations on Georges Bank. *Journal of Marine Research* 6: 54-73.

Steele, J.H. 1984. A global ocean flux study. *EOS* 65: 684.

Steele, J.H., and E.W. Henderson 1992. The role of predation in plankton models. *Journal of Plankton Research* 14(1): 157-172.

Truscott, J.E., and J. Brindley 1994. Equilibria, stability and excitability in a general class of plankton population models. *Philosophical Transactions of the Royal Society of London, Series A* 347: 703-718.

Wroblewski, J.S., J.L. Sarmiento, and G.R. Flierl 1988. An ocean basin scale model of plankton dynamics in the North Atlantic. (1) Solutions for the climatological oceanographic conditions in May. *Global Biogeochemical Cycles* 2: 199-218.

Chapter 5

Conclusions

CONCLUSIONS

Phytoplankton biomass has been found to be distributed in a continuous manner across entire ranges of size classes. Observations show that the abundance of organisms per size class is inversely proportional to their body mass. This relatively conservative property of marine ecosystems is of great relevance since the size structure of the phytoplankton community dictates the composition and structure of the rest of the ocean food web. Size distribution models were used in an attempt to enhance understanding of the causes and consequences of the size structure of planktonic ecosystems.

Platt (1985) argues that the biomass spectrum provides an operationally viable, alternative taxonomy that contains latent information about community physiology and metabolism that cannot be obtained from a conventional taxonomic description. Size distribution models provide insight into the energy flow and transfer efficiency along the size gradient in complex pelagic food webs without the necessity to define distinct trophic levels or to distinguish taxonomic groups (Gaedke, 1995). Thus, given that most physiological rates, (e.g. growth and respiration rates, and generation time) scale allometrically with organism size, it is worthwhile to consider basing pelagic ecosystem studies on size-dependent principles. The "general" biomass spectrum model presented in this thesis provides a natural way of obtaining size spectra from ecological dynamics in plankton ecosystems, through analysis of the steady state solutions of the general model. This is proposed as an area for further work.

The size distribution of planktonic organisms with respect to organism size suggests the occurrence of a continuum of functional groups owing to the close relationships between body mass and many physiological and ecological properties of pelagic organisms (Gaedke, 1992). A possible consequence at higher hierarchical levels of organization of this empirically well established observation is that the reaction time of the organisms to fluctuating environmental conditions and the seasonal variability of abundance may depend on organism size as well. Additionally, these physiological and ecological parameters are closely coupled to spatial and temporal scales of the ecosystem, adding to the predictive power of size-structured models in the analysis of the structure and function of pelagic ecosystems.

The use of size as an aggregation scheme for dynamic simulation models provides a combination of reductionism and holism useful for exploring the ecological properties of plankton ecosystems. Among the drawbacks to generalizing biological and ecological processes

(e.g. based on size), we find that there will always be groups of organisms, which will negate the allometric rules chosen. The allometric relationships between organism size and various model parameters will not apply in all cases. In addition, these relationships are usually predictable over a large range of body size, but within any narrow size range, there may be considerable variability. Thus, real size spectra will not necessarily be as smooth as that predicted from size distribution models (Borgmann, 1987). However, the use of allometric relationships is not intended to aid biologists in the study of individual species. Its contribution resides in the ability to estimate parameters for use in ecological models of plankton communities. The size relationships are objective estimators of ecological parameters and therefore have applications in the study and understanding of pelagic ecosystems.

Size distribution models obviate the problem of parameter estimation common in ecological modeling studies. In addition, the results of the model simulations can be validated against any system, since the parameters are not specifically related to any particular ecological system. The model can be applied to diverse planktonic ecosystems to test hypotheses regarding the structure and function of those systems, thus improving the predictive power of the model. Ideally, one would be able to construct a reasonably simple model with a high degree of geographical robustness, in the sense that the same size-structured model will give reasonably accurate predictions of biological production in all the major parts of the world ocean. Model predictions can be used to direct field research and analyze current ecological theories. The combination of the analysis of plankton biomass spectra and biophysical measurements will aid in the prediction of the spatio-temporal distribution and productivity of marine plankton (Zhou and Huntley, 1997). Size spectra developed from the "distributed grazing" model simulations show that the allometric structure chosen determines the resulting steady state size structure of the ecosystem. This is shown in the analysis of the unnormalized and normalized spectral slopes in chapter 4.

Marine primary production is generally assumed to be limited by nitrogen. However, there are areas of the world ocean (e.g. the subarctic Pacific and Antarctic Ocean) in which nitrate is not fully utilized and remains at high levels throughout the summer. It has been argued (Martin and Fitzwater, 1988) that production in these areas may be limited by a micronutrient such as iron. Size distribution models can be used to enhance understanding of the causes and consequences of micronutrient limitation. They can also be used to study the effects of enrichment processes (e.g. iron fertilization) on the size structure of the planktonic community.

As illustrated in chapter 4, the "distributed grazing" model proposed can be used to predict the transient response of the community (in terms of the effects on the size structure of the ecosystem) to nutrient enrichment processes. The model shows the succession of size classes as a result of the enrichment process. Understanding of these changes is essential in analyzing the potential biological effects and changes in the food web promoted by these enrichment scenarios. Models will also help in understanding the role of marine biota in natural nutrient cycles, with relevant atmospheric and climatic implications.

The representation used for describing the community effects of the enrichment process is an extreme simplification of phytoplankton nutrient uptake dynamics. It is conceivable to adapt the structure of the model to allow for the presence of an additional limiting nutrient (e.g. a micronutrient such as iron) and to define the phytoplankton growth function in terms of the uptake of the two nutrients considered. Competitive advantages (in nutrient uptake and growth) between size classes can also be integrated in the model structure to account for the differential response of phytoplankton size classes to enrichment processes.

REFERENCES

Borgmann, U. 1987. Models on the slope of, and biomass flow up, the biomass size spectrum. *Canadian Journal of Fisheries and Aquatic Sciences* 44 (Suppl.2): 136-140.

Gaedke, U. 1992. Identifying ecosystem properties: a case study using plankton biomass size distributions. *Ecological Modelling* 63: 277-298.

Gaedke, U. 1995. A comparison of whole-community and ecosystem approaches (biomass size distributions, food web analysis, network analysis, simulation models) to study the structure, function and regulation of pelagic food webs. *Journal of Plankton Research* 17(6): 1273-1305.

Martin, J.H., and S.E. Fitzwater 1988. Iron deficiency limits phytoplankton growth in the north-east Pacific subarctic. *Nature* 331: 341-343.

Platt, T. 1985. Structure of the marine ecosystem: its allometric basis. In Ulanowicz, R.E., and Platt, T. (eds.) *Ecosystem theory for biological oceanography.* Canadian Bulletin of Fisheries and Aquatic Sciences 213: 55-64.

Zhou, M., and M.E. Huntley 1997. Population dynamics theory of plankton based on biomass spectra. *Marine Ecology Progress Series* 159: 61-73.